DESIGN OF NOVEL TRANSFORMABLE PLANAR STRUCTURAL LINKAGES WITH ANGULATED SCISSOR UNITS

A Thesis Submitted to
The Graduate School of Engineering and Sciences of
İzmir Institute of Technology
In Partial Fulfillment of the Requirements for the Degree of

MASTER OF SCIENCES

in Architecture

by
Müjde YAR

December 2016
İZMİR

We approve the thesis of **Müjde YAR**

Examining Committee Members:

Assoc. Prof. Dr. Koray KORKMAZ
Department of Architecture, İzmir Institute of Technology

Assist. Prof. Dr. Gökhan KİPER
Department of Mechanical Engineering, İzmir Institute of Technology

Assoc. Prof. Dr. Ahmet Vefa ORHON
Department of Architecture, Dokuz Eylül University

28 December 2016

Assoc. Prof. Dr. Koray KORKMAZ
Supervisor, Department of Architecture
İzmir Institute of Technology

Assoc. Prof. Dr. Şeniz ÇIKIŞ
Head of the Department of Architecture

Prof. Dr. Bilge KARAÇALI
Dean of the Graduate School of Engineering and Sciences

ACKNOWLEDGEMENTS

I would like to express my sincere gratitude to my supervisor, Assoc. Prof. Dr. Koray KORKMAZ for his generous support, guidance and encouragement.

I would like to express my special thanks to Assist. Prof. Dr. Gökhan KİPER for his constructive criticisms and remarkable helps.

Also I am grateful to Assoc. Prof. Dr. Ahmet Vefa ORHON for his valuable suggestions.

Finally, I am grateful to Oğuz UNCU for his patience and endless support during my studies. Above all, I would like to express my deepest gratitude to my family for their endless love and encouragement.

ABSTRACT

DESIGN OF NOVEL TRANSFORMABLE PLANAR STRUCTURAL LINKAGES WITH ANGULATED SCISSOR UNITS

In this dissertation, the primary objective is to propose a novel geometrical construction technique in order to construct a planar and single degree of freedom structural linkage that can transform between concave and convex configurations. In the literature, most of the deployable structures transform between two known configurations: stowed and deployed. Especially, the deployable structures with radial movement capability have a fixed center point. Starting this point of view, current study deals with a new type of angulated scissor structural linkage that can change its form between bended upward and bended downward configurations by moving the center point of the structure along a direction. In other words, it can change its curvature during the transformation process. The most important point of the study is the usage of kite and dart loops to construct angulated scissor linkages. The geometry of kite or its concave version dart loop provides to obtain angulated scissor bars. The angulated scissor unit, that is composed of the mentioned angulated bars, is different from the existing ones in the literature because they do not provide deployability conditions like known angulated scissor units. Thus, the planar structure that is composed of new type of angulated scissor units has different transformation capability. It transforms between bended upward and downward configurations. In this study, modelling and simulation with computer soft wares have been used as a research method. The proposed structural linkage has been modelled using Solidworks®. As a part of the position analysis, the variations of the structure according to different parameters have been exposed in Microsoft Excel®.

ÖZET

AÇILI MAKAS BİRİMLERİ İLE YENİ DÜZLEMSEL DÖNÜŞEBİLİR STRÜKTÜREL MEKANİZMALARIN TASARIMI

Bu tezin temel amacı; dışbükey ve içbükey biçimler arasında dönüşebilen, düzlemsel ve tek serbestlik dereceli, hareketli bir yapı elde etmeye yönelik yeni bir geometrik konstrüksiyon yöntemi sunmaktır. Literatürdeki çoğu hareketli strüktür toplanıp açılmak gibi bilinen iki durum arasında şekil değiştirebilmektedir. Özellikle radyal hereket kabiliyetine sahip sistemlerin hareket esnasında merkez noktaları sabit kalmaktadır. Buradan yola çıkarak literatürdeki bu eksiklikliği gidermek adına, bu çalışma yeni açılı makas sistemlerinden oluşan, merkez noktası belirli bir doğrultu üzerinde hareket eden ve eğriliği değişebilen hareketli strüktürel mekanizmalar üzerinedir. Çalışmanın en önemli noktalarından biri dışbükey ve içbükey deltoid devrelerinin açılı makas birimlerinden oluşan strüktürler elde etmek amaçlı kullanılmasıdır. Deltoid devreleri birleştirilerek açılı makas çubukları elde edilebilmektedir. Bu şekilde elde edilmiş açılı makas birimi literatürde var olanlardan farklı özelliklere sahiptir. Bu nedenle, bu açılı makas birimleriyle oluşturulmuş düzlemsel strüktür daha fazla hareket kabiliyetine sahiptir. Çalışmada, araştırma yöntemi olarak bilgisayar ortamında modelleme ve benzeşim teknikleri kullanılmıştır. Önerilen strüktür Solidworks® ortamında modellenmiştir. Pozisyon analizinin bir parçası olarak strüktürün değişen parametrelerle elde edilen varyasyonları Microsoft Excel® ortamında incelenmiştir.

TABLE OF CONTENTS

LIST OF FIGURES.....ix

CHAPTER 1. INTRODUCTION 1
1.1. Definition of the Study.....1
1.2. Scope and Objectives of the Study.....2
1.3. Methodology 3
1.4. Significance of the Study and Contributions 3
1.5. Outline of the Thesis 3

CHAPTER 2. REVIEW OF LITERATURE.....5
2.1. Deployable Bar Structures.....5

CHAPTER 3. ANALYSIS OF LOOPS OF SCISSOR LINKAGES 18
3.1. Planar Scissor Units.....18
3.2. General Deployability Condition.....19
3.3. Geometric Properties of Quadrilateral Loops 20
3.4. Analysis of Scissor Linkages 23
3.4.1. Translational Scissor Units.....23
3.4.1.1. Translational Scissor Linkages with Identical Rhombus Loops 24
3.4.1.2. Translational Scissor Linkages with Identical Parallelogram Loops 25
3.4.1.3. Translational Scissor Linkages with Identical Kite Loops.....27
3.4.1.4. Translational Scissor Linkages with Arbitrary Rhombus Loops 28
3.4.2. Polar Scissor Units.....30
3.4.2.1. Polar Scissor Linkages with Identical Kite Loops.....30
3.4.2.2. Polar Scissor Linkages with Arbitrary Kite Loops.....32
3.4.3. Angulated Scissor Units.....34
3.4.3.1. Angulated Scissor Linkages with Identical and Similar Rhombus Loops 36

3.4.3.2. Angulated Linkages with Different Rhombus Loops 39
3.4.3.3. Angulated Scissor Linkages with Identical and Similar Parallelogram Loops.....42
3.5. Conclusion 45

CHAPTER 4. GEOMETRICAL CONSTRUCTION METHOD OF PLANAR ANGULATED SCISSOR LINKAGES 47
4.1. Loop Assembly Method.....47
4.1.1. Geometric Construction of Multi-Loop Linkages by Identical Rhombi 47
4.1.2. Geometric Construction of Irregular Expanding Polygons with Similar Rombi.....50
4.2. Conclusion 51

CHAPTER 5. ASSEMBLY OF KITE AND DART LOOPS 52
5.1. Assembly of Kite Loops 52
5.2. Assembly of Dart Loops 60
5.3. Conclusion 67

CHAPTER 6. ANALYSIS OF THE ASSEMBLIES OF KITE AND DART LOOPS 68
6.1. Geometrical Conditions of Angulated Scissor Linkage Composed of Kite Loops.....68
6.1.1. Flat Position of Kite Loops.....68
6.1.2. Bended Downward Position of Kite Loops.....70
6.1.3. Bended Upward Position of Kite Loops 72
6.2. Geometrical Conditions of Angulated Scissor Linkage Consist of Dart Loops 74
6.2.1. Flat Position of Dart Loops 75
6.2.2. Bended Downward Position of Dart Loops.....76
6.2.3. Bended Upward Position of Dart Loops.....78
6.3. Position Analysis 80
6.4. Conclusion 86

CHAPTER 7. CONCLUSION 87

REFERENCES 88

LIST OF FIGURES

Figure **Page**

Figure 2.1. Movable theatre 6
Figure 2.2. Foldable reticular dome 6
Figure 2.3. Expandable space-frame structure 7
Figure 2.4. Swimming pool in Seville 8
Figure 2.5. Singly-curved foldable barrel vault 8
Figure 2.6. Angulated scissor unit 9
Figure 2.7. Hoberman's kinetic sculpture: Expanding Geodesic Dome 9
Figure 2.8. Iris Dome 10
Figure 2.9. Hoberman Arch in 2002 Winter Olympics 10
Figure 2.10. Generalized angulated elements 11
Figure 2.11. Multi-angulated scissor structure 11
Figure 2.12. Deployable structure composed of multi-angulated elements 11
Figure 2.13. Deployable roof structure 11
Figure 2.14. Scissor unit with various hinge points and the structure constructed with 10
Figure 2.15. Expanding helicoid 11
Figure 2.16. Expanding hypar 11
Figure 2.17. Arbitrary doubly-curved translational structures 14
Figure 2.18. Deployable catenoid 15
Figure 2.19. Transformation sequence of Cable-scissor arch 15
Figure 2.20. Three types of Modified scissor-like elements 16
Figure 2.21. 4-DoF planar scissor arch structure composed of M-SLEs and SLEs 16
Figure 2.22. Adaptive roof structure composed of scissor arches 17
Figure 2.23. Perspective and top view of the proposed scissor-hinge shell structure 17
Figure 3.1. Basic scissor units a) Translational unit, b) Polar unit, c) Angulated unit ($\beta 1$, $\beta 2$, and $\beta 3$ are deployment angles) 18
Figure 3.2. Diagrammatic of scissor linkage 20
Figure 3.3. Classification of quadrilaterals 20
Figure 3.4. Hierarchies of simple quadrilaterals 21
Figure 3.5. A kite, showing its pairs of equal length sides, the axis of symmetry and bisector of opposite angles 22

Figure 3.6. a) Convex kite b) concave kite, is referred to as a dart 22
Figure 3.7. Translational scissor unit (β is deployment angle)..... 23
Figure 3.8. Translational linkage with identical bars..... 24
Figure 3.9. Identical rhombus loops of a translational scissor linkage..... 25
Figure 3.10. Translational linkage with different bars and with scissor hinges at their midpoints 26
Figure 3.11. Identical parallelogram loops of translational scissor linkage 26
Figure 3.12. Translational linkage with different bars and with scissor hinges at their midpoints 27
Figure 3.13. Identical kite loops of translational scissor linkage..... 28
Figure 3.14. Translational linkage with arbitrary bar lengths and with scissor hinges eccentrically placed 29
Figure 3.15. Different rhombus loops of translational scissor linkage..... 29
Figure 3.16. Polar scissor unit 30
Figure 3.17. Linkage formed by polar units with identical bars and with scissor hinges eccentrically placed 31
Figure 3.18. Identical kite loops of polar scissor linkage 32
Figure 3.19. Linkage formed with arbitrary polar units and mid-scissor hinges eccentrically placed 33
Figure 3.20. Different kite loops of polar scissor linkage 33
Figure 3.21. Angulated Scissor Units a) Hoberman's Symmetrical AE (φ=ψ), b) Type I Equilateral AE (φ≠ψ) and c) Type II Similar AE (φ=ψ and $l_1/l_4=l_2/l_3$) 34
Figure 3.22. Partial radially deployed closed ring scissor linkage with angulated units 37
Figure 3.23. Identical rhombus loops forming angulated scissor linkage 37
Figure 3.24. Radially deployed scissor linkage with angulated units..... 38
Figure 3.25. Similar rhombus loops forming angulated scissor linkage 39
Figure 3.26. Assembly of one type of Equilateral AEs 40
Figure 3.27. Different rhombus loops forming angulated scissor linkage..... 40
Figure 3.28. Assembly of Equilateral AEs with unequal semi-length..... 41
Figure 3.29. Assembly of various rhombus loops forming angulated scissor linkage ... 42
Figure 3.30. Assembly of identical Similar generalized angulated elements 43
Figure 3.31. Assembly of identical parallelogram loops aligned on arc of a circumference..... 43
Figure 3.32. Assembly of two different Similar Angulated Elements..... 44

Figure 3.33. Assembly of two different type of parallelogram loops aligned on arc of a circumference 45
Figure 4.1. Geometric construction of translational linkage with loop assembly method 48
Figure 4.2. Geometric construction of the angulated scissor structure forming a circular arc 48
Figure 4.3. Geometric construction of the angulated scissor linkage forming a circle .. 49
Figure 4.4. Geometric construction of the angulated scissor structure forming ellipse . 49
Figure 4.5. Geometric construction of irregular expanding polygon with similar rhombi 50
Figure 4.6. Irregular expanding polygon composed of angulated and translational units 51
Figure 5.1. Flat configuration of the assembled identical kite loops 53
Figure 5.2. Angulated scissor unit with equal semi lengths and kink angles created with identical kites 53
Figure 5.3. Angulated scissor linkage formed by identical kite loops 54
Figure 5.4. The bending upward motion of the linkage modelled on Solidworks 55
Figure 5.5. The bending downward motion of the linkage modelled on Solidworks..... 56
Figure 5.6. Flat configuration of the assembled similar kite loops with identical interior angles but different semi-lengths 56
Figure 5.7. Angulated scissor unit with different semi-lengths and equal kink angles created with similar kites 57
Figure 5.8. Angulated scissor linkage formed by similar kite loops with identical interior angles but different semi-lengths 57
Figure 5.9. Flat configuration of the assembled different kite loops with equal semi-lengths but different interior angles 58
Figure 5.10. Angulated scissor unit with equal semi lengths and different kink angles created with different kites 58
Figure 5.11. Angulated scissor linkage formed by different kite loops with equal semi-lengths but different interior angles 58
Figure 5.12. Flat configuration of the assembled different kite loops 59
Figure 5.13. Angulated scissor unit with different semi lengths and different kink angles created with different kites 59

Figure 5.14. Angulated scissor linkage formed by different kite loops with different semi-lengths and interior angles 60
Figure 5.15. Flat configuration of the assembled identical dart loops 60
Figure 5.16. Angulated scissor unit with equal semi-lengths and kink angles created with identical darts 61
Figure 5.17. Angulated scissor linkage formed by identical dart loops 61
Figure 5.18. The bending upward motion of the linkage modelled on Solidworks 62
Figure 5.19. The bending downward motion of the linkage modelled on Solidworks... 62
Figure 5.20. Flat configuration of the assembled similar dart loops with identical interior angles but different semi-lengths 63
Figure 5.21. Angulated scissor unit with different semi-lengths and equal kink angles created with similar darts 63
Figure 5.22. Angulated scissor linkage formed by similar dart loops with identical interior angles but different semi-lengths 64
Figure 5.23. Flat configuration of the assembled different dart loops with different interior angles but equal semi-lengths 64
Figure 5.24. Angulated scissor unit with equal semi-lengths and different kink angles created with different darts 65
Figure 5.25. Angulated scissor linkage formed by different dart loops with different interior angles but equal semi-lengths 65
Figure 5.26. Flat configuration of the assembled different dart loops with different interior angles and semi-lengths 66
Figure 5.27. Angulated scissor unit with different semi-lengths and kink angles created with different darts 66
Figure 5.28. Angulated scissor linkage formed by different dart loops with different interior angles and semi-lengths 66
Figure 6.1. Kinematic diagram of the flat configuration of the linkage 69
Figure 6.2. Kinematic diagram of the bended downward position of the linkage..... 70
Figure 6.3. Kinematic diagram of the bended upward position of the linkage..... 73
Figure 6.4. Kinematic diagram of the flat configuration of the linkage 75
Figure 6.5. Kinematic diagram of the bended downward configuration of the linkage . 77
Figure 6.6. Kinematic diagram of the bended upward configuration of the linkage..... 79
Figure 6.7. Kinematic diagram of the linkage 81
Figure 6.8. The position of the linkage when c=50 and θ_1~35º 82

Figure 6.9. Analytical position analysis of the angulated scissor linkage in the position of c=50 and θ_1~35º 84
Figure 6.10. Initial position of the linkage c=59,88 cm, θ1 = 30º, θ2 = 56,44º, θ3 = 93,56º 85
Figure 6.11. Bended upward position of the linkage c=26,72 cm, θ1 = 30º, θ2 = 123,56º, θ3 = 26,44º 85

CHAPTER 1

INTRODUCTION

1.1. Definition of the Study

In every period, humans have strived to construct flexible buildings that could be adapted to changing human requirements and natural conditions. Kinetic architecture's primary objective is the design of adaptable building envelopes and spaces as the major components of the building using mechanical structures (Zuk & Clarke, 1970).

The term "Kinetic Architecture" was introduced by William Zuk and Roger H. Clark in the early seventies when dynamic spatial design problems were explored in mechanical systems. William Zuk and Roger Clark defined kinetic architecture as "the architectural form could be inherently being displaceable, deformable, expandable or capable of kinetic movement" (Zuk and Clark, 1970).

In recent years, human needs have changed with developing technology. Developments in some architectural areas such as construction technology, material science, and architectural computing technologies made it possible to construct deployable and transformable structures that can meet changing human needs.

Gantes (1991) defines the deployable structures as "Deployable structures is a generic name for a broad category of prefabricated structures that can be transformed from a closed compact configuration to a predetermined, expanded form in which they are stable and carry loads." Scissor mechanisms are the most preferred units for deployable systems, and there are various studies about deployable structures constructed with them. The notion of scissor structure was first introduced in 1961 by Spanish architect Piñero and followed by many researchers until today. After Piñero, these structures were further developed by Escrig and Valcarcel as in the form of new spherical grid structures that are composed of two-way and three-way scissors with several connection details (Escrig & Valcarcel, 1986a; 1986b; 1987; 1993). In addition to these developments, Chuck Hoberman, who is an architect and a mechanical engineer, made significant contributions to the literature by his designs and patents from architectural projects to the toy industry. He proposed a novel concept composed of angulated elements

that led to the design of radially deploying closed loop structures (Hoberman, 1991). In the following years, transformable structures were applied to space applications, including antennas and solar panels by Sergio Pellegrino and Zhong You. They took Hoberman's discovery a step further, and they discovered generalized angulated elements to be used as a building block (You & Pellegrino, 1997). They also discovered multi-angulated rod that reduced the number of components of the structure and the complexity of its joints.

In the literature, scissor units are classified into three main groups according to the location of scissor hinge. These are translational, polar and angulated scissor units. At the beginning of the study, scissor units are investigated on the existing classification and their kinetic movement capacity. After that, scissor structures are examined according to their loop types. In the scissor structures literature, there are three known loop types as follows: parallelogram, rhombus, and kite. Scissor structures are examined first considering the scissor unit type and then the loop type.

This dissertation deals with the angulated scissor unit that is a different type from existing ones in the literature. When the loop types of scissor units in the literature are examined, there are limited studies about using kite loops to construct angulated scissor structure (Liao & Li, 2005; Kiper & Söylemez, 2010; Hoberman, 2013). So we found out that kite loop and its concave form dart loop are capable of constructing angulated bars. The aim of the study is to design novel angulated scissor linkage composed of kite loop and its concave form as dart loop. Furthermore, how these structures move is examined when the units are assembled together. Assembly variations, geometrical and kinematic analysis of the proposed structures are investigated.

1.2. Scope and Objectives of the Study

In the present study, firstly detailed literature investigation is conducted about deployable scissor structures. Then, geometric and kinematic properties of the existing scissor units are examined. As a contribution to the literature, loop types of scissor units are also investigated.

In the present study, a geometrical construction method is proposed to obtain angulated scissor units. In the literature there is no application of kite loops to construct angulated scissor units based on Chuck Hoberman's suggestion (Hoberman, 2013). On

the other hand, Hoberman's techniques are only applied to rhombus loop. So, in this study kite loops and also its concave version (dart loop) was used to construct a novel type of angulated scissor units.

In the light of this information, Hoberman's methods were applied and developed to construct novel types of scissor linkages consist of angulated units in the form of deployable structures having the ability to change their curvature.

1.3. Methodology

First of all, detailed literature review of previous works plays an important role in this study to understand the fundamental design criteria of scissor units.

Simulation and modeling in the computer are the methods to create 2D loop structures which are further converted into 3D and investigated with Solidworks® in order to determine movement ability of the systems. Moreover, Microsoft Excel® is used to model the system in accordance with its dimensions. In this way, Excel enables to investigate transformation capacity of the systems in terms of different dimensions or angles easily.

1.4. Significance of the Study and Contributions

The major contribution of the present study is to develop geometrical construction approach for angulated scissor units consist of kite or dart loops.

1.5. Outline of the Thesis

This thesis is composed of six chapters:

Chapter 1 introduces definition of the study, scope and objectives, methodology, significance of the study and contributions, and outline of the thesis.

Chapter 2 introduces the comprehensive review of the existing studies relevant to the thesis. It is based on deployable scissor structures.

Chapter 3 states the classification of existing scissor units, general deployability condition of them and existing quadrilateral loops in the literature. Then, the geometrical

conditions of scissor linkages constructed with each of the three scissor units is presented. Regarding this, loop types of scissor linkages is analyzed.

Chapter 4 demonstrates geometrical design method for planar scissor linkages based on a rhombus, parallelogram, and kite loops.

Chapter 5 proposes a novel deployable scissor linkages composed of angulated scissor units which are obtained by kite and dart loops.

Chapter 6 deals with the geometrical kinematical conditions and the position analysis of the proposed scissor linkage.

Chapter 7 comprises all the main findings of previous chapters in summary and expresses main contributions.

CHAPTER 2

REVIEW OF LITERATURE

In this chapter, a review of existing deployable scissor linkages are presented in order to understand the developments, contributions, and deficiencies of them. Main characteristics of the existing studies are investigated regarding their geometric properties.

In the literature review the historical development of the deployable scissor structures is investigated. In this context, the most common and important examples of the deployable scissor structures are examined.

2.1. Deployable Bar Structures

Deployable scissor structures usually transform from a compact stowed configuration to an expanded functional configuration. They are used mostly in portable or temporary applications. As adaptable structures, they can be integrated either into a site as a deployable bridge in order to respond changing transportation requirements or to a building as a deployable roof for changing weather conditions.

Emilio Pérez Piñero is the pioneer who proposed a deployable structure composed of scissor-like elements (SLEs) to construct a movable theater (Figure. 2.1). The structure is composed of rigid bars and cables, and there is a need for additional cables to lock the model and to sustain stabilization after folding the structure. Different types of deployable bar structures are further developed (Piñero 1961a; 1961b).

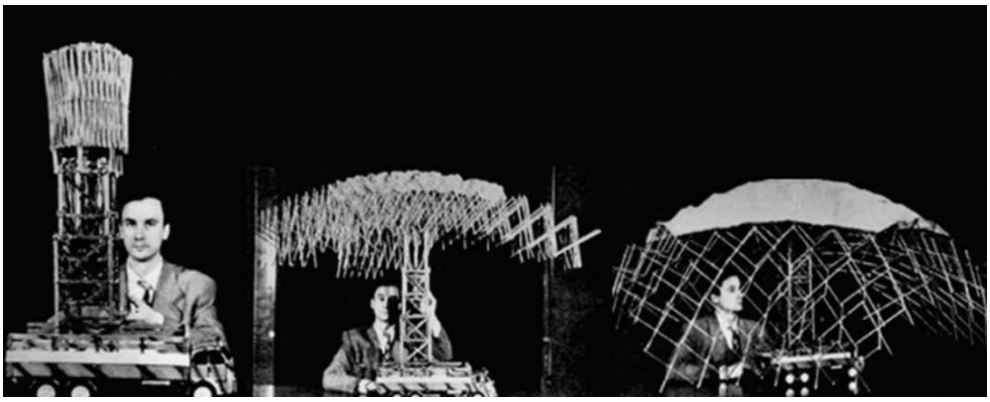

Figure 2.1. Movable theatre
(Source: © Fundación Emilio Pérez Piñero, 2017)

Piñero develops a large variety of deployable structures such as pavilions, retractable domes and temporary enclosures based on using SLEs (1962; 1965). The foldable reticular dome in Figure 2.2 contains seven modules in it. In that design, each module is capable of deploying from a compact bundle to an expanded shape. Nevertheless, in order to generate the dome shape, modules have to be deployed and stiffened on the ground and then lifted up and locked together (Belda, 2013). After the modules are connected to each other, the system is no longer deployable.

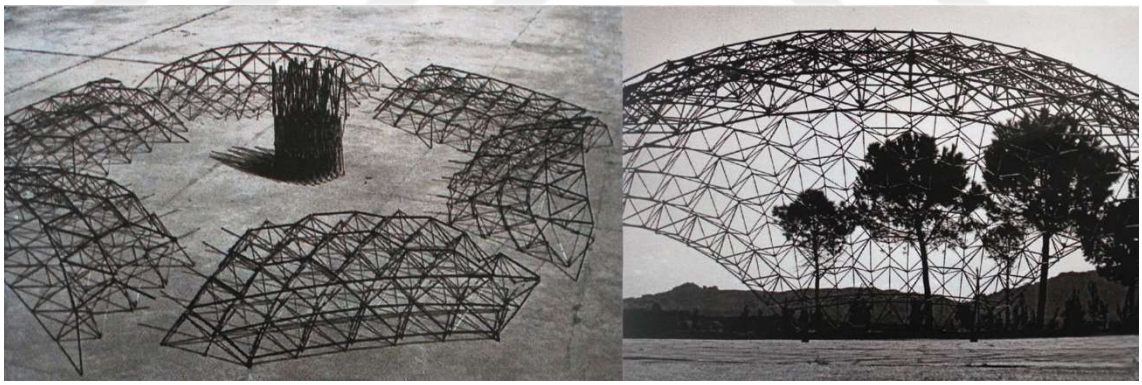

Figure 2.2. Foldable reticular dome
(Source: © Fundación Emilio Pérez Piñero, 2017)

Félix Escrig investigates deployable bar structures in detail. He is the first researcher who presented SLEs' geometric and deployability conditions, the relation between the elements, and the span of the structure (Escrig, 1984; Escrig 1985). He introduces how to obtain three-dimensional structures by intersecting SLEs in multiple directions on a grid and the way of generating curvature in such a grid by varying the location of the intermediate hinge of the SLEs. In his further studies, new spherical grid

structures composed of two-way and three-way scissors are developed (Escrig & Valcarcel, 1986a, 1986b, 1987). In addition to these developments, different kinds of deployable scissor structures include spherical and geodesic structures, quadrilateral expandable umbrella, and deployable polyhedral and compactly folded cylinder have been developed (Escrig and Valcárcel 1993; Escrig 2006).

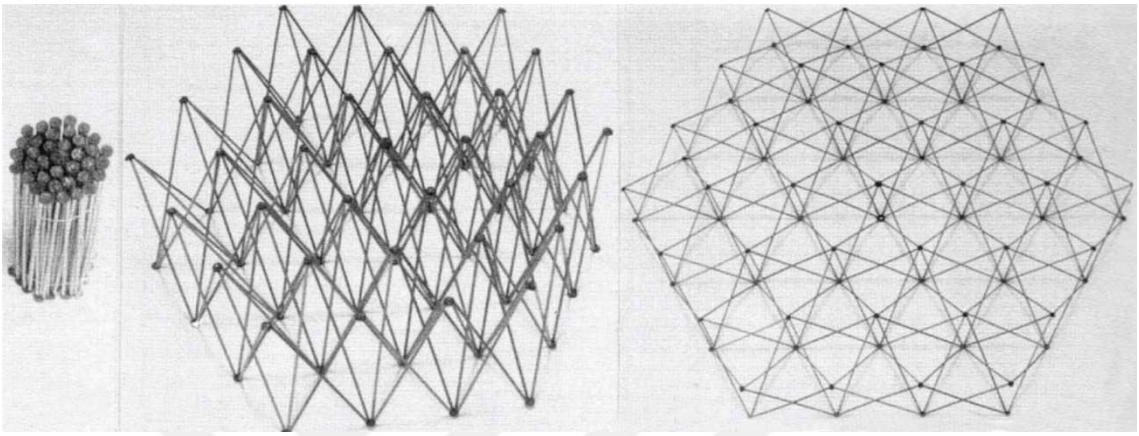

Figure 2.3. Expandable space-frame structure
(Source: Escrig, 1984)

One of the most famous examples of scissors units applied to a real life example is deployable roof structure for a swimming pool in San Pablo Sports Centre in Seville, Spain by Escrig (1996). The roof structure is based on two identical rhomboid grid structures with spherical curvature consisting of grids of equal quadrilateral SLEs in which the structure is covered with a thin fabric roof. It is unfolded from a folded configuration to an expanded form as in Figure 2.4.

Figure 2.4. Swimming pool in Seville
(Source: Wikimedia, 2016)

Escrig's foldability conditions of SLEs are further developed by Langbecker (1999) in order to find out the deployability of translational, cylindrical and spherical configurations of scissor structures and to investigate their kinematics. Moreover, by using suitable SLEs he developes many models of singly-curved foldable barrel vaults and doubly-curved synclastic structures as in Figure 2.5 (Langbecker & Albermani, 2001).

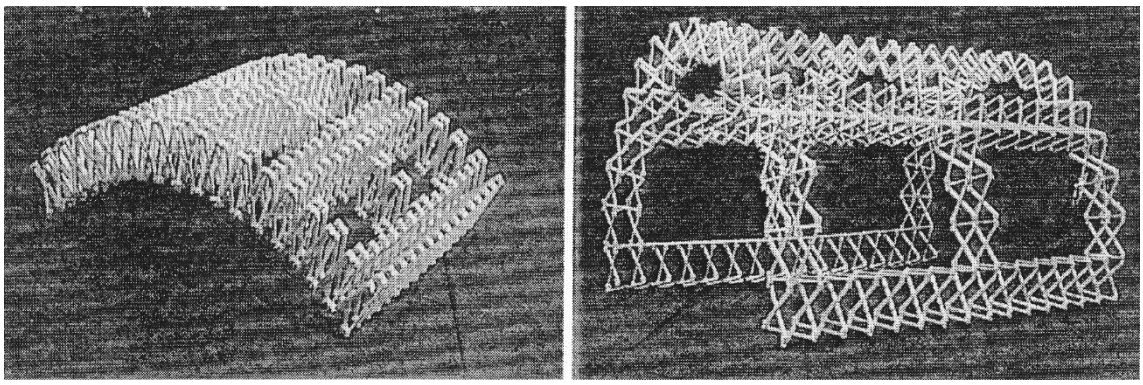

Figure 2.5. Singly-curved foldable barrel vault
(Source: Langbecker & Albermani, 2001)

The discovery of angulated elements by Chuck Hoberman (1990), composed of two identical angulated bars connected to each other by a revolute joint, brings a new perspective into the design of scissor mechanisms (Figure 2.6). This development led Hoberman to use single *DoF* scissor structures in a wide range of applications due to the fact that it creates a central opening at the center.

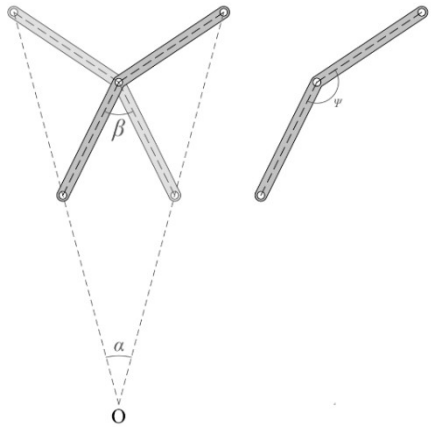

Figure 2.6. Angulated scissor unit

By using the angulated elements, Hoberman (1991) creates original works such as Hoberman Arch, Expanding Geodesic Dome, Expanding Sphere, Expanding Icosahedron and Iris Dome. Expanding Geodesic Dome structure of Hoberman is illustrated in Figure 2.7.

Figure 2.7. Hoberman's kinetic sculpture: Expanding Geodesic Dome
(Source: © Hoberman, 2016)

Another work, the Iris Dome is a lamella dome, which is based on the geometry of interlocking spirals capable of retracting radially towards the perimeter (Figure 2.8) (Hoberman, 1993).

Figure 2.8. Iris Dome
(Source: © Hoberman, 2016)

Hoberman's Arch is briefly described as follows: firstly, rigid panels are used to clad the structure comprising of six concentric rings of angulated elements, and these panels slide over one another by attaching to the individual angulated elements. (Figure 2.9).

Figure 2.9. Hoberman Arch in 2002 Winter Olympics
(Source: © Hoberman, 2016)

Hoberman is the pioneer in the design of angulated elements and his ideas inspire people to go one step further. For example, You and Pellegrino (1997) make detailed investigations about angulated scissor structures. They take Hoberman's discovery a step further, and they discover *generalized angulated elements* (Figure 2.10) to be used as a building block (You & Pellegrino, 1997).

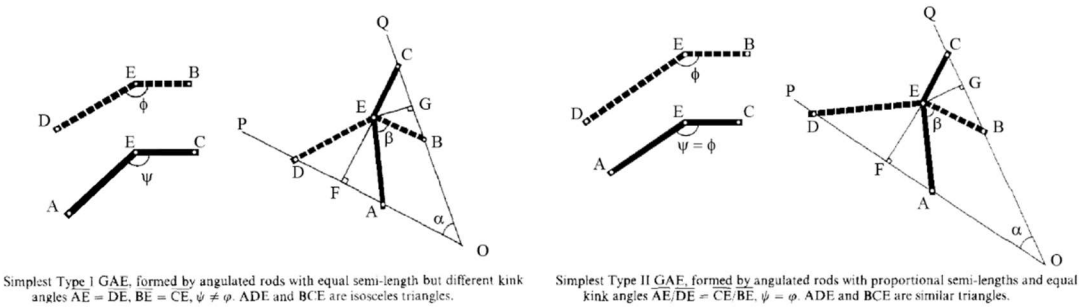

Figure 2.10. Generalized angulated elements
(Source: You & Pellegrino, 1997)

They also discover multi-angulated rod that reduced the number of components of the structure and the complexity of its joints (Figure 2.11). Kassabian, You and Pellegrino construct a deployable structure in such a way that they develop multi-angulated elements which are used to construct mounted on pinned columns (Kassabian et. al., 1999) (Figure 2.12).

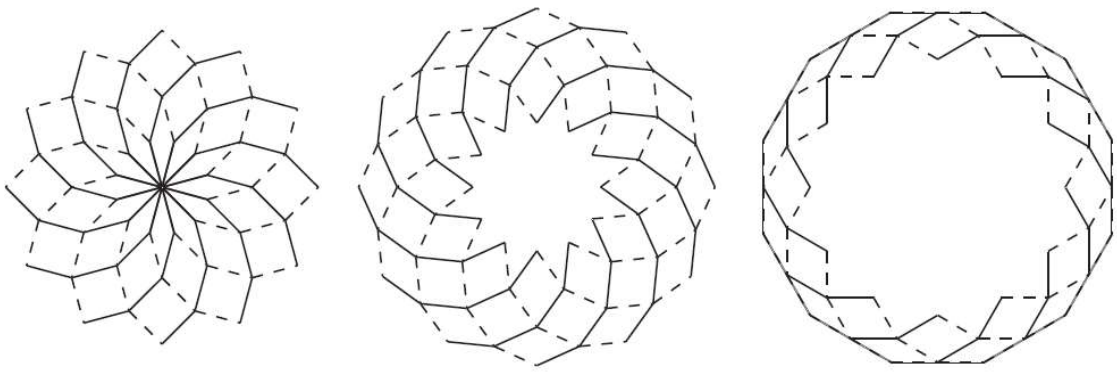

Figure 2.11. Multi-angulated scissor structure
(Source: Jensen & Pellegrino, 2002)

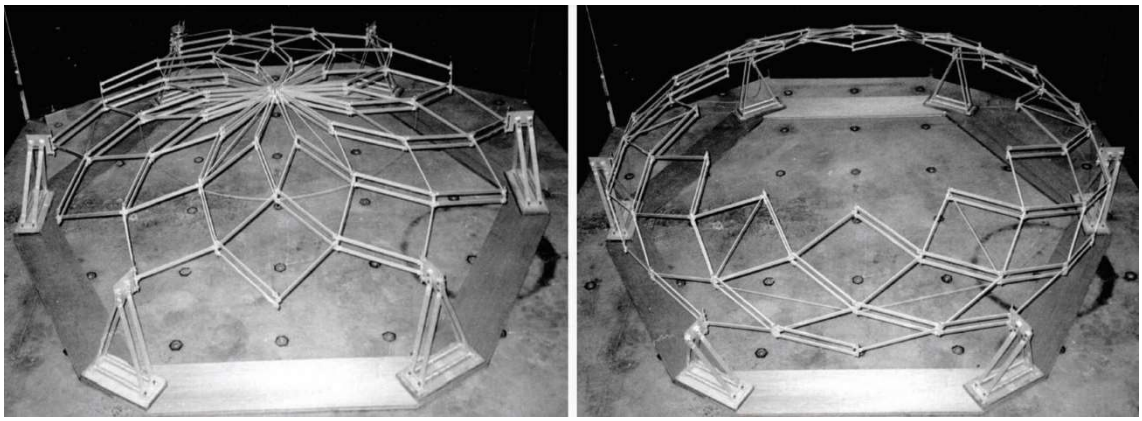

Figure 2.12. Deployable structure composed of multi-angulated elements
(Source: Kassabian, You, & Pellegrino, 1999)

Another researcher uses scissor arches composed of angulated elements in order to cover a tennis arena (Van Mele, 2008). In his design, the scissor arches are integrated with a membrane that is capable of folding and unfolding together with the scissors from one form to another instead of using a single arch which is pinned at one end. The scissor arches are cut into two and constructed two halves are pinned to spectator area which are connected at a central hinge in the closed configuration. On the other hand, he does not have a chance to construct the roof because that kind of a bar structure is not convenient for a long span. As a result, he prefers to use a movable supporting structure and cables to provide structural resistance against the service loads as shown in the Figure 2.13.

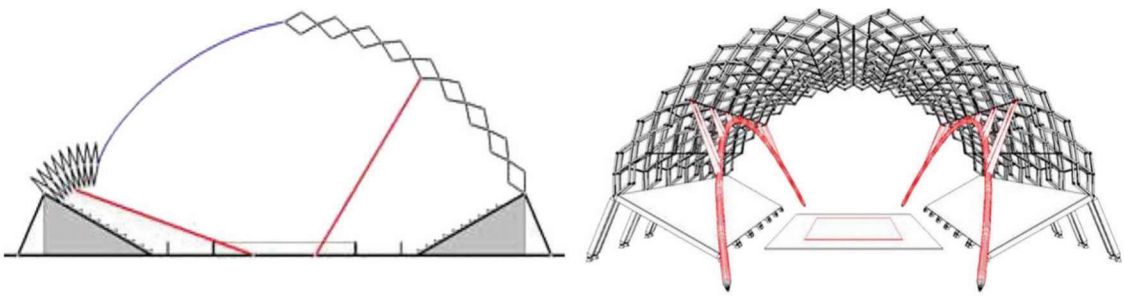

Figure 2.13. Deployable roof structure
(Source: Van Mele, 2008)

Different type of scissor units can also obtain the curved structures rather than using basic scissor units. Rippmann and Sobek develop a new scissor unit consisting of various intermediate hinge points as in Figure 2.14. They also design a novel structure constituting of different geometric shapes by switching the locations of the hinge points in the design of basic scissor structure as indicated in Figure 2.14 (Rippmann, 2007). At first look, the system seems like flexible, but it is not the case because the system has single DoF.

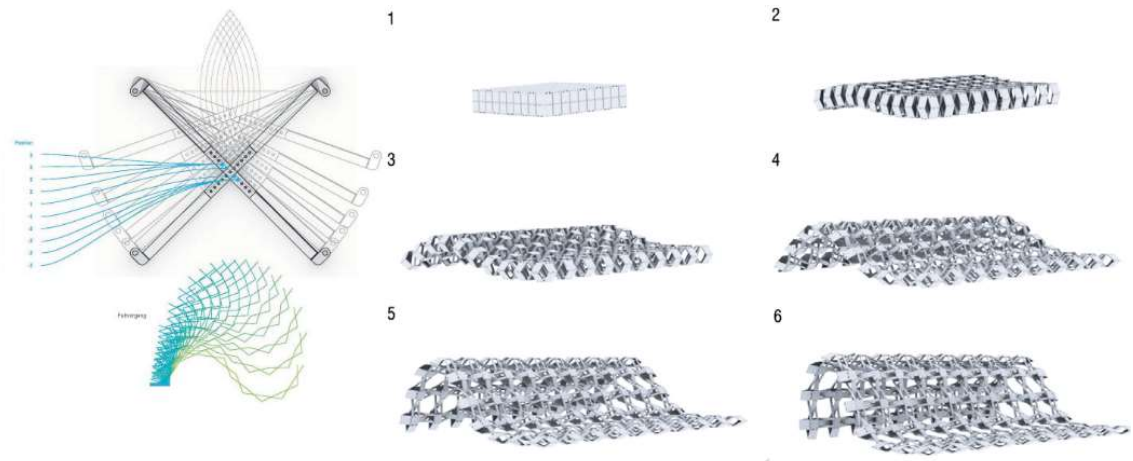

Figure 2.14. Scissor unit with various hinge points and the structure constructed with (Source: Rippmann, 2007)

Hoberman who is the pioneer of angulated scissor systems also developes two deployable anticlastic structures using angulated elements. Expanding Helicoid is one of the novel designs of him introduced in 1998 as shown in Figure 2.15. The structure looks like a double helix DNA structure. Another example of anticlastic structures is Expanding Hypar built in 1998 (Figure 2.16). These designs contribute to the development of deployable bar structures, but in terms of architectural perspective, it is hard to implement them in daily life due to their complex mechanisms.

Figure 2.15. Expanding helicoid
(Source: © Hoberman, 2016)

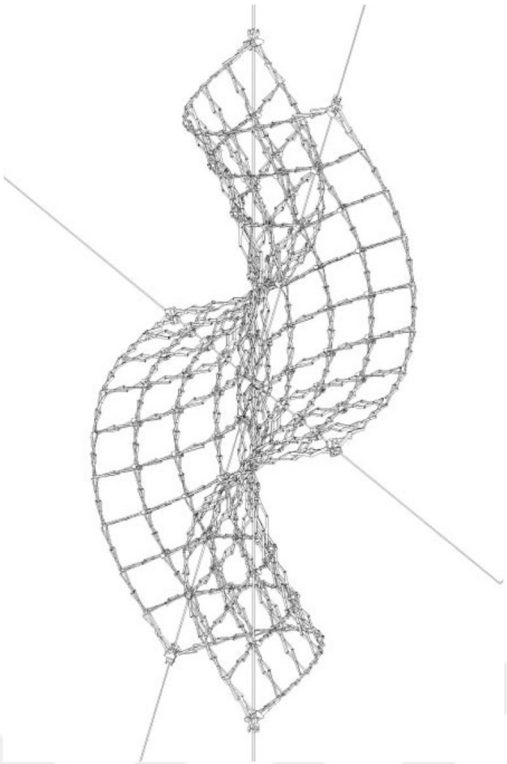

Figure 2.16. Expanding hypar
(Source: © Hoberman, 2016)

Polina Petrova developes doubly curved structures as an alternative to constant curvatures. The main aim of her work is to develop more arbitrary surfaces and suitable forms for contemporary architecture. As a result, arbitrary doubly-curved translational surfaces are developed by her (Petrova, 2008) as in Figure 2.17.

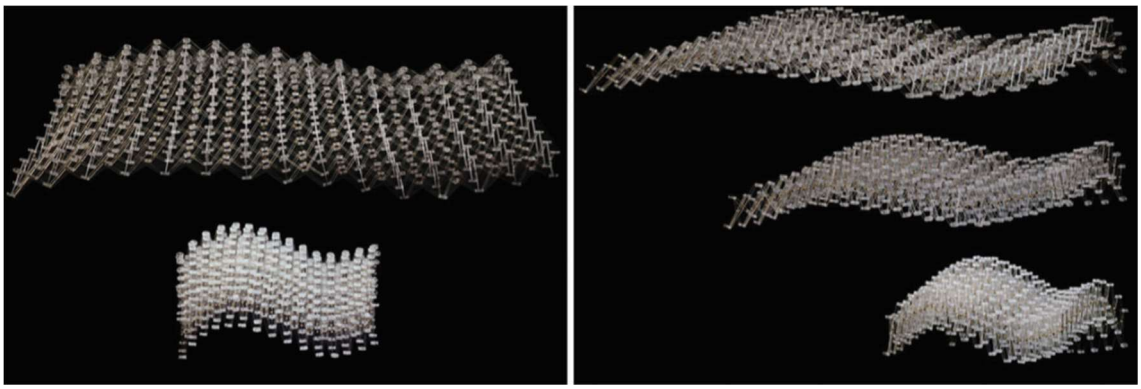

Figure 2.17. Arbitrary doubly-curved translational structures
(Source: Petrova, 2008)

In more recent works, Roovers, Mira and Temmerman (2013) reveal the potential of angulated elements to be applicable in new geometrical shapes. In order to accomplish that, they use Hoberman's Expanding Helicoid rather than using simpler curved surfaces.

In the end, they come up with a design based on a single DoF deployable catenoid structure as shown in Figure 2.18.

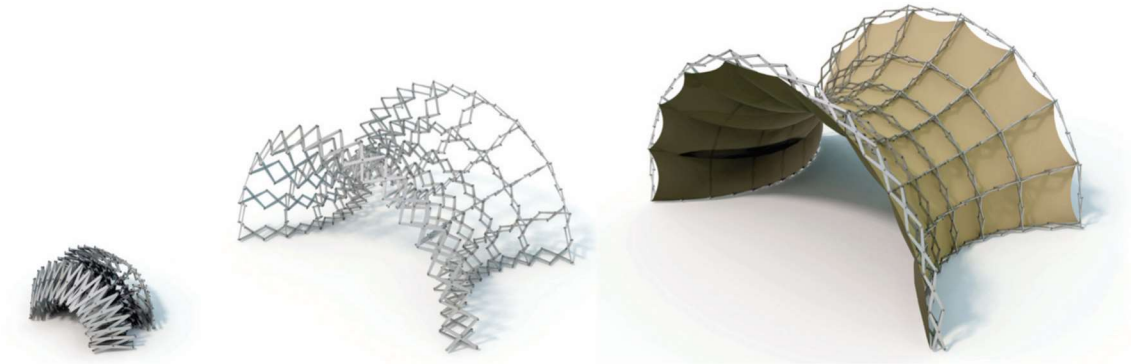

Figure 2.18. Deployable catenoid
(Source: Roovers, Mira, & De Temmerman 2013)

As being one of the novel transformable deployable structures, as compared to typical scissor-hinge structures, Cable Scissors Arch (CSA) is developed by Tsutomu Kokawa. The most important feature of that system is its ability to change its geometry without changing the span length. The structure consists of two scissor assemblies and zigzag flexible cables with pulleys. In Figure 2.19, the deployment sequence can be seen (Kokawa and Hokkaido, 1997).

Figure 2.19. Transformation sequence of Cable-scissor arch
(Source: Kokawa and Hokkaido, 1997)

In addition to the mentioned studies until so far, Akgün (2010) proposes new transformable structures based on a novel SLEs. In his design, three types of modified scissor-like element (M-SLE) are developed by adding revolute joints on various locations of a bar as shown in Figure 2.20.

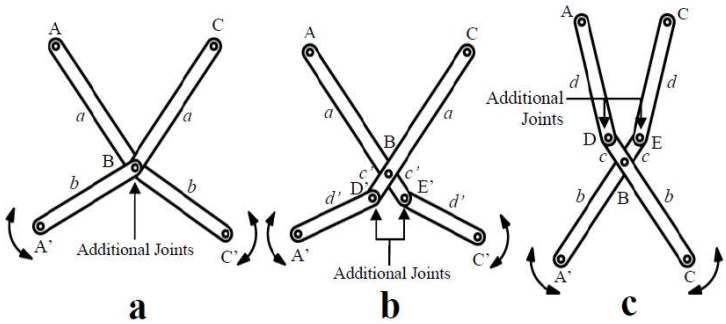

Figure 2.20. Three types of Modified scissor-like elements
(Source: Akgün, 2010)

Development of M-SLE led Akgün to introduce new adaptable scissor structures being able to transform from rectilinear geometries to different curved shapes without changing the span. As an example, 4-DoF planar scissor arch structure composed of M-SLEs and SLEs is designed as in Figure 2.21.

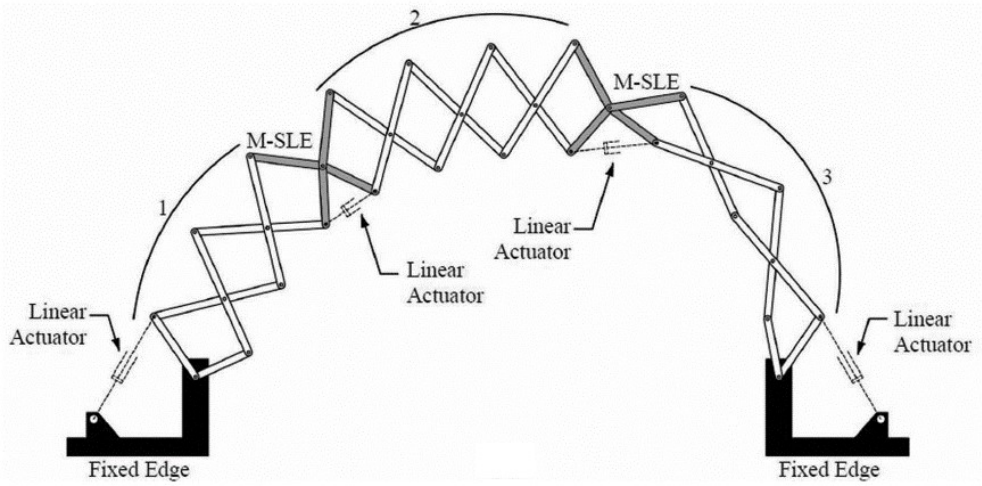

Figure 2.21. 4-DoF planar scissor arch structure composed of M-SLEs and SLEs
(Source: Akgün, 2010)

Then, Akgün uses six scissor arches to design an adaptable roof structure, which is highly flexible (Figure 2.22). Also, he designs a complex 4-DoF spatial scissor structure composed of different types of scissor units as 25 spatial SLEs (S-SLEs), 4 modified spatial scissor-like elements (MS-SLEs), 20 hybrid spatial scissor-like elements (HS-SLEs) and 8 special SLEs as shown in Figure 2.23. These scissor units give extra flexibility to the structure and becoming superior over the current examples of spatial scissor structures.

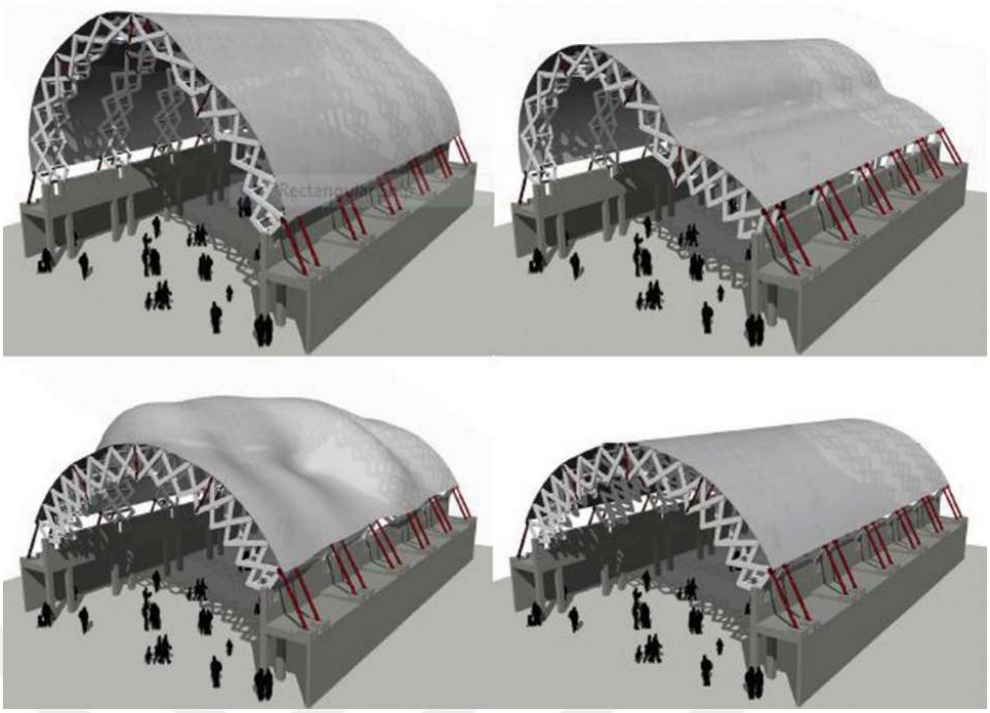

Figure 2.22. Adaptive roof structure composed of scissor arches
(Source: Akgün, 2010)

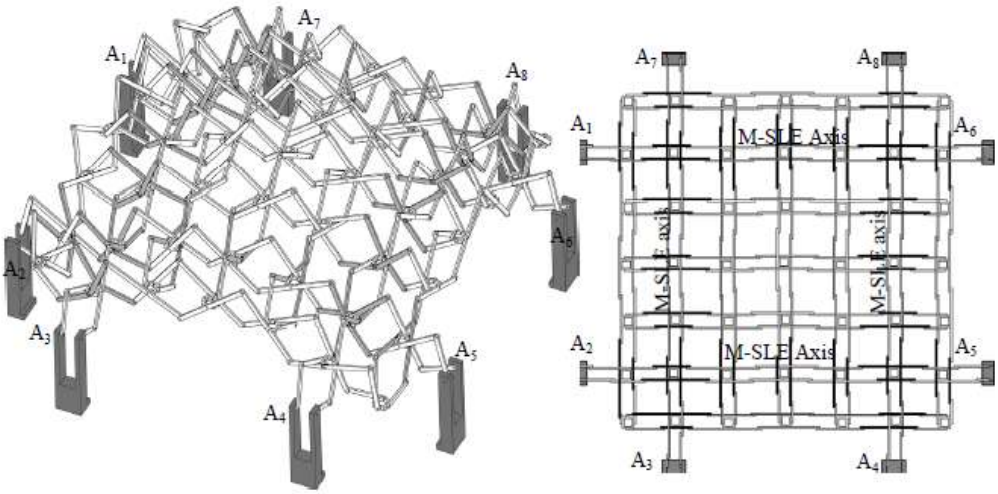

Figure 2.23. Perspective and top view of the proposed scissor-hinge shell structure
(Source: Akgün, 2010)

CHAPTER 3

ANALYSIS OF LOOPS OF SCISSOR LINKAGES

In this chapter the main scissor units are examined based on their geometrical properties. Basic scissor units are categorized into three main groups as translational, polar and angulated scissor unit. The general deployability condition of scissor linkages is investigated. In addition to this, to understand the loop types of scissor linkages, quadrilateral loops are examined. Then, scissor linkages are investigated based on their geometrical conditions and their loop types on deployed configuration.

3.1. Planar Scissor Units

This section is concerned with an explanation of the characteristics of basic scissor units. The classification of scissor units in (Maden, Korkmaz and Akgün, 2011) is followed. A scissor unit consists of two rods connecting to each other with a single DoF revolute joint (R). This revolute joint, called as a scissor hinge, allows rotation about a single axis perpendicular to their common plane. The position of the scissor hinge on the bars determine the type of the scissor unit such as translational, polar or angulated scissor unit (Figure 3.1).

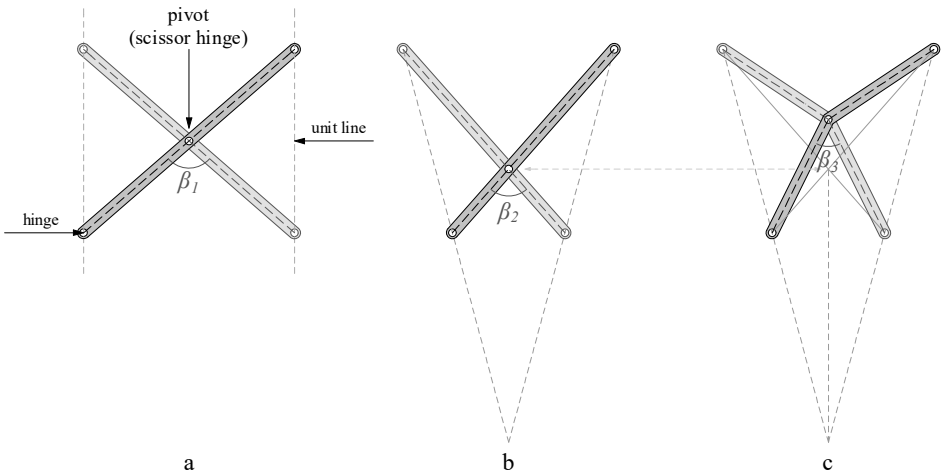

Figure 3.1. Basic scissor units a) Translational unit, b) Polar unit, c) Angulated unit (β1, β2, and β3 are deployment angles) (Reproduced from: Maden, Korkmaz, and Akgün, 2011)

*Unit line*s are imaginary lines which extend along the upper-end point of a bar and the bottom end point of the other bar. Scissor units vary according to the position of the scissor hinge and dimensions of the bars. Thus, unit lines can stay parallel to each other or intersect at one point. Each of the scissor units is characterized by its geometric properties.

3.2. General Deployability Condition

This section is concerned with explaining the geometric characteristics in order to explain the deployability conditions of scissor linkages to transform from compact (stowed) to open (deployed) configurations. The configuration of compact shape for scissor linkages brings the scissor linkage the capability of being stored. Ideally, the scissor units in compact shape should be concurrent in a line-segment form. In Figure 3.2 B_0, C_0, A_1, B_1, C_1, A_2, B_2, C_2, A_3, B_3, and C_3 will be collinear in the stowed configuration. The distance between C_1B_1 can be found by applying the cosine law to $C_1A_0B_1$ and $C_1A_1B_1$ triangles:

$$|C_1B_1| = a_i^2 + b_i^2 - 2a_ib_icos(\gamma_i) = a_{i+1}^2 + b_{i+1}^2 - 2a_{i+1}b_{i+1}cos(\gamma_{i+1}) \tag{3.1}$$

In the stowed configuration $\gamma_i = \gamma_{i+1} = \pi$ so Eq. (3.2) reduces to:

$$a_i + b_i = a_{i+1} + b_{i+1} \tag{3.2}$$

This equation is derived by Escrig (1985) for foldability of planar scissor structural linkages. It reveals that the sum of the lengths of bars on both sides of the unit line should be equal to each other. This equation can only be applied to translational and polar scissor units that are formed by straight bars.

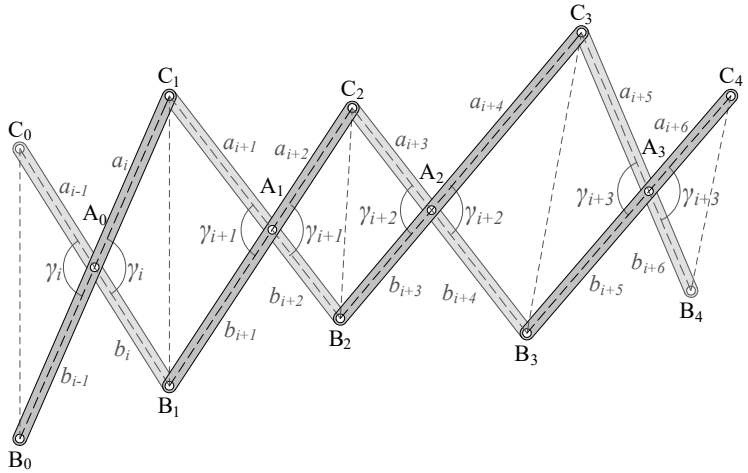

Figure 3.2.. Diagrammatic of scissor linkage
(Reproduced from: Maden, Korkmaz, and Akgün, 2011)

3.3. Geometric Properties of Quadrilateral Loops

A quadrilateral is defined as a particular geometric shape with four sided polygons which is composed of four points (a.k.a. vertices) orderly joined by straight line segments (a.k.a. sides). There are three classifications of quadrilaterals (Leonard, Lewis, Liu & Tokarsky, 2014): convex, simple and nonsimple (Figure 3.3). Whether convex or concave, if the sides of a quadrilateral do not cross each other, it is called a simple quadrilateral. A quadrilateral with intersecting sides is nonsimple quadrilateral (Figure 3.3).

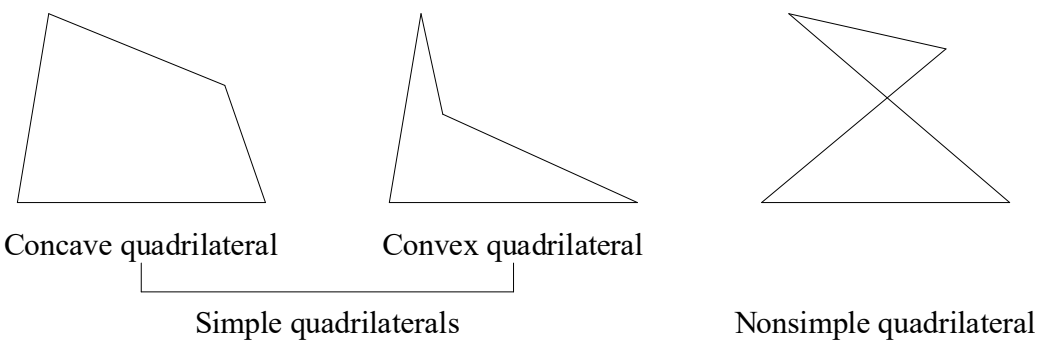

Figure 3.3. Classification of quadrilaterals
(Reproduced from: Leonard, Lewis, Liu & Tokarsky, 2014)

The most regular quadrilateral is named as the square. A square is a quadrilateral with all sides, and interior angles are equal. Interior angles sum up to 360° in a

quadrilateral, so all interior angles of a square are 90°. An equiangular quadrilateral is called a rectangle. All angles are equal to 90°. A rhombus is defined as an equilateral quadrilateral with all sides equal to each other (Usiskin, Z., Griffin, J., Witonsky, D., & Willmore, E. 2008).

In all mentioned quadrilaterals, square, rectangle, or rhombus' sides are parallel. When the opposite sides of a quadrilateral are parallel, it is known as a parallelogram.

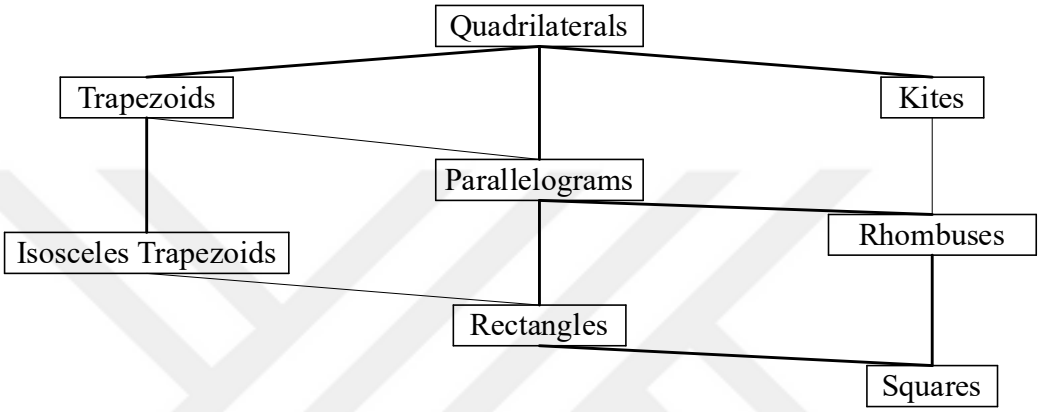

Figure 3.4. Hierarchies of simple quadrilaterals
(Source: Usiskin, Griffin, Witonsky, & Willmore, 2008)

A quadrilateral which has two pairs of adjacent sides of equal length is called as a kite (Figure 3.5.). In the special case where all four sides are the same length, the kite satisfies the definition of a rhombus. One of the two diagonals (q) divides the kite into two isosceles triangles, and the other one (p) divides into two congruent triangles (symmetry axis) as illustrated in Figure 3.5. The symmetry axis is also the bisector of opposite angles. Two opposite angles that are located on opposite sides of the axis of symmetry are equal to each other (angles at C and D in Figure 3.5) (Usiskin, et. al. 2008).

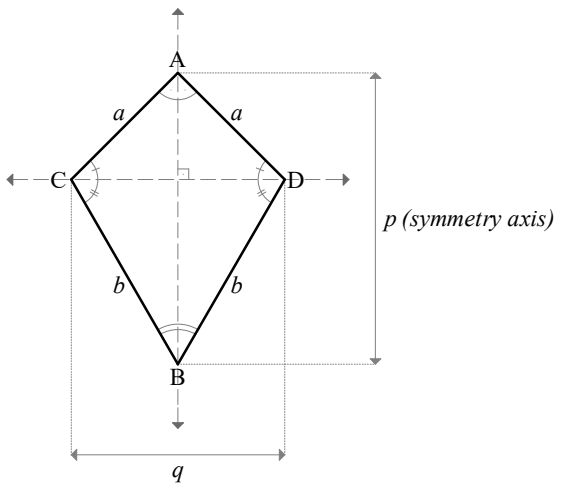

Figure 3.5. A kite, showing its pairs of equal length sides, the axis of symmetry and bisector of opposite angles (Reproduced from: Usiskin, et. al. 2008)

The geometrical form of the kite may be either convex and concave (Figure 3.6). The word "kite" generally represents the convex form (Figure 3.6.a). When the kite is concave, it is referred to as a "dart" (Figure 3.6.b). Kite and dart are examples of quadrilaterals with perpendicularly crossing diagonals. A square and a rhombus also have perpendicularly crossing diagonals (Usiskin, et. al. 2008).

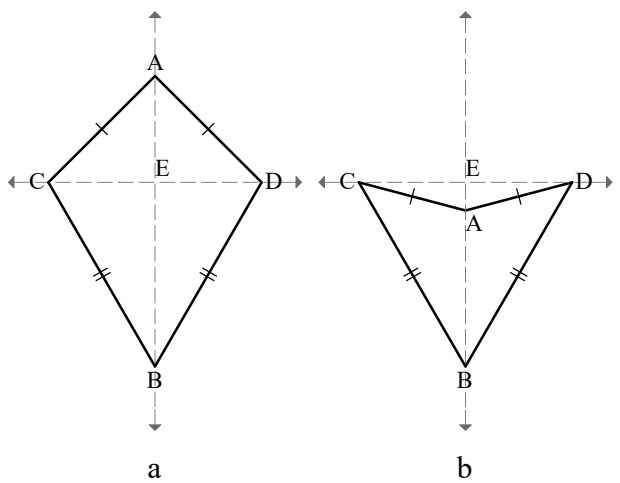

Figure 3.6. a) Convex kite b) concave kite, is referred to as a dart (Reproduced from: Usiskin, et. al. 2008)

3.4. Analysis of Scissor Linkages

In this section, scissor linkages consist of basic scissor units are investigated. The geometrical conditions of scissor linkages are examined. Also, the loop types of scissor linkages are analyzed.

3.4.1. Translational Scissor Units

Translational scissor units, also called rectilinear units, consist of two straight rods connected by a scissor hinge. In order to provide a translational movement, unit lines must be parallel to each other during deployment and stowed process, which is the most specific characteristics of the translational units. As the deployment angle β (Maden, Korkmaz, and Akgün, 2011) changes the translational unit deploys accordingly, which means the distance t changes.

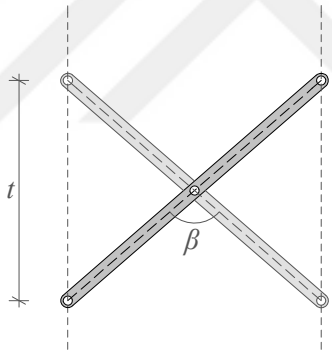

Figure 3.7. Translational scissor unit (β is deployment angle)

According to the De Temmerman (2007) there are two types of translational scissor units that are plane and curved translational units. The curved translational scissor unit is the version of plane translational unit with different semi lengths. So, in this thesis we only consider one translational unit.

There are different types of translational units varying with the location of scissor hinge and size of rods.

3.4.1.1. Translational Scissor Linkages with Identical Rhombus Loops

The first type translational scissor linkage consists of translational scissor units with *2l* bar lengths with equal partial lengths. The resulting translational linkage makes a rectilinear movement. This type of translational linkage is the basic scissor linkage known as lazy-tong mechanism (De Temmerman, 2007). Unit lines always keep parallel to each other during the deployment. The condition of this type scissor linkage mechanism could be formulized as (Maden, Korkmaz, and Akgün, 2011):

$$|B_0A_1| = |A_1C_1| = |C_0A_1| = |A_1B_1| = \ldots = |A_5C_5| = |C_4A_5| = |A_5B_5| = l \qquad (3.3)$$

When we observe the linkage in the deployed configuration, it is seen that loops of the linkage are identical rhombi (Figure 3.8).

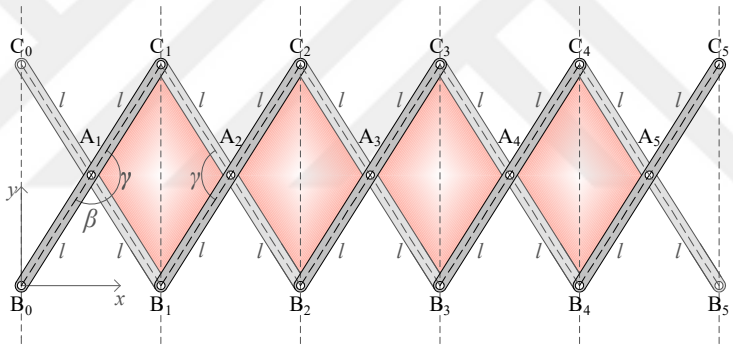

Figure 3.8. Translational linkage with identical bars
(Reproduced from: Maden, Korkmaz, and Akgün, 2011)

It is observed that loops of the linkage occur by translating a rhombus along one direction (Figure 3.9). The translational scissor unit with equal lengths are obtained because the side lengths of a rhombus are equal to *l*. The summation of collinear sides of two rhombi (for example C_1A_2 and A_2B_2; B_1A_2 and A_2C_2) is equal to one bar length of the scissor unit (2*l*) as illustrated in Figure 3.9.

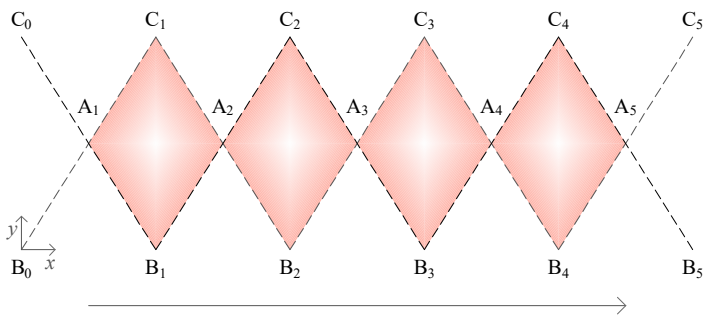

Figure 3.9. Identical rhombus loops of a translational scissor linkage

3.4.1.2. Translational Scissor Linkages with Identical Parallelogram Loops

The second type of translational linkage consist of scissor units with different partial lengths (l_1+l_2). During the deployment process of the translational scissor linkage the unit lines that pass through the axes of hinges remain parallel to each other. The condition of this type of scissor linkage can be formulized as (Maden, Korkmaz, and Akgün, 2011):

$$|C_0A_1| = |A_1B_1| = |C_1A_2| = |A_2B_2| = \ldots = |C_4A_5| = |A_5B_5| = l_1 \tag{3.4}$$

$$|B_0A_1| = |A_1C_1| = |B_1A_2| = |A_2C_2| = \ldots = |B_4A_5| = |A_5C_5| = l_2 \tag{3.5}$$

When we examine the linkage it is observed that the loops of the linkage are identical parallelogram loops in the deployed configuration (Figure 3.10).

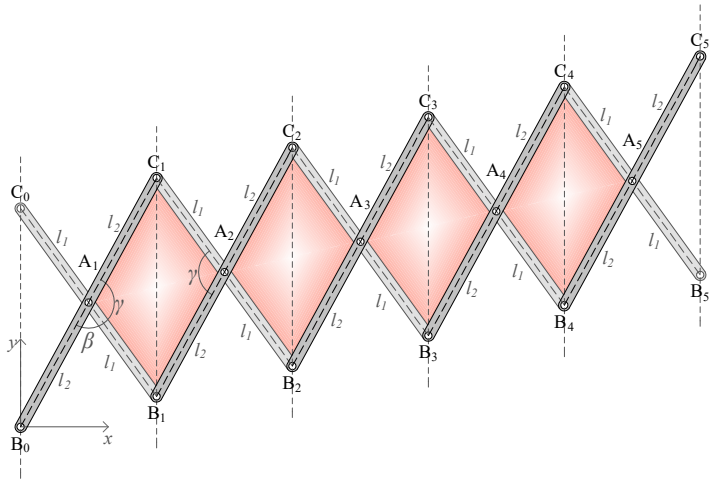

Figure 3.10. Translational linkage with different bars and with scissor hinges at their midpoint (Reproduced from: Maden, Korkmaz and Akgün, 2011)

Clearly, loops of the linkage are obtained by translating a parallelogram along a line. The summation of short sides (l_1) (for example C_1A_2 and A_2B_2) of two parallelograms is equal short bar length ($2l_1$) of the scissor unit while the summation of the long sides (l_2) (for example B_1A_2 and A_2C_2) of two parallelograms is equal the long bar length ($2l_2$) of the scissor unit as can be seen from Figure 3.11.

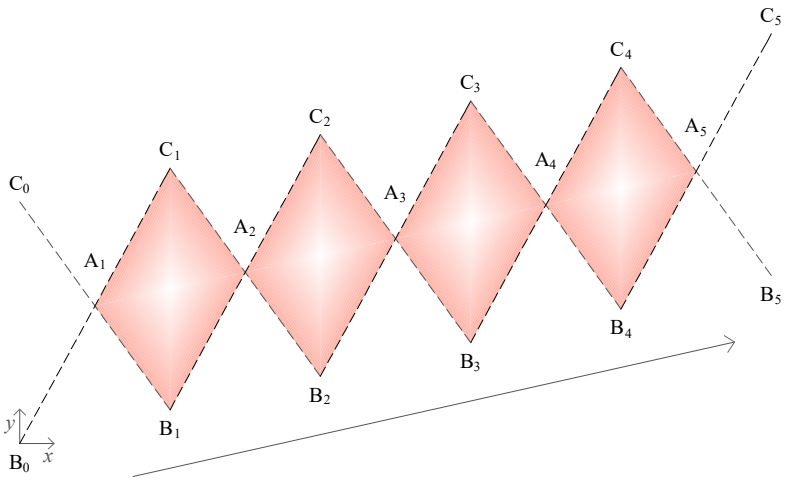

Figure 3.11. Identical parallelogram loops of translational scissor linkage

3.4.1.3. Translational Scissor Linkages with Identical Kite Loops

The third type of translational linkage is formed by assembling translational scissor unit with different bar lengths, with its reflected one. During the deployment process unit lines of the linkage remain parallel to each other. The condition of this type scissor linkage can be formulized as (Maden, Korkmaz, and Akgün, 2011):

$$|C_0A_1| = |A_1B_1| = |B_1A_2| = |A_2C_2| = \ldots = |C_4A_5| = |A_5B_5| = l_1 \tag{3.6}$$

$$|B_0A_1| = |A_1C_1| = |C_1A_2| = |A_2B_2| = \ldots = |B_4A_5| = |A_5C_5| = l_2 \tag{3.7}$$

The linkage is formed by assembling one translational scissor unit with an identical reflected one. It is observed that the loops of the linkage are identical kite loops in the deployed configuration (Figure 3.12).

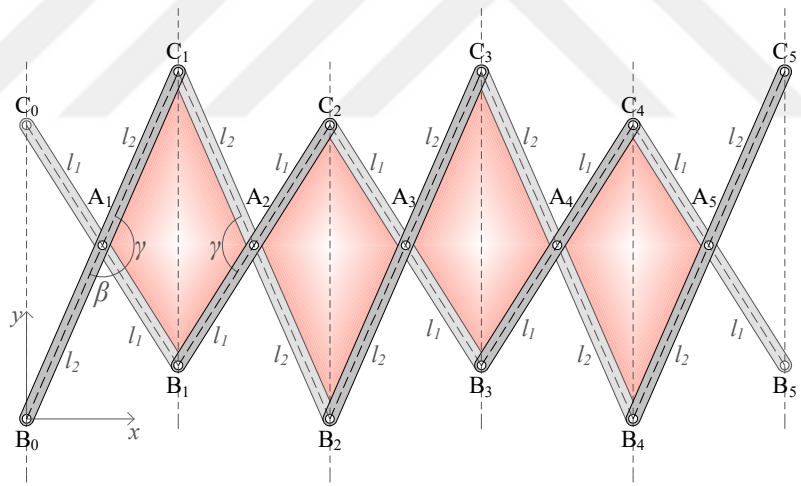

Figure 3.12. Translational linkage with different bars and with scissor hinges at their midpoints (Reproduced from: Maden, Korkmaz, and Akgün, 2011)

Loops of the linkage are obtained by glide-reflection operation (combination of translation and reflection) of a kite loop along a line (Figure 3.13). The summation of long sides of two adjacent kites (l_2) (for example C_1A_2 and A_2B_2) is equal to the long bar length ($2l_2$) of the scissor unit while the summation of the short sides (l_1) (for example B_1A_2 and A_2C_2) of two adjacent kites is equal to the short bar length ($2l_1$) of the scissor unit as can be seen in Figure 3.13.

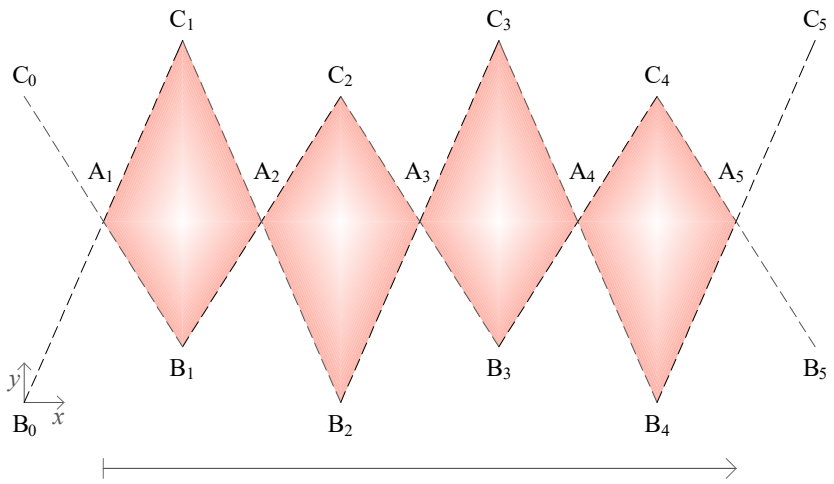

Figure 3.13. Identical kite loops of translational scissor linkage

3.4.1.4. Translational Scissor Linkages with Arbitrary Rhombus Loops

The fourth type of translational linkage is formed by assembling different translational scissor units. During the deployment process unit lines of the linkage remain parallel to each other. The condition for this type of linkage can be written as (Maden, Korkmaz, and Akgün, 2011):

$$|B_0A_1| = |C_0A_1| = l_0,\ |A_1B_1| = |A_1C_1| = |B_1A_2| = |C_1A_2| = l_1,\ \dots,$$
$$|A_4B_4| = |A_4C_4| = |B_4A_5| = |C_4A_5| = l_4,\ |A_5B_5| = |A_5C_5| = l_5 \tag{3.8}$$

When the linkage that is formed by different translational scissor units is examined, it is observed that the loops of the linkage are different kite loops in the deployed configuration.

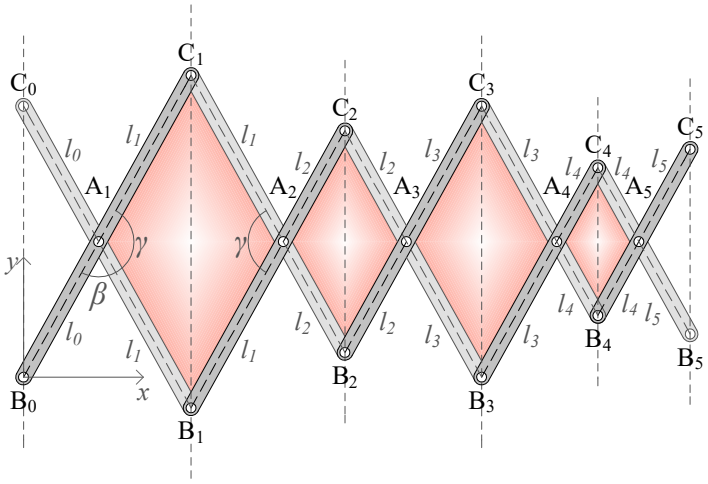

Figure 3.14. Translational linkage with arbitrary bar lengths and with scissor hinges eccentrically placed (Reproduced from: Maden, Korkmaz and Akgün, 2011)

It can be observed that the linkage can be obtained by assembling rhombi with different side lengths but identical interior angles along a line. The summation of the collinear sides (for example C_1A_2 and A_2B_2) of two rhombi gives a bar length of a scissor unit (Figure 3.15). Different rhombi can form a translational scissor linkage as long as unit lines remain parallel to each other.

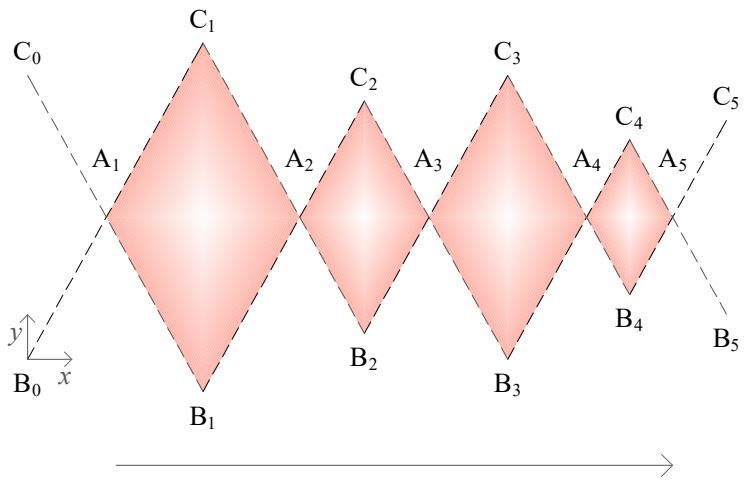

Figure 3.15. Different rhombus loops of translational scissor linkage

3.4.2. Polar Scissor Units

If the unit lines of a scissor unit are no longer parallel to each other and all intersect at the same point, a polar scissor unit is obtained. It is possible to obtain circular motion with polar scissor units.

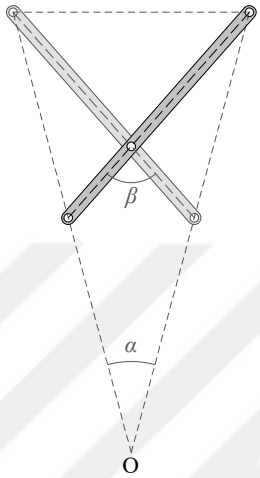

Figure 3.16. Polar scissor unit

A polar scissor unit is obtained by joining two straight bars in mirror symmetry with an eccentric scissor hinge. Eccentric hinge means that the hinge is not at the midpoints of the bars. A linkage with a polar scissor unit makes a circular movement with variable curvature. However, the curvature changes slightly during the motion while the subtended angle changes drastically. Unit lines intersect at a center while the segment angle α varies while the linkage deploys (Figure 3.16). The middle hinges of the scissor units are on a concentric circle at a specific instant during the deployment process. The loops of the deployed polar scissor linkage are kite loops. According to the sizes of polar units, loops can form different kites.

Different polar units are obtained by varying the location of scissor hinges and sizes of the rods.

3.4.2.1. Polar Scissor Linkages with Identical Kite Loops

The first type of polar linkage consists of scissor units with two identical straight bars with the eccentric hinge on them. The result of connecting identical polar units is a

scissor linkage that can make a circular movement by uniformly changing its curvature. As the characteristics of a polar scissor linkage suggest, all unit lines intersect at a specific point. The deployability condition of this scissor linkage can be formulized as (Maden, Korkmaz, and Akgün, 2011):

$$\frac{|A_1B_0|}{|A_1C_1|}=\frac{|A_1B_1|}{|A_1C_0|}=\frac{|A_2B_1|}{|A_2C_2|}=\frac{|A_2B_2|}{|A_2C_1|}=\ldots=\frac{|A_5B_4|}{|A_5C_5|}=\frac{|A_5B_5|}{|A_5C_4|} \tag{3.9}$$

The bars are identical; therefore (Maden, Korkmaz, and Akgün, 2011):

$$|C_0A_1| = |A_1C_1| = |C_1A_2| = |A_2C_2| = \ldots = |C_4A_5| = |A_5C_5| = l_1 \tag{3.10}$$

$$|B_0A_1| = |A_1B_1| = |B_1A_2| = |A_2B_2| = \ldots = |B_4A_5| = |A_5B_5| = l_2 \tag{3.11}$$

When the linkage is examined, it is observed that each loop of the linkage are identical kite loops in the deployed configuration (Figure 3.17).

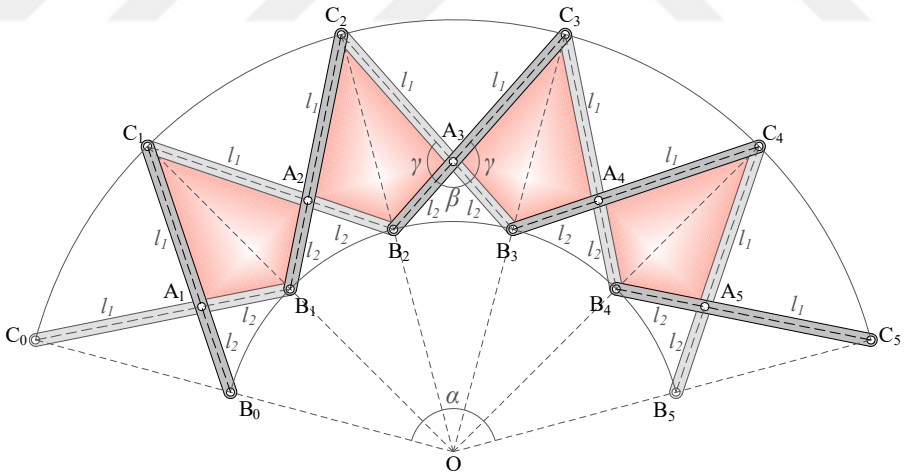

Figure 3.17. Linkage formed by polar units with identical bars and with scissor hinges eccentrically placed (Reproduced from: Maden, Korkmaz, and Akgün, 2011)

It is observed that, when a kite loop is duplicated by rotating about a center point, these kites create the loops of the scissor linkage formed by identical polar scissor units (Figure 3.18). The summation of collinear sides of two kite loops (for example C_1A_2 and

A_2B_2) give the total side length of a bar (l_1+l_2) of the scissor unit (Figure 3.18). Thus, scissor linkage formed by identical polar scissor units is obtained.

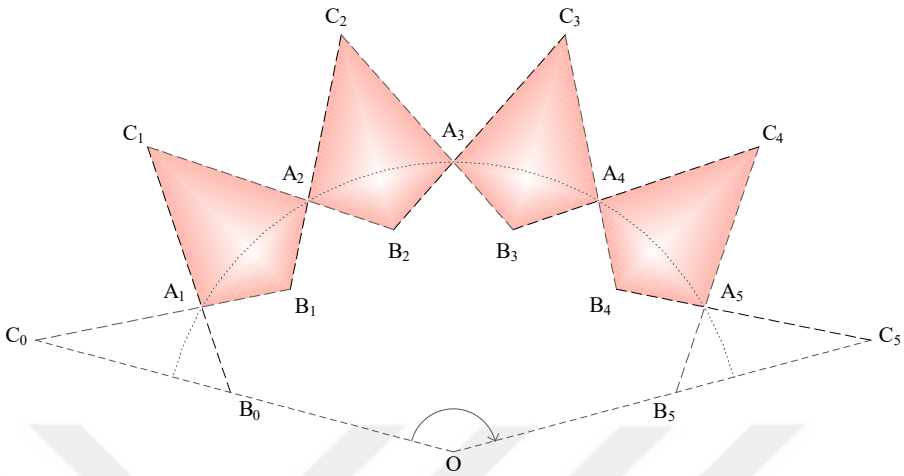

Figure 3.18. Identical kite loops of polar scissor linkage

3.4.2.2. Polar Scissor Linkages with Arbitrary Kite Loops

The second type of polar linkage consists of different polar scissor units that have different straight bars with eccentric hinges on them. Although the lengths of bars can vary, the sum of the lengths of both sides of the unit line should be equal to each other (Eq. 3.13). The result of connecting different polar units is a scissor linkage that can make a circular movement with uniformly changing curvature. The condition of this type scissor structural mechanism can be formulized as (Maden, Korkmaz, and Akgün, 2011):

$$\frac{|A_1B_0|}{|A_1C_1|} \neq \frac{|A_1B_1|}{|A_1C_0|} \neq \frac{|A_2B_1|}{|A_2C_2|} \neq \frac{|A_2B_2|}{|A_2C_1|} \neq \ldots \neq \frac{|A_5B_4|}{|A_5C_5|} \neq \frac{|A_5B_5|}{|A_5C_4|} \tag{3.12}$$

$$|C_0A_1| = l_0,\ |B_0A_1| = l_1,\ |A_1C_1| = |C_1A_2| = l_2,$$
$$|A_1B_1| = |B_1A_2| = l_3,\ \ldots,\ |A_5C_5| = l_{10},\ |A_5B_5| = l_{11} \tag{3.13}$$

When the linkage is examined in the deployed configuration, it can be seen that the loops of the linkage are different kites (Figure 3.19).

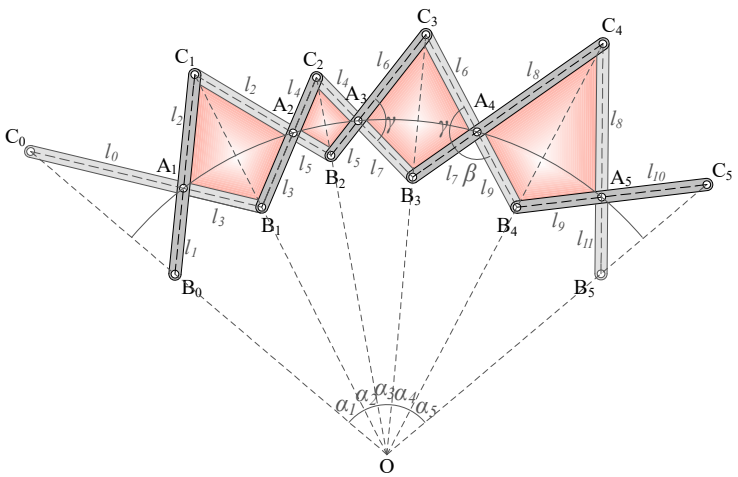

Figure 3.19. Linkage formed with arbitrary polar units and mid-scissor hinges eccentrically placed (Reproduced from: Maden, Korkmaz, and Akgün, 2011)

It can be deduced that, when different kite loops are duplicated by rotating about a center point, these kites create the loops of the scissor linkage formed by different polar scissor units (Figure 3.20). The summation of collinear sides of two kite loops (for example C_1A_2 and A_2B_2) give the total side length of a bar of the scissor unit (Figure 3.15). Thus, scissor linkage formed by different polar scissor units is obtained.

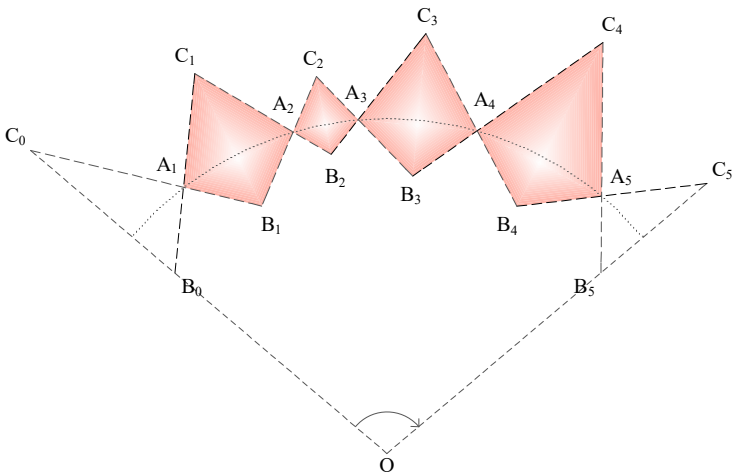

Figure 3.20. Different kite loops of polar scissor linkage

3.4.3. Angulated Scissor Units

Angulated unit comprises of two angulated bars which have a kink with an angle instead of straight bars. While translational and polar units have linear and circular deployment respectively, angulated scissor units are capable of making radial deployment about a center. Angulated scissor unit was first discovered by Chuck Hoberman in 1990 (Hoberman, 1990). Hoberman's angulated unit comprise two angulated bars that have equal kink angles ($\psi = \varphi$) (Figure 3.21a).

In addition to Hoberman's angulated scissor unit, You and Pellegrino (1997) discovered *generalized angulated elements* (*GAEs*) that are *Equilateral Angulated Element* (*AE*) (Type I) and *Similar AE* (Type II). These elements, as well as Hoberman's symmetrical angulated element, subtend a constant angle during folding.

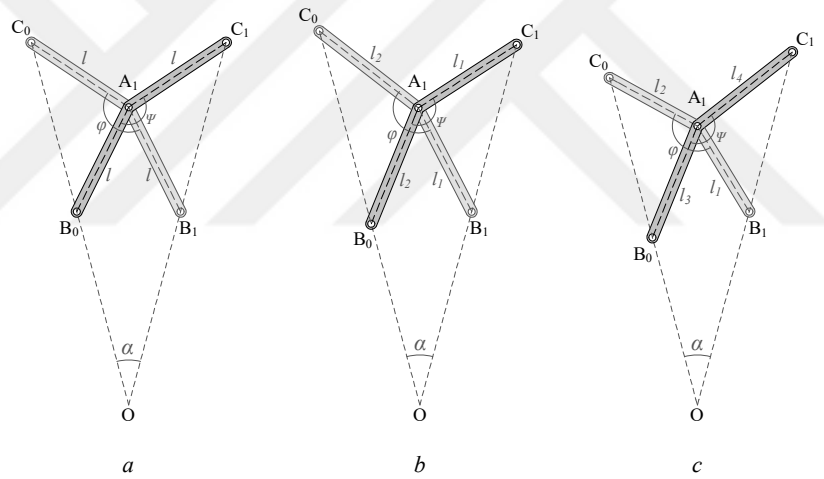

Figure 3.21. Angulated Scissor Units a) Hoberman's Symmetrical AE (φ=ψ), b) Type I Equilateral AE (φ≠ψ) and c) Type II Similar AE (φ=ψ and $l_1/l_4=l_2/l_3$)

The relationship between kink angles and segment angle can be demonstrated in Eq. 3.14 (You and Pellegrino, 1997):

$$\alpha = 180° - \left(\frac{\varphi + \psi}{2}\right) \tag{3.14}$$

While translational and polar units have linear and circular deployment respectively, angulated scissor units are capable of making radial deployment about a center with a uniformly varying curvature. The hinges of the linkage lie on concentric

circles at a specific instant during the deployment. The segment angle (α) between two unit lines of an angulated scissor unit remains constant during the deployment whereas it varies in polar units (Jensen, 2004).

The first type of angulated unit is the Hoberman's symmetrical AE (Figure 3.21a). It is obtained by connecting two identical isosceles angulated bars, and they have equal kink angles:

$$|A_1B_0| = |A_1\,C_1| = |A_1B_1| = |A_1C_0| \tag{3.15}$$

$$\varphi = \Psi \tag{3.16}$$

The segment angle α always remains constant. The relationship between segment angle and the kink angles is given by:

$$\alpha = 180^{o} - \Psi = 180^{o} - \varphi \tag{3.17}$$

Hoberman (1990, 1991) has shown that the above derivation can be extended to nonsymmetrical angulated elements, which are still made of identical angulated rods. It satisfies the following conditions (You and Pellegrino, 1997):

$$|A_1B_0| = |A_1\,C_0| \text{ and } |A_1B_1| = |A_1C_1| \tag{3.18}$$

$$\varphi = \Psi \tag{3.19}$$

The second type of angulated units is Equilateral AE (Figure 3.21b) formed by angulated rods with equal semi-length but not necessarily equal kink angles. It satisfies the following conditions (You and Pellegrino, 1997):

$$|A_1B_0| = |A_1C_0| \tag{3.20}$$

$$|A_1B_1| = |A_1C_1| \tag{3.21}$$

$$\varphi \neq \Psi \tag{3.22}$$

Although kink angles are different, the segment angle always remains constant. The relationship between segment angle and kink angles is indicated as (You and Pellegrino, 1997):

$$\alpha = 180° - \frac{\Psi + \varphi}{2} \tag{3.23}$$

The third type of angulated units is the Similar AE (Figure 3.21c) formed by angulated rods with proportional semi-lengths and having equal kink angles. Deployability condition for this type of unit is (You and Pellegrino, 1997):

$$\frac{|A_1B_0|}{|A_1C_0|} = \frac{|A_1C_1|}{|A_1B_1|} \tag{3.24}$$

$$\varphi = \Psi \tag{3.25}$$

The segment angle always remains constant. The relationship between segment angle and kink angles is indicated in Equation 3.26:

$$\alpha = 180° - \Psi = 180° - \varphi \tag{3.26}$$

3.4.3.1. Angulated Scissor Linkages with Identical and Similar Rhombus Loops

The first type of angulated scissor linkage consists of identical angulated bars with equal semi-lengths and equal kink angles, that is Hoberman's Symmetrical AEs. The result of connecting identical angulated units is a scissor linkage that can make a radial movement by uniformly varying curvature. As the characteristics of angulated scissor linkage, all unit lines intersect at a point. The geometrical condition of this scissor linkage can be formulized as (Maden, Korkmaz, Akgün, 2011):

$$|A_1B_0| = |A_1C_0| = |A_1B_1| = |A_1C_1| = |A_2C_1| = |A_2B_1| = \ldots = |A_5B_5| = |A_5C_5| = l \tag{3.27}$$

When the linkage that is formed by identical isosceles angulated scissor units is examined, it is observed that the loops of the linkage are identical kite loops in the deployed configuration (Figure 3.22).

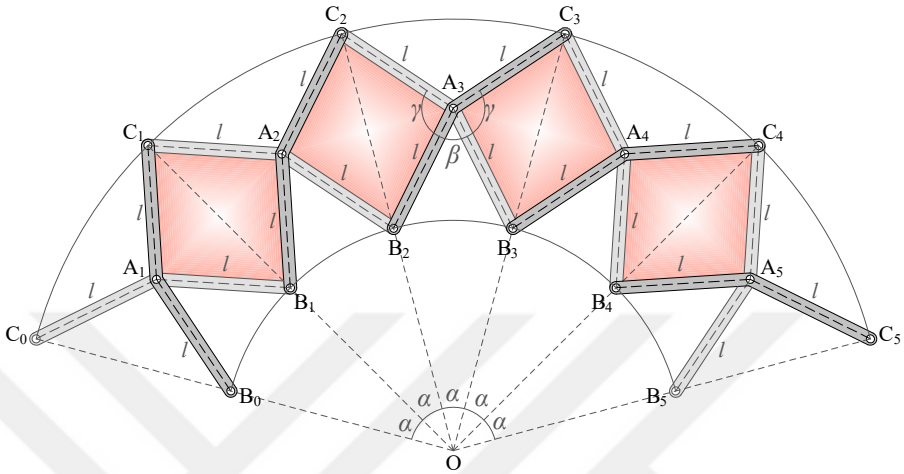

Figure 3.22. Partial radially deployed closed ring scissor linkage with angulated units (Reproduced from: Maden, Korkmaz, Akgün, 2011)

It is observed that, when a rhombus loop is duplicated by rotating about a center point (Figure 3.23), these rhombi create the loops of the scissor linkage formed by identical angulated scissor units. The two sides of two adjacent rhombus loops (for example C_2A_2 and A_2B_1) constitutes an angulated bar of the scissor unit (Figure 3.23). Thus, scissor linkage formed by identical angulated scissor units is obtained.

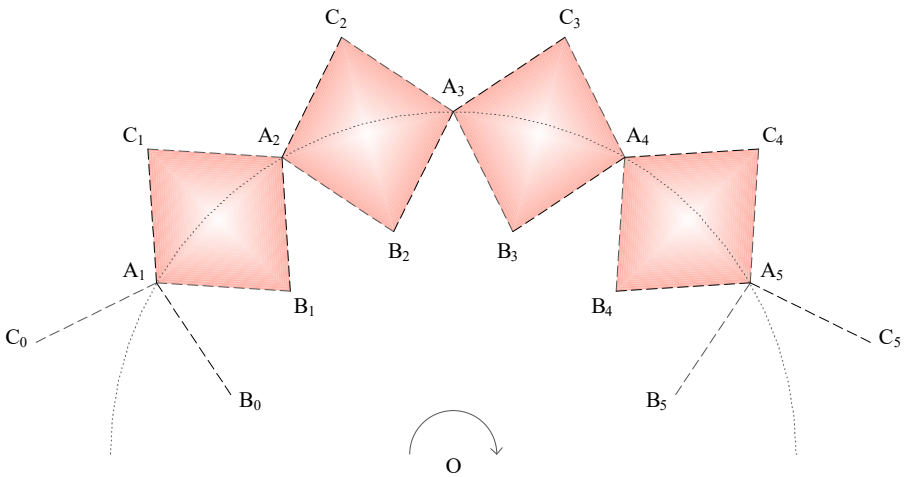

Figure 3.23. Identical rhombus loops forming angulated scissor linkage

The second type of angulated scissor linkage consists of identical angulated bars with the unequal semi-lengths (l_1 and l_2) but equal kink angles, which is a more general form of Hoberman's angulated unit. The result of connecting identical angulated units is a scissor linkage that can make a radial movement by uniformly varying curvature. Once again, all unit lines intersect at a point. The geometrical condition of this scissor linkage can be formulized as:

$$\begin{aligned}|A_1B_0| = |A_1C_0| = |A_2B_2| = |A_2C_2| = |A_3B_2| = |A_3C_2| = \ldots \\ = |A_5B_4| = |A_5C_4| = l_1\end{aligned} \tag{3.28}$$

$$|A_1B_1| = |A_1C_1| = |A_2B_1| = |A_2C_1| = \ldots = |A_5B_5| = |A_5C_5| = l_2 \tag{3.29}$$

When the linkage that is formed by identical angulated scissor units is examined, it is observed that the loops of the linkage are similar kite loops with same interior angles in the deployed configuration (Figure 3.24).

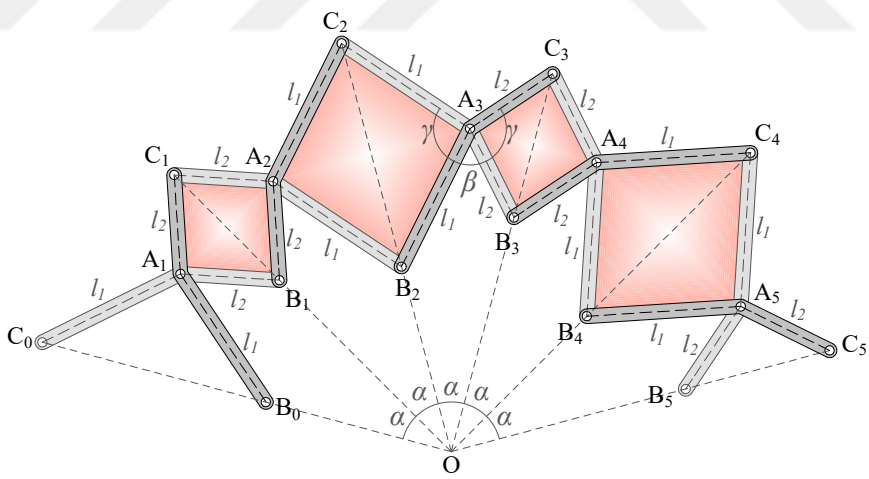

Figure 3.24. Radially deployed scissor linkage with angulated units

It is observed that, when two similar rhombus loops (such as rhombus $A_1B_1A_2C_1$ and rhombus $A_2B_2A_3C_2$) are duplicated by rotating about a center point (Figure 3.25), these rhombi create the loops of the scissor linkage formed by identical angulated scissor units with unequal semi-lengths. The two sides of two adjacent rhombus loops (for

example C_2A_2 and A_2B_1) constructs an angulated bar of the scissor unit (l_1+l_2) (Figure 3.25). Thus, scissor linkage formed by identical angulated scissor units is obtained.

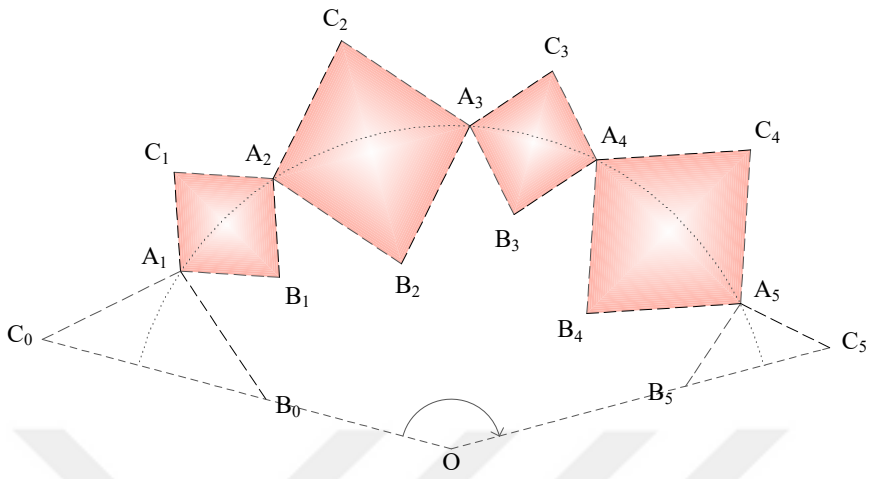

Figure 3.25. Similar rhombus loops forming angulated scissor linkage

3.4.3.2. Angulated Linkages with Different Rhombus Loops

The third type of angulated scissor linkage consists of identical equilateral AEs. The linkage makes a radial movement with a uniformly varying curvature with respect to the center point. The geometric properties of this scissor linkage can be formulized as:

$$|A_1B_1| = |A_1C_1| = |A_2B_1| = |A_2C_1| = |A_3B_3| = |A_3C_3| = |A_4B_3| = |A_4C_3| = l_1 \quad (3.30)$$

$$|A_1B_0| = |A_1C_0| = |A_2B_2| = |A_2C_2| = |A_3B_2| = |A_3C_2| = |A_4B_4| = |A_4C_4| = l_2 \quad (3.31)$$

For the linkage that is constructed by equilateral AEs, segment angles of all units would be the same and remain constant during the motion of the linkage. When the linkage is examined, it is observed that the loops of the linkage composed of two different rhombi in the deployed configuration (Figure 3.26).

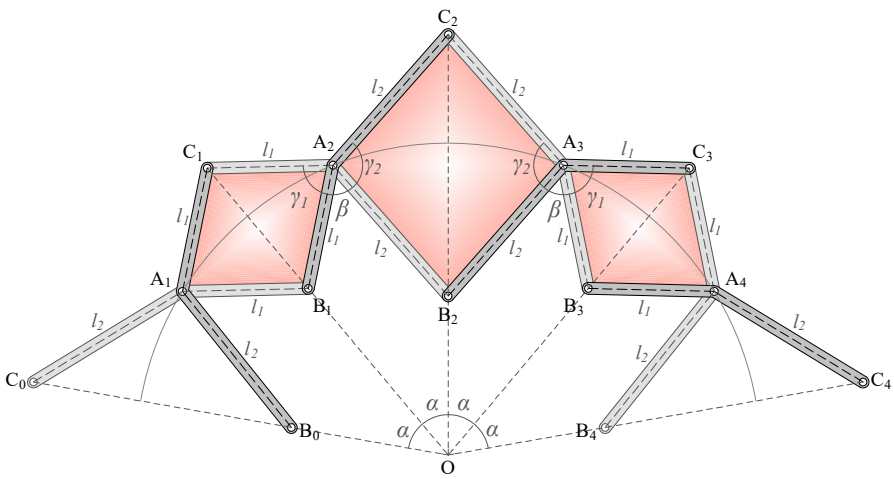

Figure 3.26. Assembly of one type of Equilateral AEs

It is observed that, when two different rhombi are duplicated by rotating about a center point (Figure 3.27), these rhombi create the loops of the scissor linkage formed by Equilateral AEs. The two sides of two adjacent rhombus loops (for example C_2A_2 and A_2B_1) constitutes an angulated bar of the scissor unit. Thus, scissor linkage formed by identical equilateral AEs is obtained.

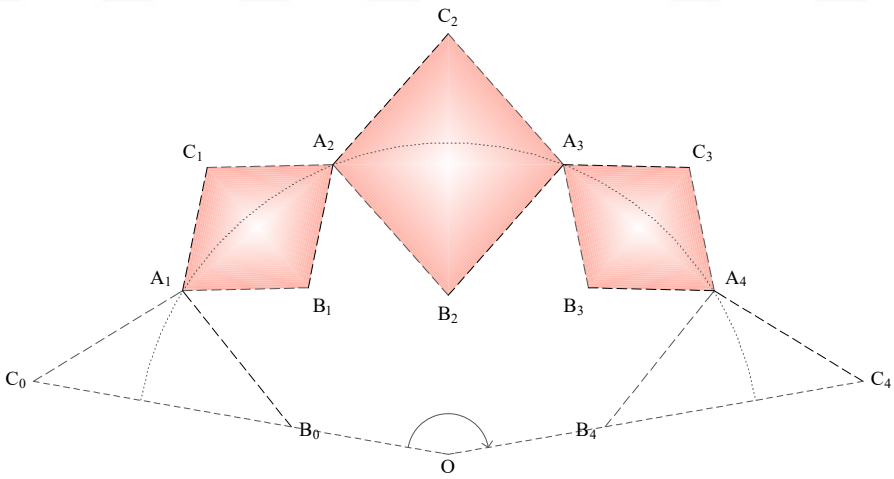

Figure 3.27. Different rhombus loops forming angulated scissor linkage

The fourth type of angulated scissor linkage consists of different Equilateral AEs. The linkage makes a circular movement with a constant curvature with respect to the center point. Because there is more one type of Equilateral AEs forming the linkage unit lines intersect at different points as defining a circle. The geometrical condition of this scissor linkage can be formulized as:

$$|A_1B_0| = |A_1C_0| = l_1,\ |A_1B_1| = |A_1C_1| = |A_2B_1| = |A_2C_1| = l_2,$$
$$|A_2B_2| = |A_2C_2| = |A_3B_2| = |A_3C_2| = l_3, \tag{3.32}$$

If we use different Equilateral AEs with different partial lengths and different kink angles (Figure 3.28), segment angle of all units would be different. However, for each unit, the segment angle remains constant during the deployment process. Thus, the sum of the segment angles also remains constant that is expressed in equation 2.34 (You and Pellegrino, 1997):

$$\alpha_{sum} = \alpha_1 + \alpha_2 + \alpha_3 + \ldots + \alpha_n \tag{3.33}$$

When the linkage is examined, it is observed that the loops of the linkage composed of more than two different rhombi in the deployed configuration (Figure 3.28).

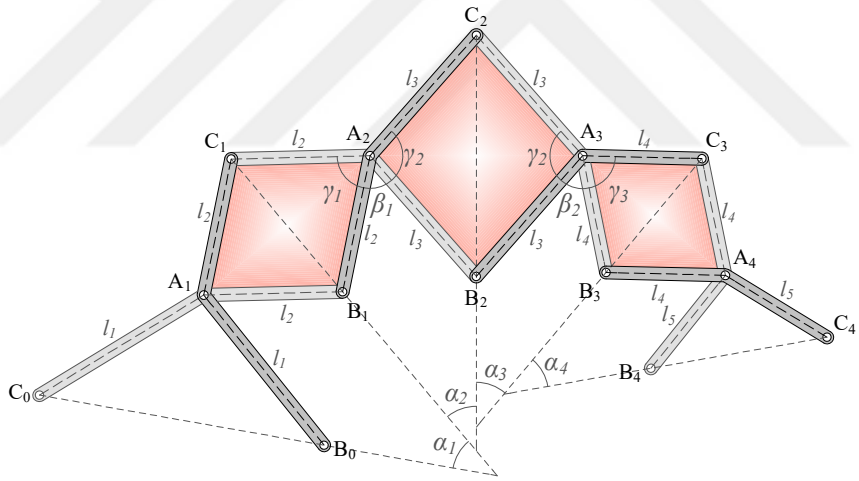

Figure 3.28. Assembly of Equilateral AEs with unequal semi-length
(Reproduced from: You & Pellegrino, 1997))

It is observed that, when different rhombi are multiplied respectively by rotating according to one point (Figure 3.29), they create the loops of the scissor linkage formed by different Equilateral AEs. The summation of transverse sides of two rhombus loops (for example C_2A_2 and A_2B_1) give the total side length of one angulated bar of the one scissor unit. Thus, scissor linkage formed by different Equilateral AEs is obtained.

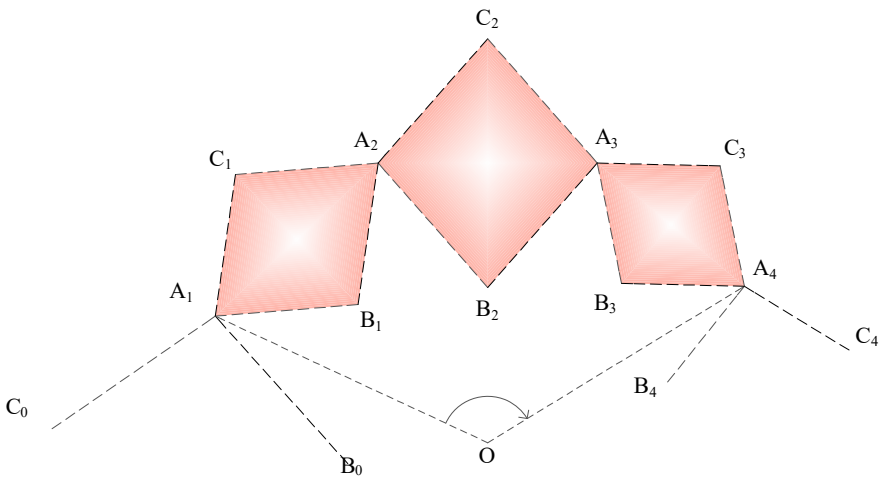

Figure 3.29. Assembly of various rhombus loops forming angulated scissor linkage

While in Figure 3.27 the linkage consists of two types of rhombi with various corner angles, in Figure 3.29 the loops of the linkage are different rhombi. To sum up, we can obtain angulated scissor linkage formed by Equilateral AEs by assembling rhombus loops that are rotated on the arc of the circumference. There can be two or more different rhombus loops.

3.4.3.3. Angulated Scissor Linkages with Identical and Similar Parallelogram Loops

The fourth type of angulated scissor linkage consists of identical, similar AEs. The linkage makes a radial movement with constant curvature with respect to the centre point. Because there is one type of Similar AE forming the linkage unit lines intersect at different point as defining a circle. The deployability condition of this scissor linkage can be formulized as:

$$\frac{|A_1B_0|}{|A_1C_0|}=\frac{|A_1C_1|}{|A_1B_1|}=\frac{|A_2B_1|}{|A_2C_1|}=\frac{|A_2C_2|}{|A_2B_2|}=\frac{|A_3B_2|}{|A_3C_2|}=\frac{|A_3C_3|}{|A_3B_3|}=\ldots=\frac{|A_5B_4|}{|A_5C_4|}=\frac{|A_5C_5|}{|A_5B_5|} \tag{3.34}$$

For the linkage that is constructed by identical Similar AEs, segment angles of all units would be the same and remain constant during the motion of the linkage. When the linkage is examined it is observed that the loops of the linkage composed of identical parallelograms in the deployed configuration (Figure 3.30).

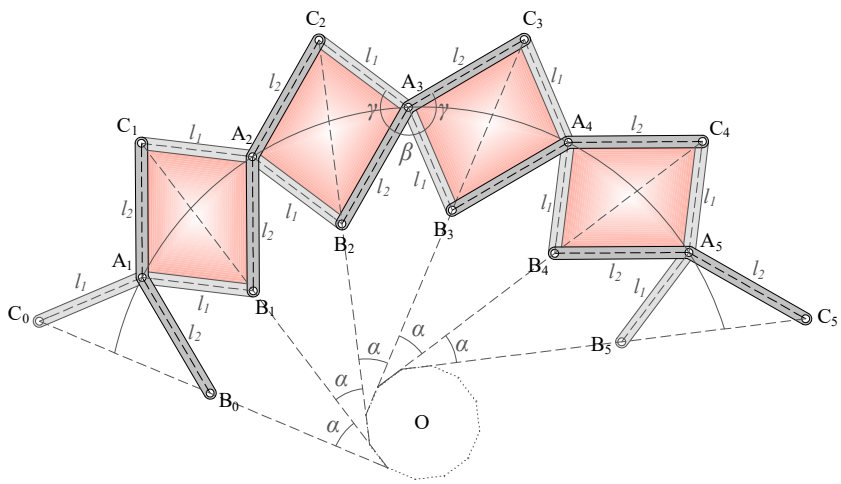

Figure 3.30. Assembly of identical Similar generalized angulated elements

It is observed that, when one parallelogram loop is multiplied by rotating according to one center point of the rotation (Figure 3.31), these rhombi create the loops of the scissor linkage formed by identical angulated Similar AEs. With the identical parallelogram loops, there is only one type of Similar AE exist. The summation of transverse sides of two rhombus loops (for example C_2A_2 and A_2B_1) give the total side length of one angulated bar of the scissor unit (Figure 3.31). Thus, scissor linkage formed by identical Similar AEs is obtained.

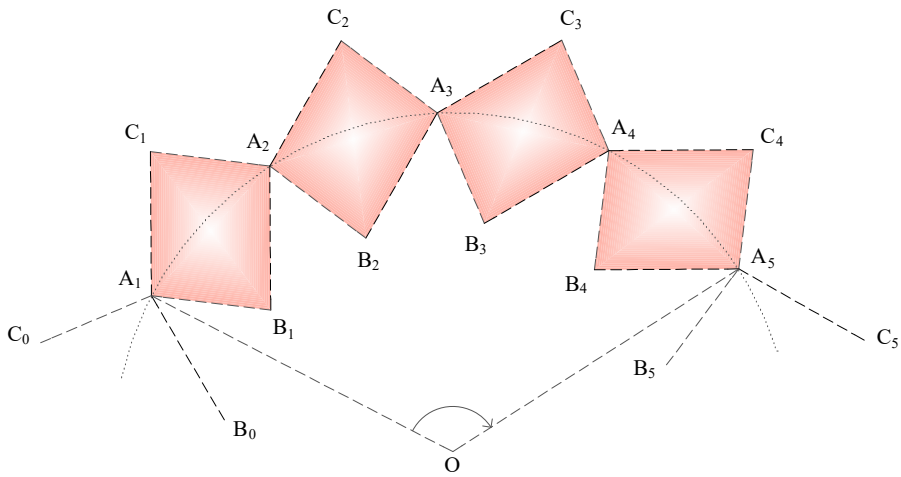

Figure 3.31. Assembly of identical parallelogram loops aligned on arc of a circumference

If we use different Similar AEs, segment angle of all units would be different. But for each unit, the segment angle remains constant during the deployment process. Thus,

the sum of the segment angles also remains constant that is expressed in equation 3.35 (You and Pellegrino, 1997):

$$\alpha_{sum} = \alpha_1 + \alpha_2 + \alpha_3 + \ldots + \alpha_n \tag{3.35}$$

In Figure 3.32 there is one Similar AE with different partial lengths forming the linkage. Thus, it is observed that there are two similar parallelograms with identical interior angles in the deployed configuration of the linkage.

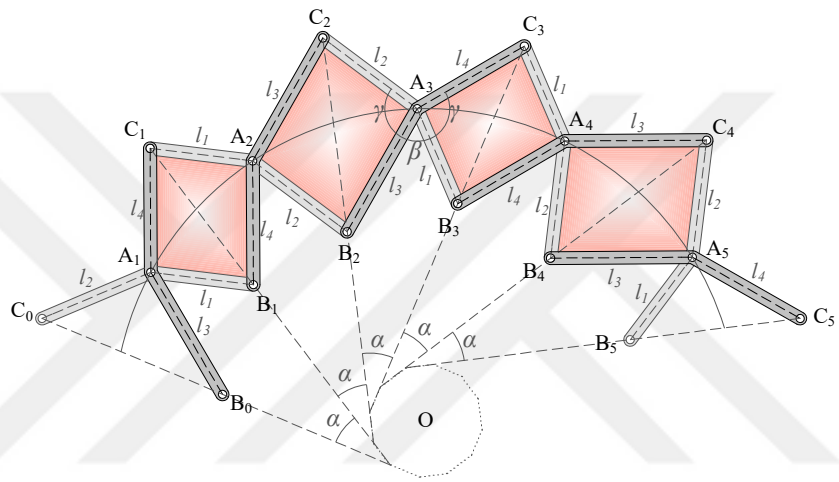

Figure 3.32. Assembly of two different Similar Angulated Elements

It is observed that, when two similar parallelogram loops are multiplied by rotating according to one center point of the rotation (Figure 3.33), these rhombi create the loops of the scissor linkage formed by identical angulated Similar AEs. The summation of transverse sides of two rhombus loops (for example C_2A_2 and A_2B_1) give the total side length of one angulated bar of the scissor unit (Figure 3.33). Thus, scissor linkage formed by Similar AEs is obtained.

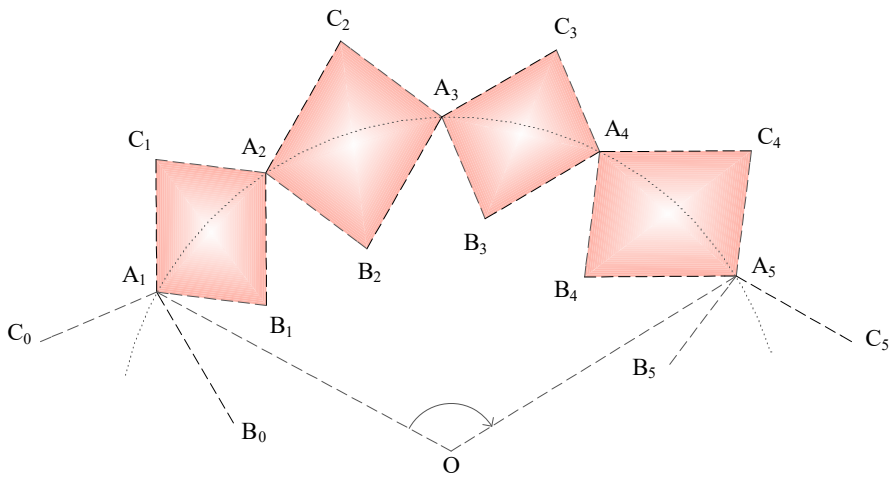

Figure 3.33. Assembly of two different type of parallelogram loops aligned on arc of a circumference

3.5. Conclusion

This chapter first reviews the geometric features of existing scissor units. Then the loop types of scissor linkages are investigated. It is observed that there are three types of loops forming scissor linkages. Those are a parallelogram, rhombus, and kite.

It is important to consider what kind of movement -translational or radial- the linkage has and what kind of scissor unit the structure consists of when connecting the loops to each other.

In order to obtain translational scissor linkages, we can use each of the three types of loops. Rhombuses and parallelograms are assembled end to end to obtain straight rods; while one kite loop must be assembled with its mirror symmetric one in order to get straight rods. Otherwise, angulated rods are obtained instead of straight ones. Because of the identical rods and parallel unit lines, there always be the similar loops in translational scissor linkages. It can be observed that the loops of translational scissor linkages would be parallelograms, rhombuses or kites.

It has been observed that polar scissor linkages are only obtained by assembling kite loops. Deployable structures formed by polar scissor units are capable of making the circular deployment. Therefore, kite loops are duplicated about the center point of rotation in order to obtain a polar scissor linkage. Also, it is important to get straight rods from the assembly of kite loops. Kites can be identical or different.

It has been observed that angulated scissor units are only derived from rhombus or parallelogram loops. According to the foldability conditions of angulated scissor units, loops of the linkage can be identical rhombuses or different rhombuses, identical parallelograms or different parallelograms.

CHAPTER 4

GEOMETRICAL CONSTRUCTION METHOD OF PLANAR ANGULATED SCISSOR LINKAGES

This chapter concentrates on the geometrical construction method of angulated scissor linkages formed by rhombus loops. According to this construction method, it is proved that single DoF deployable scissor linkages can be constructed by using rhombus loops. It reveals that deployable scissor linkages, whose geometry is not only circular (Hoberman, 2013) but also irregular polygonal linkages (Kiper, & Söylemez, 2010), can be obtained with this construction method.

4.1. Loop Assembly Method

All 2D or 3D deployable scissor structures are multi-loops mechanisms. When deployable structures formed by angulated scissor units are investigated, it is observed that the segment angles between unit lines remain constant during the deployment process. In order to obtain constant segment angles, angulated units are assembled to each other in such a way that each loop is a parallelogram or rhombus.

According to the loop analysis of scissor linkages mentioned before, a scissor structural linkage may comprise rhombus, parallelogram or kite loops. In this context, there are some studies about constructing irregular polygonal scissor linkages with rhombus loops (Liao & Li, 2005; Kiper & Söylemez, 2010). Also, in an MIT lecture note, Hoberman (2013) introduces a method for the geometric construction of expanding polygons composed of angulated scissor units. He assembles identical or similar rhombi.

4.1.1. Geometric Construction of Multi-Loop Linkages by Identical Rhombi

Firstly, Hoberman connects identical rhombuses to each other at their corners (Fig. 4.1a). In Figure 4.1b scissor rods are drawn by offsetting the lines to both of the two

sides of the rod axes equally. Thus, a translational scissor structure is obtained with identical rods. The corners where rhombi connect to each other represent the scissor hinge of a scissor unit, while the top and the bottom corners of the rhombi represent revolute joints where scissor units connect to each other. During the motion of the linkage, scissor hinges and other revolute joints of the linkage move on parallel lines. Therefore, the unit lines which are drawn from the top points of the rhombuses to bottom ones, remain parallel during the motion (Fig. 4.1b).

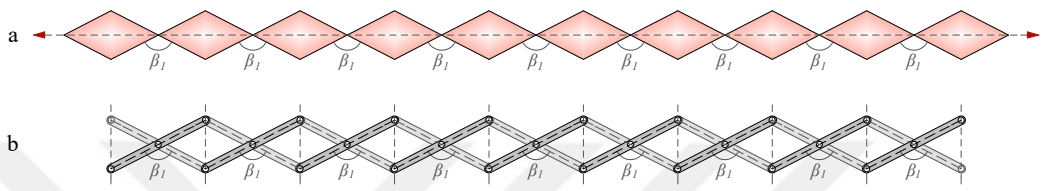

Figure 4.1. Geometric construction of translational linkage with loop assembly method (Reproduced from: Hoberman, 2013)

When identical rhombi are assembled to each other as aligned on the arc of a circle, the deployment angle (β) between rhombi is determined as shown in Figure 4.2a. In this assembly type, the edges of rhombi identify the axes of angulated rods. This assembly mode of rhombi gives us angulated scissor linkage formed by identical angulated scissor units. When we draw unit lines, we can see that they intersect at the center of a circle (Figure4.2b). Scissor hinges and other revolute joints draw concentric circles of variable radius during the motion of the structure.

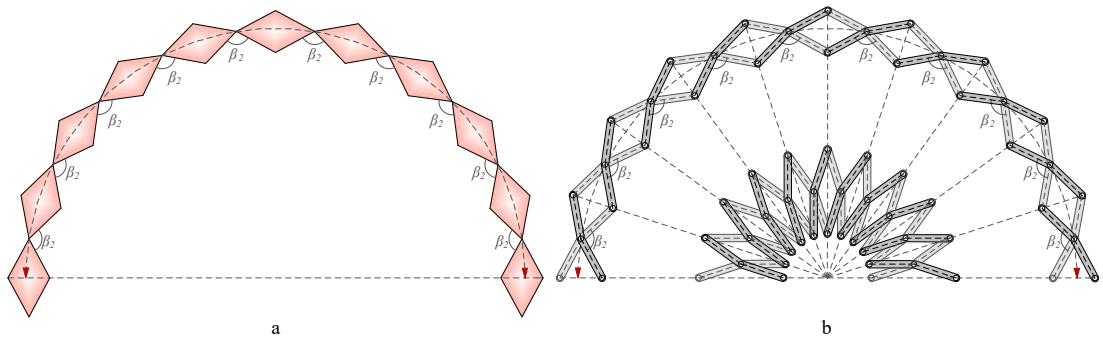

Figure 4.2. Geometric construction of the angulated scissor structure forming a circular arc (Reproduced from: Hoberman, 2013)

In Figure 4.3a identical rhombi are assembled in a way to create a circular multi-loop linkage. In this case, each of the angulated scissor units is identical. Unit lines intersect at the center of the circle (Figure 4.3b and Figure 4.3c).

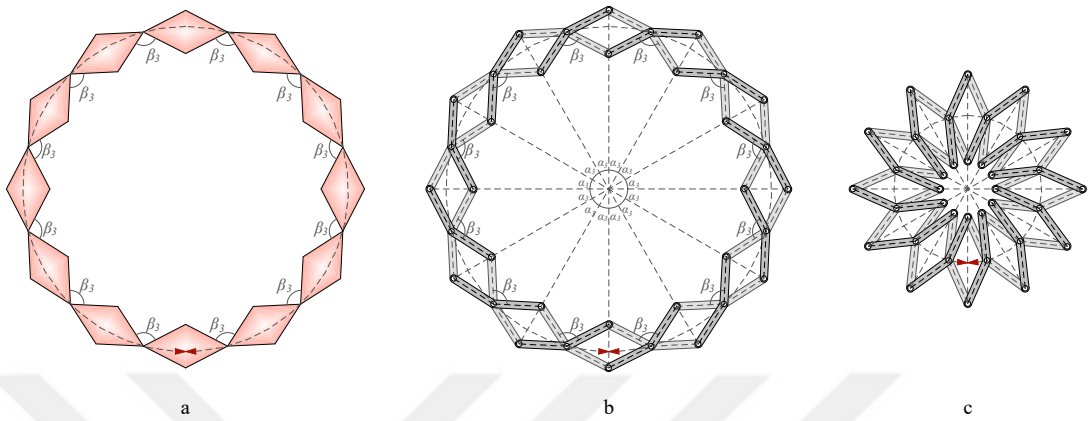

Figure 4.3. Geometric construction of the angulated scissor linkage forming a circle (Reproduced from: Hoberman, 2013)

In Figure 4.4 identical rhombi are assembled in a way to create an elliptical multi-loop structure. In this case, the deployment angle between rhombi is different because an ellipse has non-constant curvature. There are different types of angulated scissor units forming the linkage. There are many points where unit lines intersect because of the different kink angles of angulated units (Figure 4.4b and Figure 4.4c).

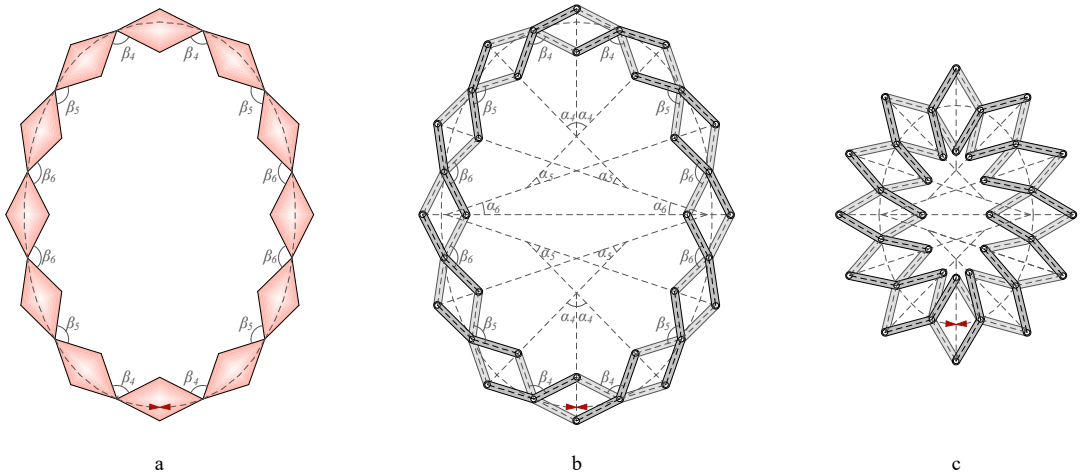

Figure 4.4. Geometric construction of the angulated scissor structure forming ellipse (Reproduced from: Hoberman, 2013)

4.1.2. Geometric Construction of Irregular Expanding Polygons with Similar Rhombi

Generally, for polygonal scissor linkages are expected to deploy keeping the angles and side length proportions of the base polygon. In order to provide dilative transformation, the polygon has to have an inscribing circle, rather than be cyclic (Kiper & Söylemez, 2010). Irregular expanding polygons composed of angulated scissor units can be constructed with the same method explained above.

In Figure 4.5 there are similar rhombi which have equal interior angles but different dimensions. Kink angles of angulated bars for every scissor unit vary because the deployment angles between rhombi are different from each other. In this case, unit lines of angulated scissor units intersect at various points.

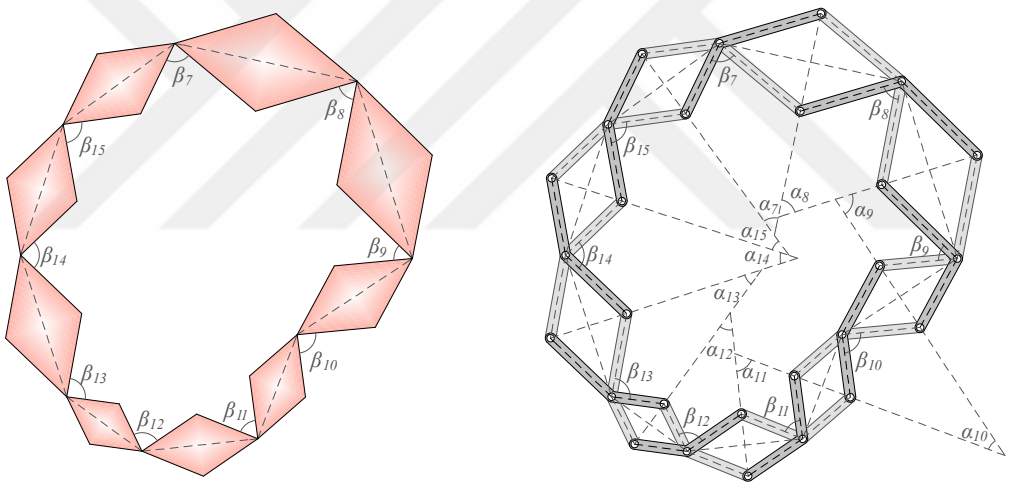

Figure 4.5. Geometric construction of irregular expanding polygon with similar rhombi (Reproduced from: Hoberman, 2013)

It is possible to attach rhombi to each side of the desired polygonal geometry. Rhombi side lengths are half of the scaled polygon sides (Kiper & Söylemez, 2010). According to the deployment angle between rhombi, scissor units can be different such as angulated or translational scissor units. In Figure 4.6 there are two types of scissor units as translational and angulated scissor units.

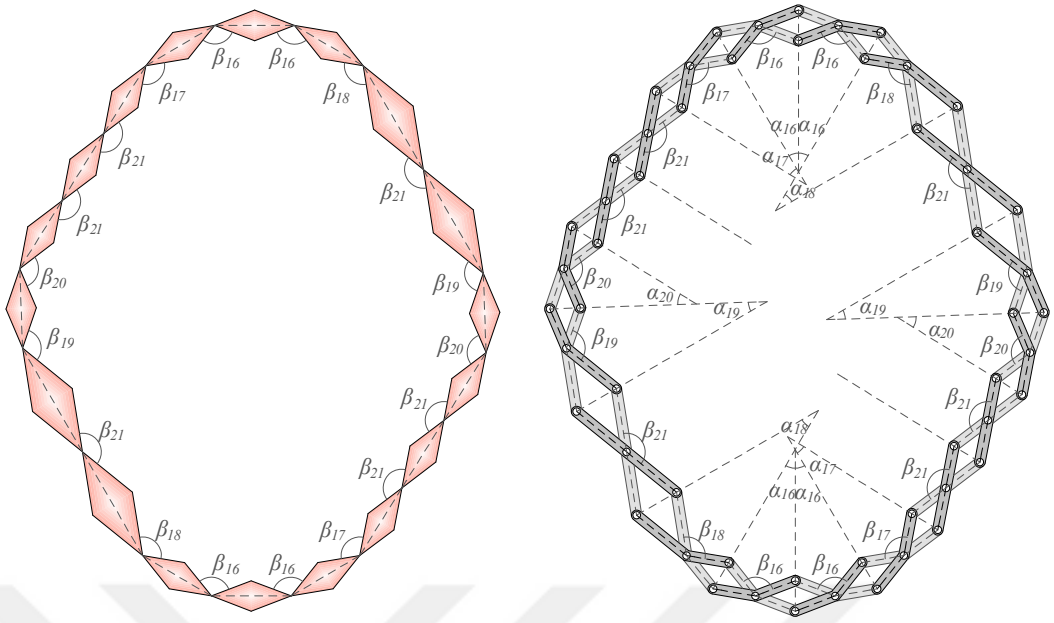

Figure 4.6. Irregular expanding polygon composed of angulated and translational units (Reproduced from: (Hoberman, 2013))

4.2. Conclusion

According to the construction method, only rhombus loops are used. Rhombi can be identical or similar in order to construct a deployable linkage. Circular, polygonal or irregular polygonal geometries can be obtained. It is observed that angulated scissor units and translational scissor units can be obtained by assembling rhombus loops.

CHAPTER 5

ASSEMBLY OF KITE AND DART LOOPS

This Chapter proposes a study of assembly variations of kite and dart loops. When aforementioned studies are taken into, it has been observed that angulated elements can be obtained when kite loops are assembled to each other. In addition to this, dart loops are assembled for the first time to obtain angulated scissor elements. For this purpose, different conditions for assembling kite and dart loops are investigated. Ultimately, a new type of scissor linkage is obtained that can transform between convex and concave configurations.

There are four different conditions for the assembling kite and dart loops. Possible conditions can be listed as follows for two of the kite or dart loops of a system:

1. Short side lengths are equal, long side lengths are equal, and interior angles are equal (identical kite or dart loops)
2. Short side lengths are different and long side lengths are different, but interior angles are equal (similar kite or dart loops)
3. Short side lengths are equal and long side lengths are equal, but interior angles are different (different kite or dart loops)
4. Short side lengths are different and long side lengths are different. Also interior angles are different (different kite or dart loops)

5.1. Assembly of Kite Loops

For the first assembly condition, identical kite loops are assembled in a flat configuration where the symmetry axes are parallel to each other and perpendicular to the x-axis as illustrated in Figure 5.1:

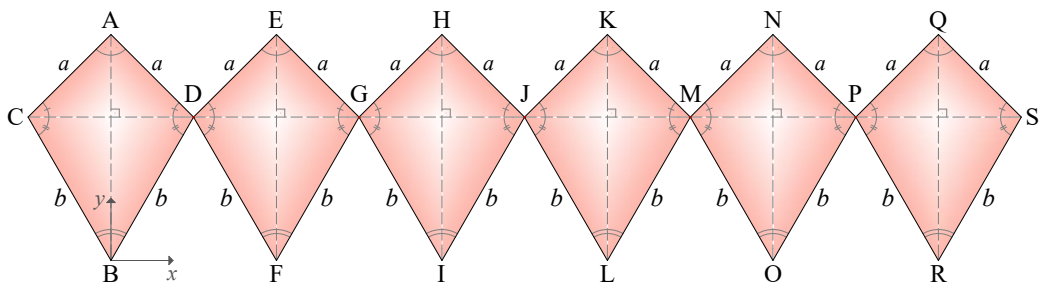

Figure 5.1. Flat configuration of the assembled identical kite loops

Scissor units are detected from the assembly type of the kite loops. It can be observed that there are angulated scissor units generated from the sides of the kite loops (for example |AD| and |DF|, |ED| and |BD|) that define the axes of the angulated bars. An angulated scissor unit resides between two symmetry axes (Figure 5.2). By defining the scissor units, symmetry axes represent unit lines. The connection point of the kite loops (for example point D) determines the scissor hinge of an angulated scissor unit. It is observed that, Hoberman's nonsymmetrical angulated elements are obtained from the assembly of identical kite loops. But the obtained scissor unit (Figure 5.2) is different from the Hoberman's unit. While the Hoberman's unit is obtained from the assembly of similar rhombuses, this new type of angulated unit it is obtained from the assembly of identical kite loops.

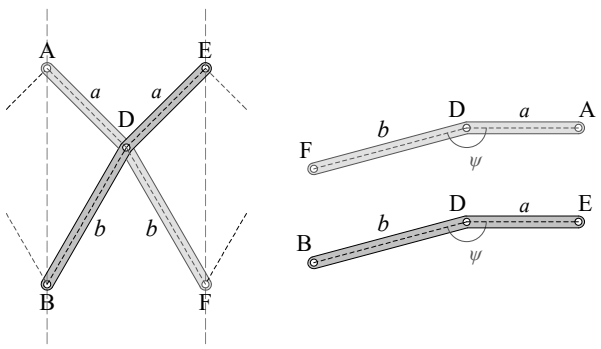

Figure 5.2. Angulated scissor unit with equal semi lengths and kink angles created with identical kites

The scissor linkage composed of mentioned angulated elements is illustrated in flat configuration in Figure 5.3. The point A is assumed as the fixed point of the linkage.

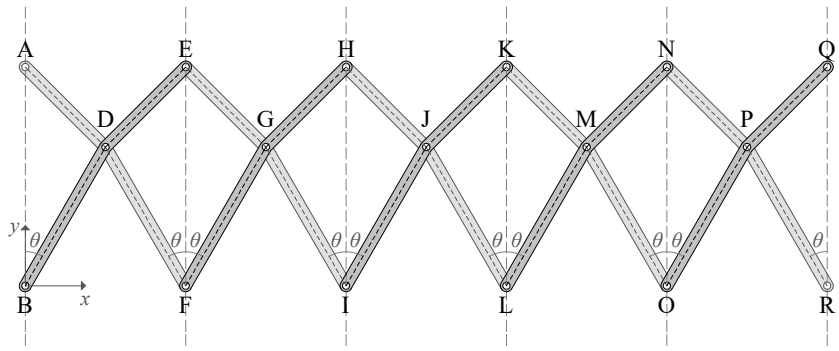

Figure 5.3. Angulated scissor linkage formed by identical kite loops

The new type angulated scissor linkage also was modeled on Solidworks® as illustrated in Figure 5.4 and Figure 5.5. The transformation capability of a single DoF deployable linkage which is constructed by assembling the kite loops is shown. This linkage is investigated under three different situations. For the first situation, the linkage is in the flat configuration. It is seen that unit lines are parallel to each other so the curvature is equal to zero. The second situation is bended upward configuration (Figure 5.4). This is accomplished by moving point B (Figure 5.3) along the y-axis as well as the angle θ of kite loop changes at the same time. After some point, when the loops of the linkage become triangles, if the linkage continues to bend up concave kites become convex kites. The linkage continues bending upward. The third situation is bended downward configuration (Figure 5.5). The angle θ decreases. Loops of the linkage remain as kites. Due to the fact that the segment angles varying during the deployment, center point, which is formed by unit lines intersection, is translated on y-axis. As a result, the radius of curvature changes.

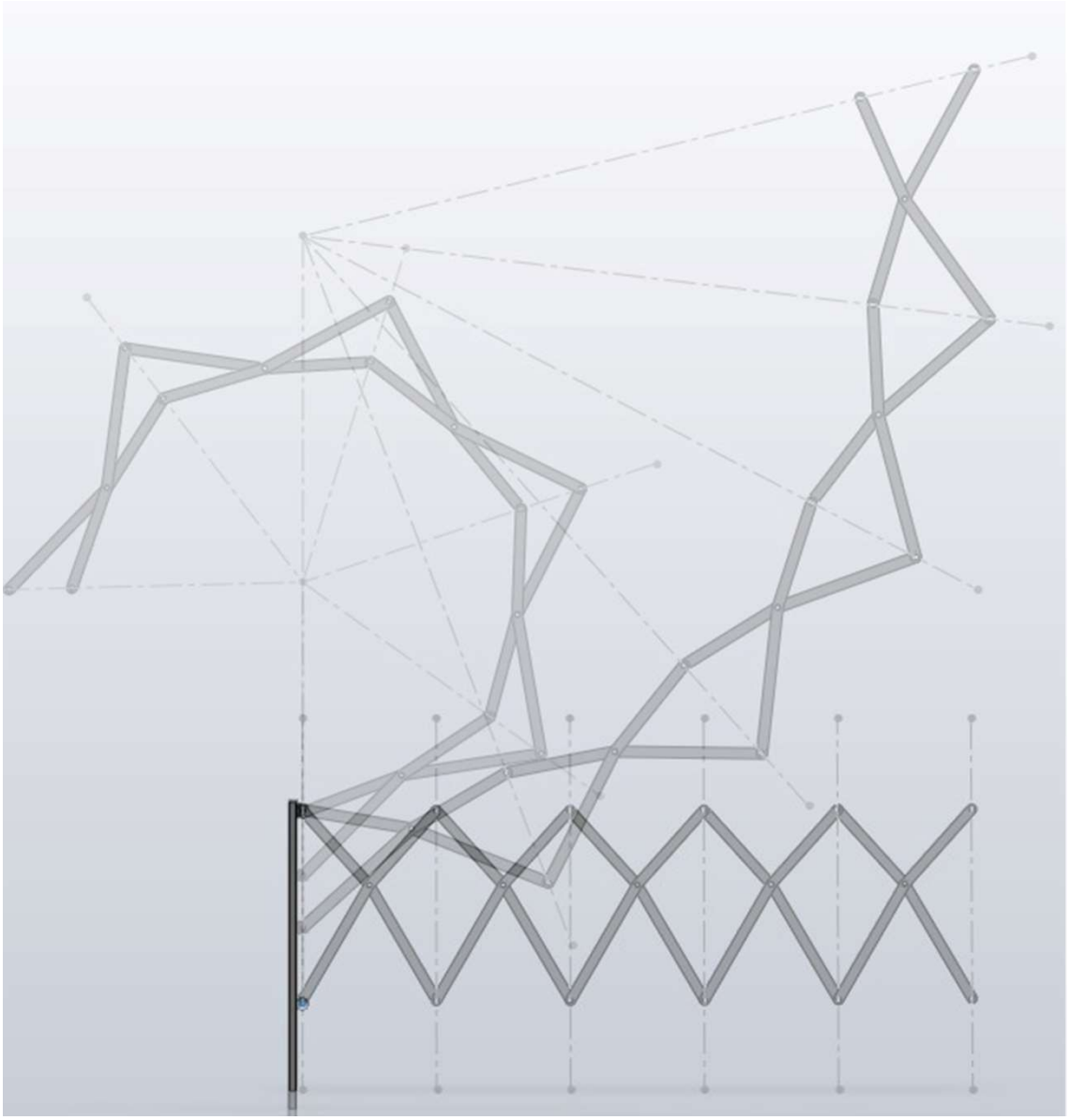

Figure 5.4. The bending upward motion of the linkage modelled on Solidworks

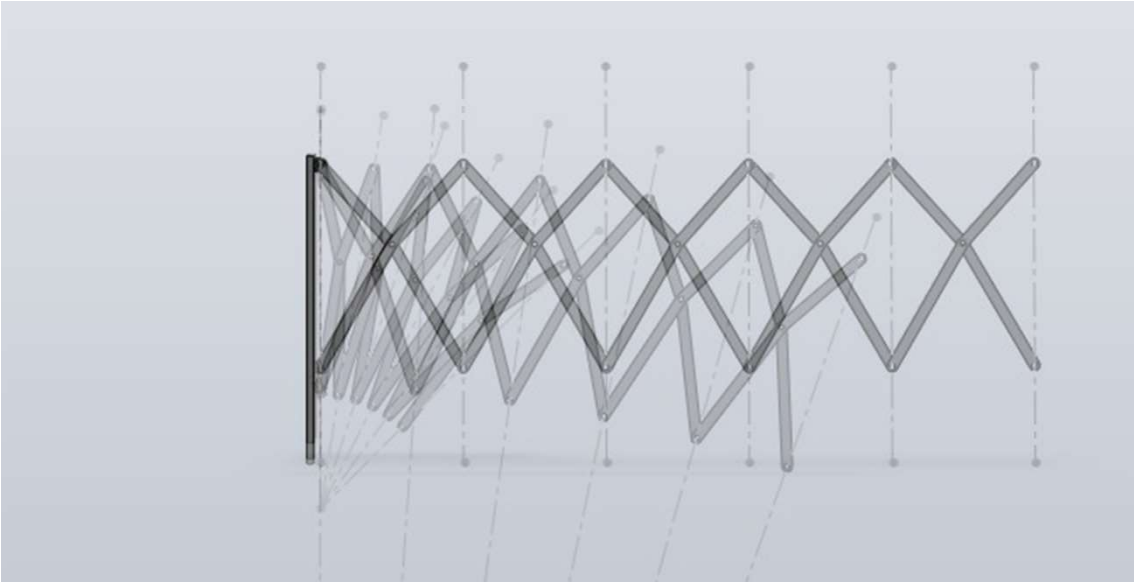

Figure 5.5. The bending downward motion of the linkage modelled on Solidworks

In the second type of assembly, there are two types of kites. Interior angles are equal to each other, but semi lengths are different (Fig. 5.6). As a first step, two kinds of kites are assembled in a flat configuration in a sequence where symmetry axes are parallel to each other and perpendicular to the x-axis.

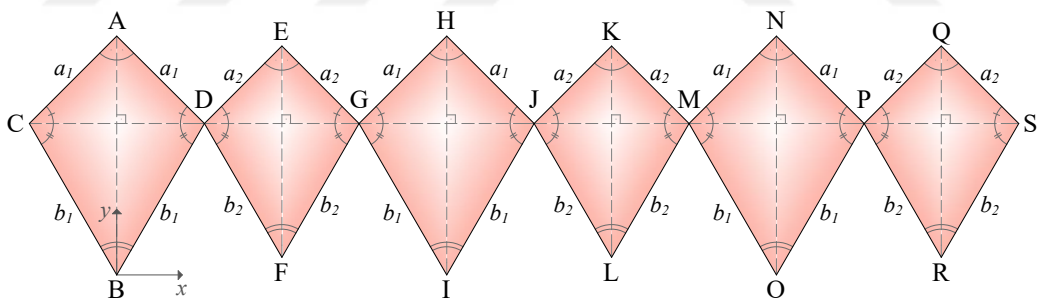

Figure 5.6. Flat configuration of the assembled similar kite loops with identical interior angles but different semi-lengths

After the assembly, angulated scissor unit is detected from the assembly type of the kite loops that have different semi-lengths but equal kink angles. In the second type of assembly, the type of angulated scissor units obtained are different from the first one. Because of the identical interior angles of kites, kink angles of the angulated bars of the scissor unit are equal to each other. But the angulated elements of a scissor unit are different from each other (Figure 5.7). If the proportions of short sides and long sides are equal to each other, similar GAEs are obtained. But the obtained scissor unit (Figure 5.7) is different from the Type II unit. While the Type II unit is obtained from the assembly

of identical or similar parallelograms, this new type of angulated unit it is obtained from the assembly of similar kite loops.

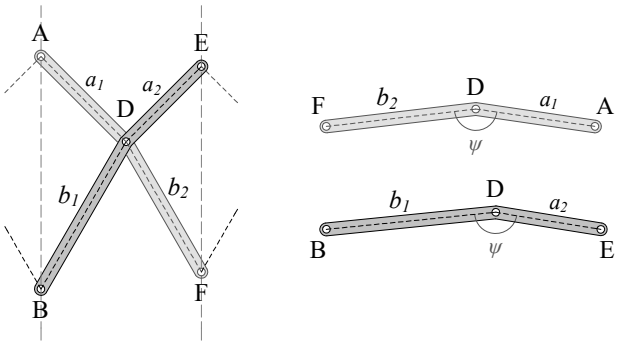

Figure 5.7. Angulated scissor unit with different semi-lengths and equal kink angles created with similar kites

At first, unit lines of angulated scissor units are parallel to each other (Figure 5.8).

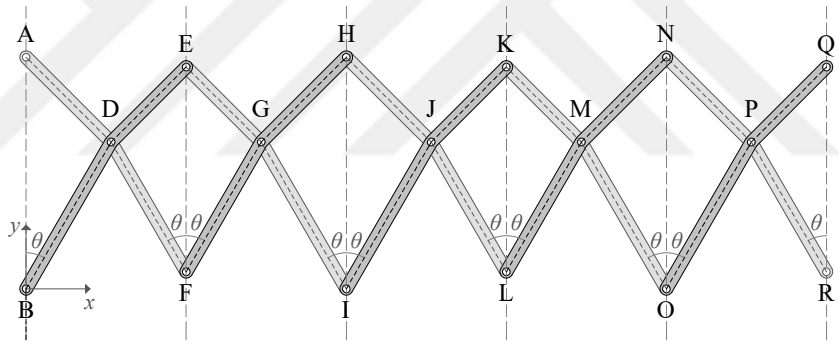

Figure 5.8. Angulated scissor linkage formed by similar kite loops with identical interior angles but different semi-lengths

For the second type of assembly of the kite loops, the obtained angulated scissor linkage has the same transformation capacity as the first one. The linkage transforms between bended upward and bended downward configurations. The center point of the linkage, where the unit lines intersect, moves along the *y*-axis during the motion of the linkage. Thus the curvature of the linkage changes.

According to the third type of assembly, there are two types of kites whose semi-lengths are equal to each other, but interior angles are different (Figure 5.9).

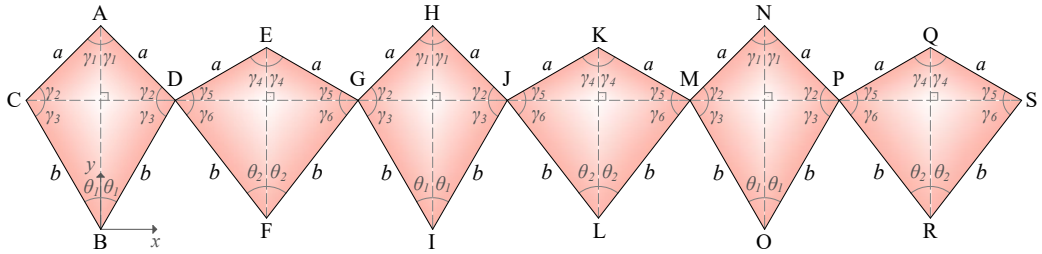

Figure 5.9. Flat configuration of the assembled different kite loops with equal semi-lengths but different interior angles

Considering the assembly of kites in a flat configuration, there exists angulated scissor unit, that has equal semi-lengths but different kink angles (Figure 5.10). Thus, Equilateral GAEs are obtained. But the obtained scissor unit in Figure 5.10 is different from the Type I unit. While the Type I unit is obtained from the assembly of different rhombuses, this new type of angulated unit it is obtained from the assembly of different kite loops.

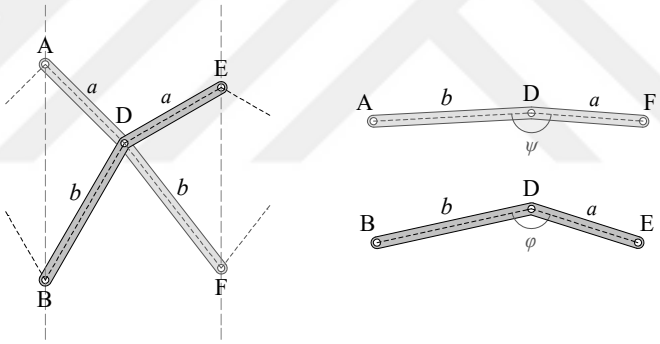

Figure 5.10. Angulated scissor unit with equal semi lengths and different kink angles created with different kites

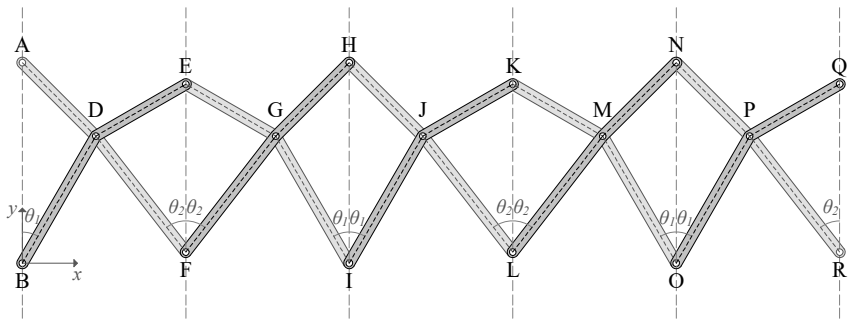

Figure 5.11. Angulated scissor linkage formed by different kite loops with equal semi-lengths but different interior angles

For this assembly, the motion of the linkage has the same transformation capability with previous ones. It can bend up and down. The center point of the linkage, where the unit lines intersect, moves along the *y*-axis during the motion of the linkage. When the linkage bends upward unit lines intersect at the positive side of the *y* axis and when the linkage bends downward unit lines intersect at the negative side of the *y* axis.

In the fourth type of assembly of kite loops, there are two types of kites, not only interior angles but also semi-lengths are different from each other (Figure 5.12).

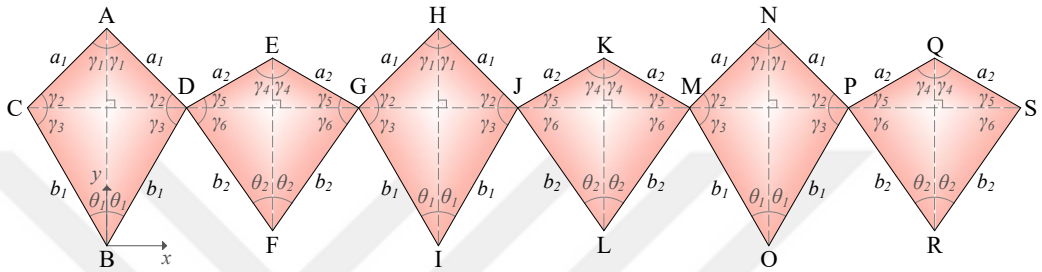

Figure 5.12. Flat configuration of the assembled different kite loops

For this condition, there exist an angulated scissor unit, which possesses different semi lengths and kink angles (Figure 5.13).

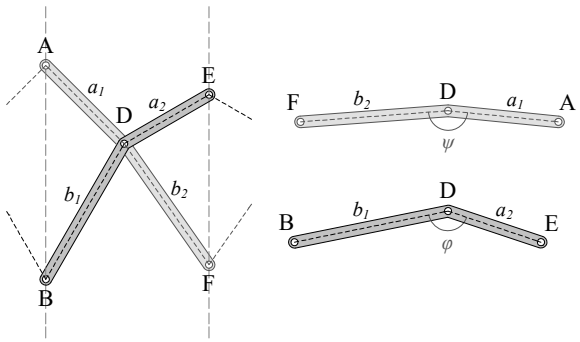

Figure 5.13. Angulated scissor unit with different semi lengths and different kink angles created with different kites

The scissor linkage for the fourth condition (Figure 5.14) has also the same transformation capacity with the other linkages.

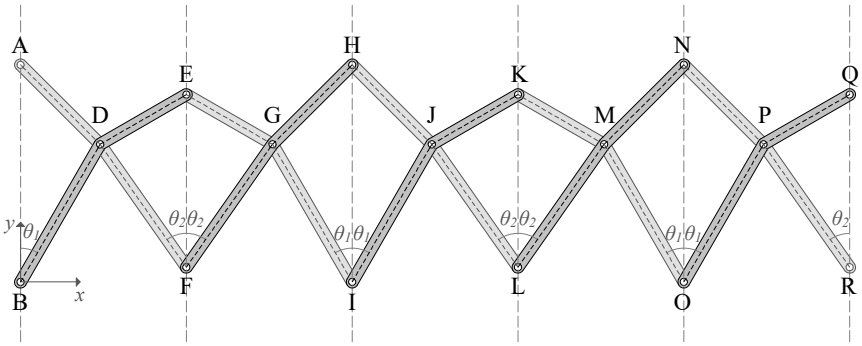

Figure 5.14. Angulated scissor linkage formed by different kite loops with different semi-lengths and interior angles

5.2. Assembly of Dart Loops

For the first condition of the assembly mode, there are identical darts illustrated in Figure 5.15. Firstly, identical dart loops are assembled in a flat configuration where the symmetry axes are parallel to each other and perpendicular to the horizontal-axis.

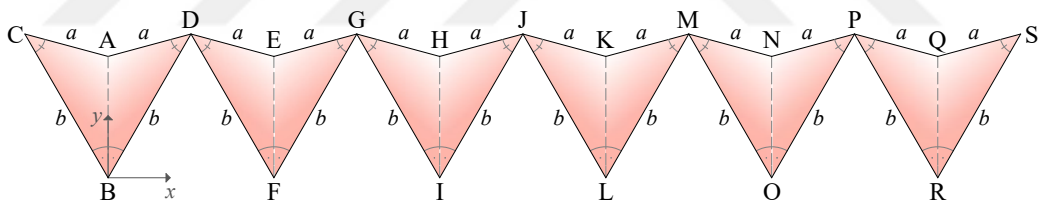

Figure 5.15. Flat configuration of the assembled identical dart loops

Scissor units are detected from the assembled dart loops. It can be observed that there are angulated scissor units generated from the sides of the dart loops (for example |AD| and |DF|, |ED| and |BD|) that define the axes of the angulated bars. An angulated scissor unit resides between two symmetry axes (Figure 5.16). Once an angulated scissor unit is defined between the two symmetry axes, symmetry axes define the unit lines of the angulated scissor unit. The connection point of the dart loops (for example point D) determines the scissor hinge of an angulated scissor unit. It is observed that, Hoberman's nonsymmetrical angulated elements are obtained from the assembly of identical dart loops. But the obtained scissor unit (Figure 5.16) is different from the Hoberman's unit.

While the Hoberman's unit is obtained from the assembly of similar rhombuses, this new type of angulated unit it is obtained from the assembly of identical dart loops.

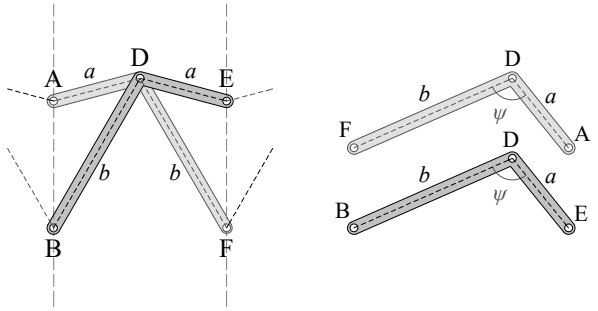

Figure 5.16. Angulated scissor unit with equal semi-lengths and kink angles created with identical darts

The scissor linkage composed of mentioned angulated elements is illustrated in Figure 5.17. The point A is assumed as the fixed point of the linkage and point B is the movable point of the linkage.

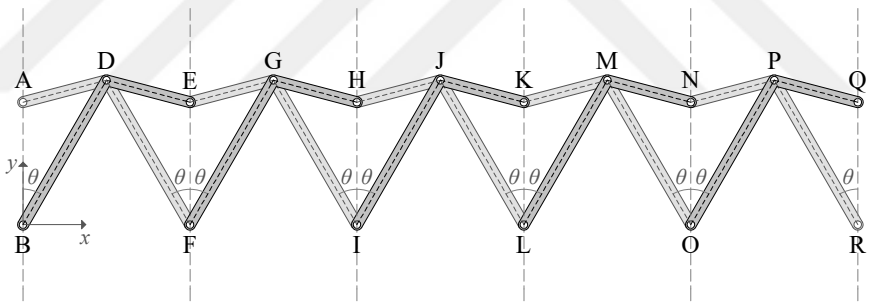

Figure 5.17. Angulated scissor linkage formed by identical dart loops

The new type angulated scissor linkage also was modeled on Solidworks® as illustrated in Figure 5.18 and Figure 5.19. Also, the transformation capability of a single DoF deployable linkage which is constructed by assembling the identical dart loops is shown. This linkage is investigated under three different situations. For the first situation, the linkage is in the flat configuration. It is seen that unit lines are parallel to each other so the curvature is equal to zero. The second situation is bended upward configuration (Figure 5.18). This is accomplished by moving point B (Figure 5.17) along the y-axis as well as the angle θ of dart loop decreases at the same time. The linkage continues bending upward. Loops of the linkage remain as darts. The third situation is bended downward configuration (Figure 5.19). After some point, when the loops of the linkage become

triangles, if the linkage continues to bend down darts become kites. Due to the fact that the segment angles varying during the deployment, center point, which is formed by unit lines intersection, is translated on y-axis. As a result, the radius of curvature changes.

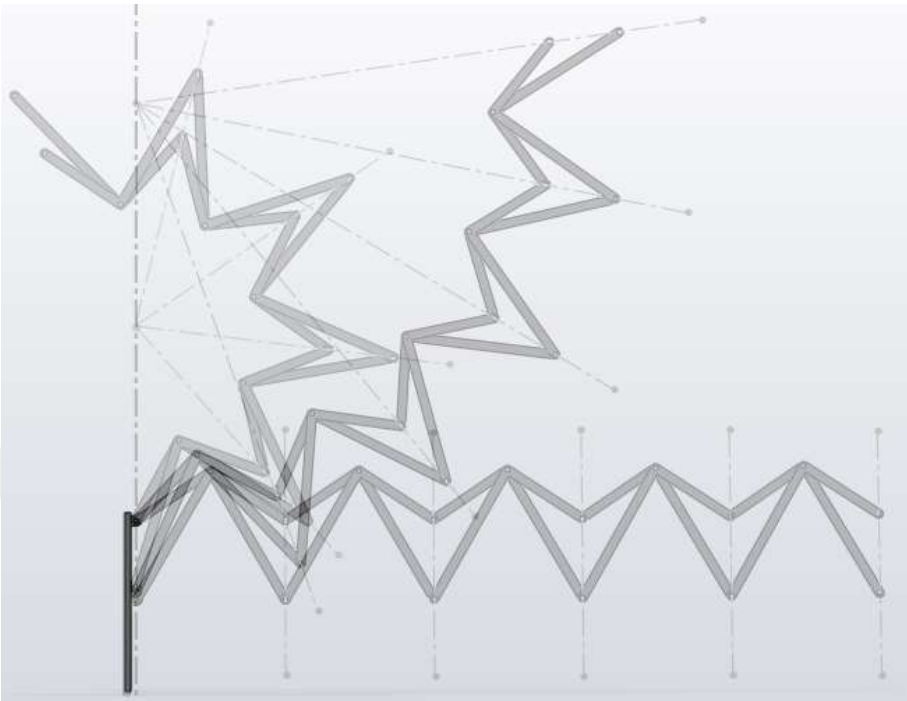

Figure 5.18. The bending upward motion of the linkage modelled on Solidworks

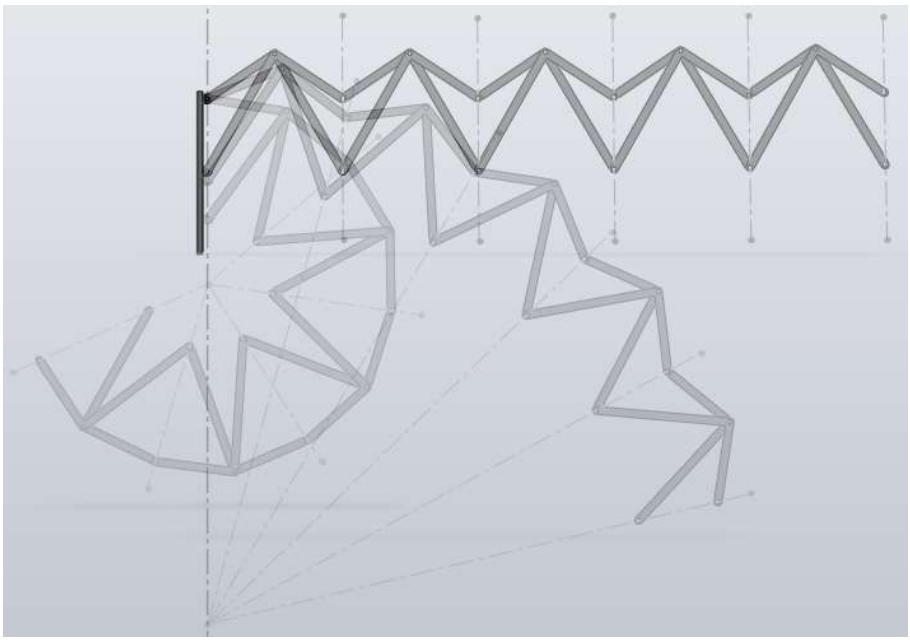

Figure 5.19. The bending downward motion of the linkage modelled on Solidworks

In the second assembly type of dart loops, there are two types of darts whose interior angles are equal to each other but semi-lengths are different (Figure 5.20). As a

first step, two types of darts are assembled in a flat configuration in a sequence where the symmetry axes are parallel to each other and perpendicular to the x-axis. After the assembly, an angulated scissor unit is detected from the assembly of two dart loops.

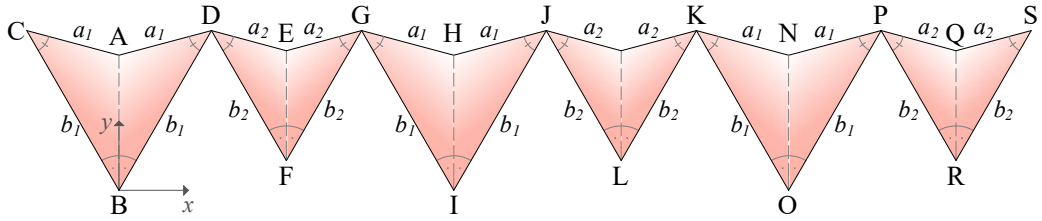

Figure 5.20. Flat configuration of the assembled similar dart loops with identical interior angles but different semi-lengths

From the second assembly type of darts, angulated scissor unit is detected that have different semi-lengths but equal kink angles. In the second type of assembly, the type of angulated scissor units obtained are different from the first one. Because of the identical interior angles of darts, kink angles of the angulated bars of the scissor unit are equal to each other. But the angulated elements of a scissor unit are different from each other (Figure 5.21). If the proportions of short sides and long sides are equal to each other, similar GAEs are obtained. But the obtained scissor unit (Figure 5.21) is different from the Type II unit. While the Type II unit is obtained from the assembly of identical or similar parallelograms, this new type of angulated unit it is obtained from the assembly of similar dart loops.

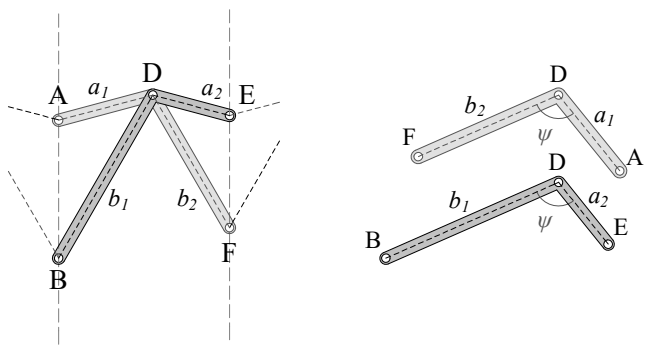

Figure 5.21. Angulated scissor unit with different semi-lengths and equal kink angles created with similar darts

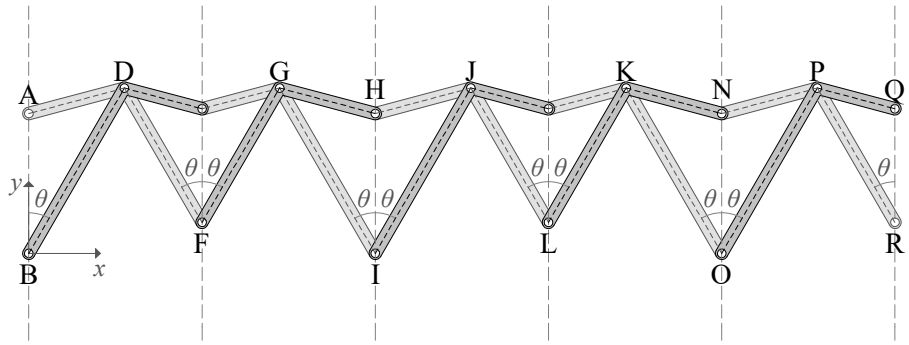

Figure 5.22. Angulated scissor linkage formed by similar dart loops with identical interior angles but different semi-lengths

For the second type of assembly of the dart loops, the obtained angulated scissor linkage (Figure 5.22) has the same transformation capacity as the first one. The linkage transforms between bended upward and bended downward configurations. Thus the curvature of the linkage changes.

According to the third assembly type, there are two types of dart loops whose semi-lengths are equal to each other but interior angles are different (Figure 5.23). An angulated scissor unit that has equal semi-lengths but different kink angles is obtained (Figures. 5.24-25).

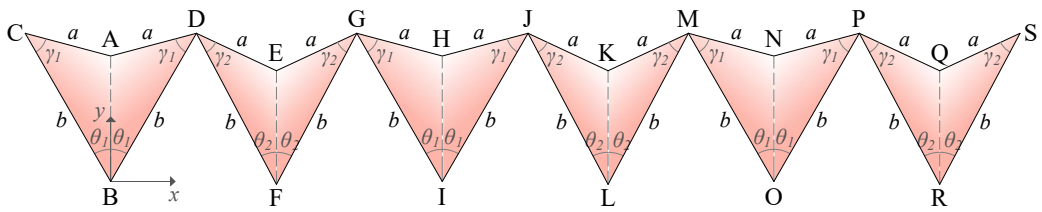

Figure 5.23. Flat configuration of the assembled different dart loops with different interior angles but equal semi-lengths

Considering the assembly of darts in a flat configuration, there exists angulated scissor unit, that has equal semi-lengths but different kink angles (Figure 5.24). Thus we can obtain Equilateral GAEs. But the new type of angulated scissor unit (Figure 5.24) is different from the Type I unit. While the Type I unit is obtained from the assembly of different rhombuses, this new type of angulated unit it is obtained from the assembly of different dart loops.

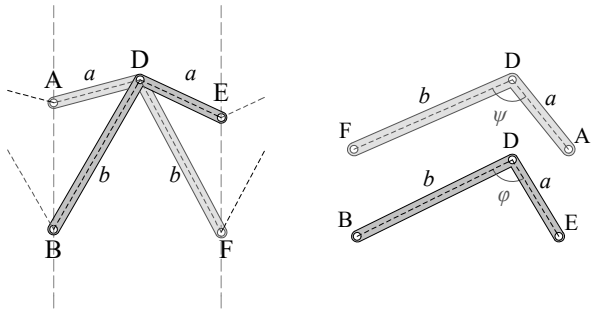

Figure 5.24. Angulated scissor unit with equal semi-lengths and different kink angles created with different darts

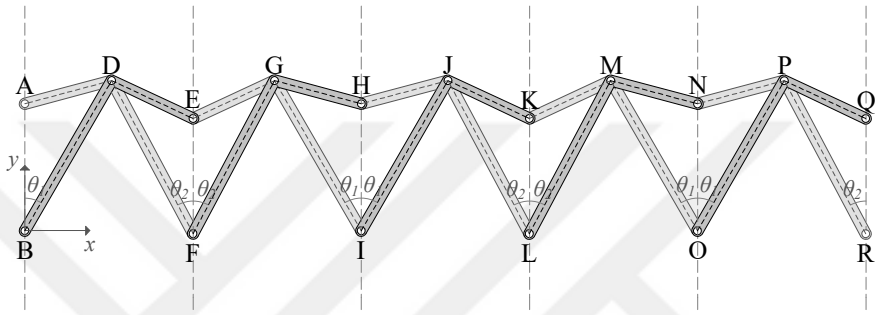

Figure 5.25. Angulated scissor linkage formed by different dart loops with different interior angles but equal semi-lengths

For this assembly (Figure 5.25), the motion of the linkage has the same transformation capability with previous ones. It can bend up and down. The center point of the linkage, where the unit lines intersect, moves along the *y* axis during the motion of the linkage. When the linkage bends upward unit lines intersect at the positive side of the *y*-axis and when the linkage bends downward unit lines intersect at the negative side of the *y*-axis.

In the fourth assembly type of dart loops, there are two types of darts with different interior angles and semi lengths (Figure 5.26). A new type of angulated element is obtained (Figure 5.27).

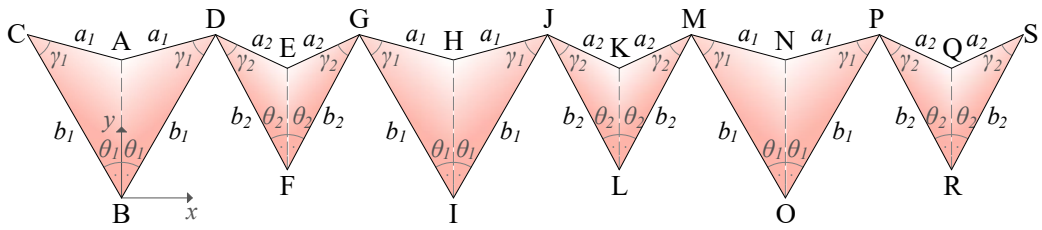

Figure 5.26. Flat configuration of the assembled different dart loops with different interior angles and semi-lengths

For this condition, there exist an angulated scissor unit, which possesses different semi lengths and kink angles (Figure 5.27).

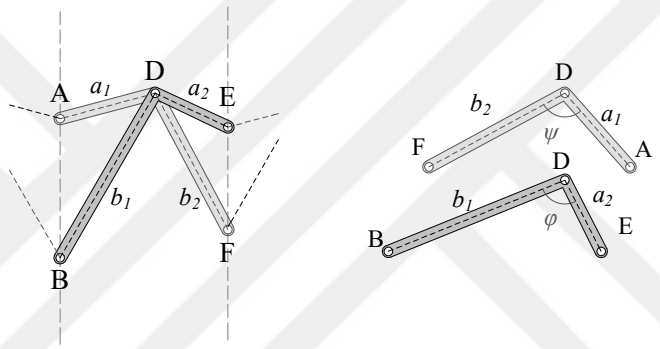

Figure 5.27. Angulated scissor unit with different semi-lengths and kink angles created with different darts

The fourth assembly has the same transformation capability with the other linkages (Figure 5.28).

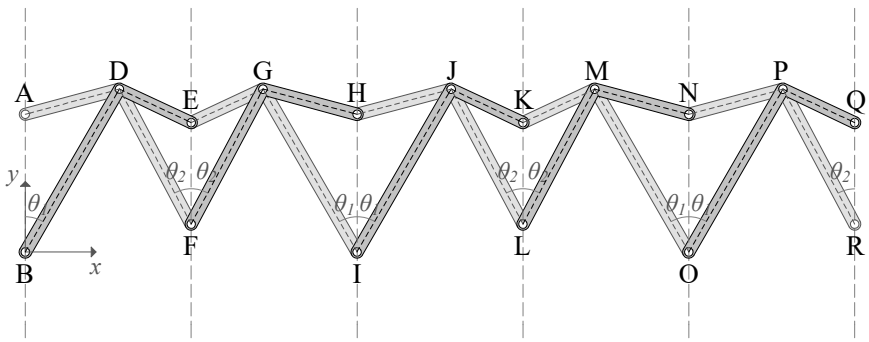

Figure 5.28. Angulated scissor linkage formed by different dart loops with different interior angles and semi-lengths

5.3. Conclusion

This Chapter reveals that angulated scissor linkages can be obtained by kite and dart loops. It is observed that using identical or different kite or dart loops do not make a difference to a transformation capability of the linkage.

In the literature, existing three type of angulated units are obtained by rhombi or parallelograms. Also, the unit lines intersect at one point and the segment angle between unit lines is constant. The angulated units obtained from kite or dart loops, have different geometrical features from the existing ones in the literature. They do not provide the existing deployability conditions for angulated scissor units in the literature. They have nonstable unit lines. The segment angle between unit lines change during the motion. Thus the linkage can transform between convex and concave configurations.

CHAPTER 6

ANALYSIS OF THE ASSEMBLIES OF KITE AND DART LOOPS

This chapter reveals the analysis of geometrical conditions of the scissor linkages constructed by assembling identical kite and dart loops. Then, the position analysis of the scissor linkage consist of identical kite loops is proposed.

6.1. Geometrical Conditions of Angulated Scissor Linkage Composed of Kite Loops

In this section three main configurations that are flat, bended downward and bended upward positions of scissor linkage consist of identical kite loops is investigated.

6.1.1. Flat Position of Kite Loops

In Figure 6.1 the kinematic diagram of the new type of angulated scissor linkage obtained by assembling identical kite loops is illustrated. Three parameters uniquely define a kite loop. The parameters are selected as the sides a and b, and half of the bottom angle θ_1.

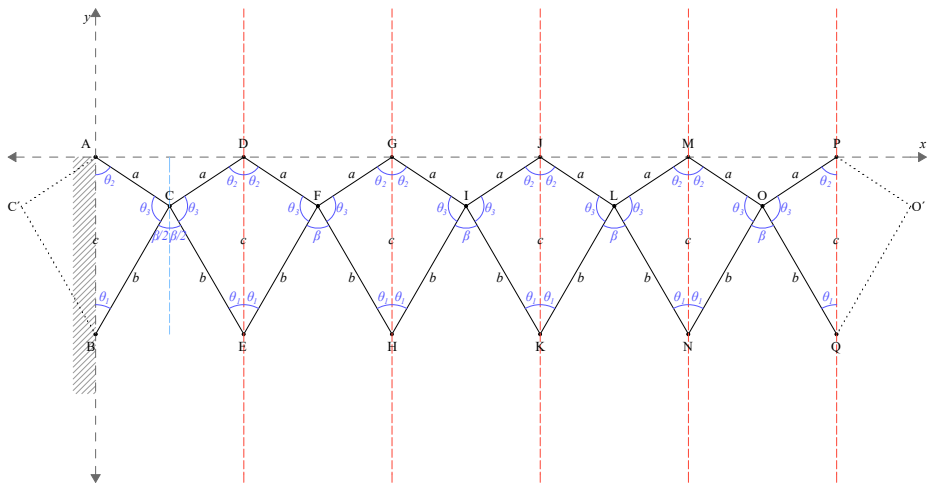

Figure 6.1. Kinematic diagram of the flat configuration of the linkage

In flat position of the linkage, unit lines of the angulated scissor units are parallel to each other. In this case, the deployment angle between the kite loops is equal the bottom angle of the kite:

$$\beta = 2\theta_1 \tag{6.1}$$

According to sine law we can calculate unknown parameters of a kite loop with the known parameters a, b, and θ_1:

$$\frac{a}{sin\theta_1} = \frac{b}{sin\theta_2} \tag{6.2}$$

$$\theta_2 = \pi - sin^{-1}\left(\frac{b.sin\,\theta_1}{a}\right) \tag{6.3}$$

By calculating the angle θ_2 we can calculate the third angle (θ_3) of the triangle ΔABC:

$$\theta_3 = 180 - (\theta_1 + \theta_2) \tag{6.4}$$

The other side length of ΔABC which is the long diagonal of the kite at the same time, is calculated by the help of cosine law:

$$c^2 = a^2 + b^2 - (2ab\cos\theta_3) \tag{6.5}$$

Kink angles are equal to each other for every angulated bar of the linkage. Kink angle of an angulated bar can be calculated as:

$$\psi = 2\theta_1 + \theta_3 \tag{6.6}$$

6.1.2. Bended Downward Position of Kite Loops

When the linkage bends downward the deployment angle decreases continuously. The unit lines intersect at a point M' (Figure 6.2) which is on the -*y* axis. At a specific configuration, points such as B, E, H, etc. lie on a small circle with radius r_{1d}, points such as C, F, I, etc. lie on a medium circle with radius r_{2d} and points such as A, D, G, etc. lie on a large circle with radius r_{3d}. As the structure further bends downward, the radii of the circles decrease, hence curvature increases. In order to calculate the segment angle α' and the deployment angle β', the value of the bottom angle (θ_1') of the kite loop needs to be known for the new position.

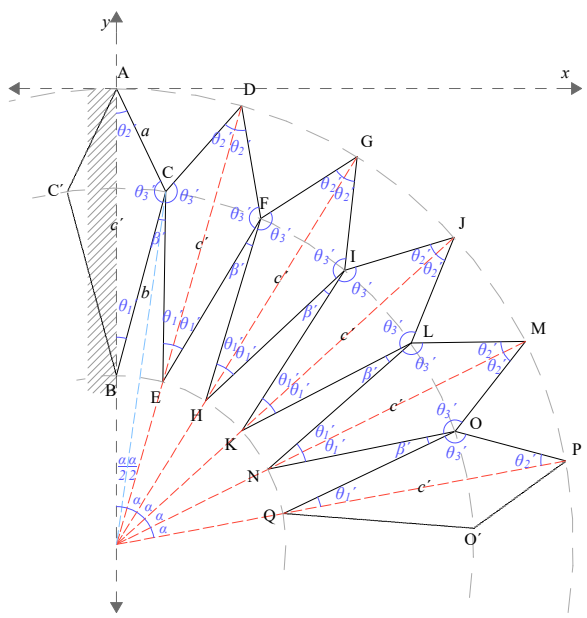

Figure 6.2. Kinematic diagram of the bended downward position of the linkage

Kink angle ψ of the angulated bar is always constant. In bended downward configuration, because the unit lines are no longer parallel to each other, the angle β' can be calculated with the help of kink angle as:

$$\psi = 2\theta_1 + \theta_3 \tag{6.7}$$

$$\beta' = \psi - \theta_3' \tag{6.8}$$

The sum of the two of the interior angles of the triangle is equal the one exterior angle. According to this condition for the triangle ΔBM′C the segment angle of one angulated unit is calculated as:

$$\frac{\alpha}{2} + \frac{\beta'}{2} = \theta_1' \tag{6.9}$$

$$\alpha = 2\theta_1' - \beta' \tag{6.10}$$

From Eq. 5.10 it is seen that in the bended downward configuration of the linkage, the segment angle is equal to the difference between the bottom angle of one kite and the deployment angle between kites.

The small radius of the bended downward configuration of the linkage can be calculated by means of the triangle ΔBM'C. According to sine law r_{1d} is found as in the equation 5.11:

$$r_{1d} = \frac{b\sin{}^{\beta'}/_{2}}{\sin{}^{\alpha'}/_{2}} \tag{6.11}$$

The medium radius can be found by the cosine law:

$$r_{2d} = -\left[r_{1d}^2 + b^2 + 2r_{1d}b\cos(\theta_1')\right]^{\frac{1}{2}} \tag{6.12}$$

The large radius can be found by the sum of the small radius and the long diagonal of the loop:

$$r_{3d} = r_{1d} + c' \tag{6.13}$$

6.1.3. Bended Upward Position of Kite Loops

When the linkage bends upward the unit lines intersect at a point M' (Figure 6.3) which is on the $+y$ axis. At a specific configuration, points such as A, D, G, etc. lie on a small circle with radius r_{1u}, points such as C, F, I, etc. lie on a medium circle with radius r_{2u} and points such as B, E, H, etc. lie on a large circle with radius r_{3u}. As the linkage further bends downward, the radii of the circles decrease, hence curvature increases. Thus the deployment angle β increases. In order to calculate the segment angle α'' and the change of the deployment angle, we need to know the new degree of the bottom angle (β'') of the kite loop for this position.

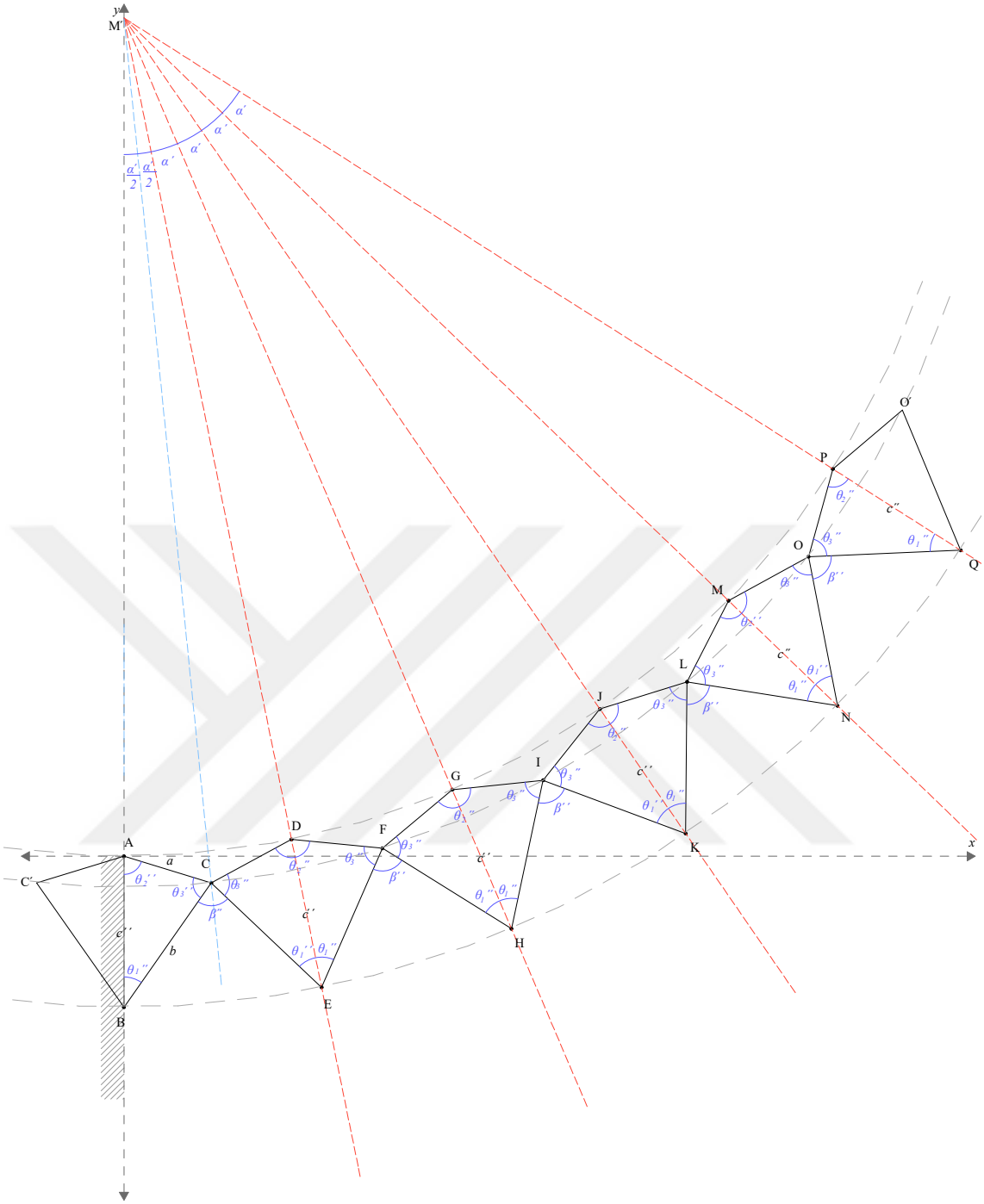

Figure 6.3. Kinematic diagram of the bended upward position of the linkage

Kink angle of the angulated bar always constant. The angle β'' can be calculated as:

$$\beta'' = \psi - \theta_3'' \tag{6.14}$$

The sum of the two of the interior angles of the triangle is equal the one exterior angle. According to this condition for the triangle Δ BM′C the segment angle of one angulated unit is calculated as:

$$\frac{\alpha'}{2} + \theta_1'' = \frac{\beta''}{2} \tag{6.15}$$

$$\alpha' = \beta'' - 2\theta_1'' \tag{6.16}$$

From Eq. 5.15 it is seen that in the bended upward configuration of the linkage, the segment angle is equal to the difference between the bottom angle of one kite and the deployment angle between kites. Compared to the downward configuration the new segment angle is negative of the one computed in Eq. 5.9.

The small radius of the bended upward configuration of the linkage can be calculated by means of the triangle ΔBM'C. According to the sine law r_{1u} is found as 6:

$$\frac{a}{\sin \alpha'/2} = \frac{r_{1u}}{\sin\left(180 - \beta''/2 - \theta_3''\right)} \tag{6.17}$$

The medium radius can be found by the cosine law:

$$r_{2u} = [r_{1u}^2 + a^2 + 2r_1 a \cos(\theta_2'')]^2 \tag{6.18}$$

The large radius can be found as the sum of the small radius and the long diagonal of the loop:

$$r_{3u} = r_{1u} + c'' \tag{6.19}$$

6.2. Geometrical Conditions of Angulated Scissor Linkage Consist of Dart Loops

In this section three main configurations that are flat, bended downward and bended upward positions of scissor linkage consist of identical dart loops is investigated.

6.2.1. Flat Position of Dart Loops

The first linkage constructed by identical dart loops is proposed by Kiper (2015). In Figure 6.4 the kinematic diagram of the scissor linkage assembly is illustrated.

The linkage assembly is formed by identical dart loops in flat configuration. In order to uniquely define a dart loop, at least three known parameters are needed which can be the sides *a* and *b*, and half of the bottom angle θ_1.

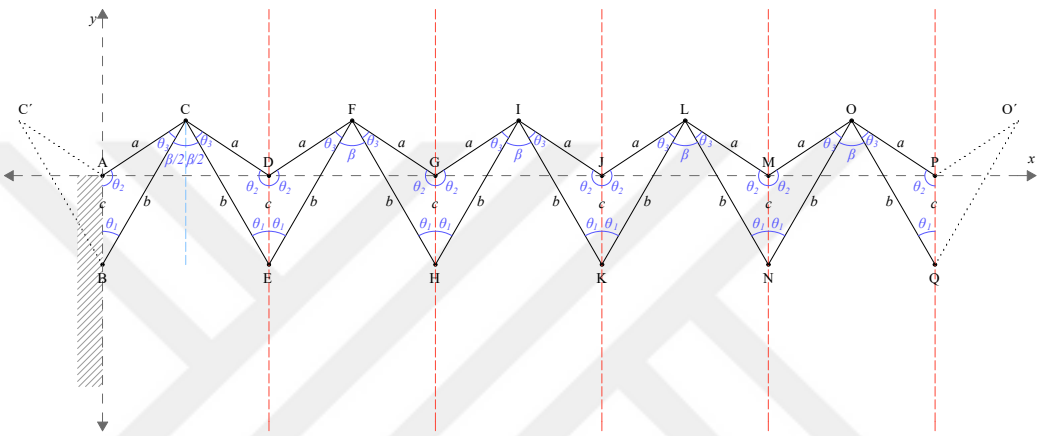

Figure 6.4. Kinematic diagram of the flat configuration of the linkage

In the flat position of the linkage, unit lines of the angulated scissor units are parallel to each other. In this case, the deployment angle between the kite loops is equal a bottom angle of the dart:

$$\beta = 2\theta_1 \tag{6.20}$$

According to the sine law the unknown parameters of a kite loop can be calculated in terms of the known parameters *a*, *b*, and θ_1:

$$\frac{a}{sin\theta_1} = \frac{b}{sin\theta_2} \tag{6.21}$$

$$\theta_2 = \pi - sin^{-1}\left(\frac{b.sin\,\theta_1}{a}\right) \tag{6.22}$$

By calculating the angle θ_2 we can calculate the third angle (θ_3) of triangle ΔABC:

$$\theta_3 = 180 - (\theta_1 + \theta_2) \tag{6.23}$$

The other side length of ΔABC which is the long diagonal of the dart at the same time, is calculated by the help of cosine law:

$$c^2 = a^2 + b^2 - (2ab \cos \theta_3) \tag{6.24}$$

Kink angles are equal to each other for every angulated bar of the linkage. Kink angle of one angulated bar can be calculated as:

$$\psi = 2\theta_1 + \theta_3 \tag{6.25}$$

6.2.2. Bended Downward Position of Dart Loops

When the linkage bends downward the deployment angle decreases continuously. Similar to the case with the kite loops, small, medium and large circles (with radii r_{1d}, r_{2d} and r_{3d}, respectively) passing through joints can be defined (Figure 6.5) The unit lines of scissor units intersect at the centre of these circle which changes moves along the -*y* axis. Thus the deployment angle β decreases. In order to calculate the segment angle α' and the change of the deployment angle β', the bottom angle (θ_1') of the dart loop for this position needs to be calculated.

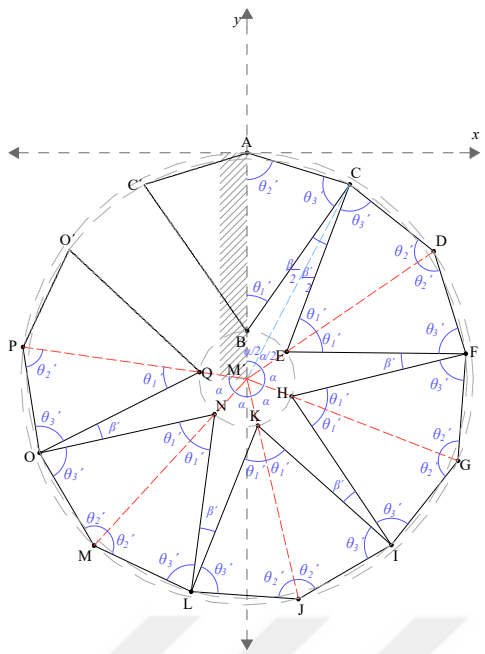

Figure 6.5. Kinematic diagram of the bended downward configuration of the linkage

Kink angle of the angulated bar always constant. In this situation, because the unit lines are no longer parallel to each other the angle β' can be calculated as:

$$\beta' = \psi - \theta_3' \tag{6.26}$$

Sum of the two of the interior angles of the triangle is equal an exterior angle. According to this condition for the triangle ΔBM′C the segment angle of one angulated unit is calculated as:

$$\frac{\alpha}{2} + \frac{\beta'}{2} = \theta_1' \tag{6.27}$$

$$\alpha = 2\theta_1' - \beta' \tag{6.28}$$

From Eq. 5.21 it is seen that in the bended downward configuration of the linkage assembly, the segment angle is equal to the difference between the bottom angle of a kite and the deployment angle between kites.

The small circle radius r_{1d} of the bended downward configuration of the linkage can be calculated by means of the triangle ΔBM′C. According to sine law r_{1d} is found as:

$$\frac{b}{\sin \alpha'/2} = \frac{r_{1d}}{\sin \beta'/2} \tag{6.29}$$

The medium radius can be found with cosine law:

$$r_{2d} = \left[r_{1d}^2 + b^2 + 2r_{1d}\, b \cos(\theta_1')\right]^{1/2} \tag{6.30}$$

The large radius can be found by the sum of the small radius and the long diagonal of the loop:

$$r_{3d} = r_{1d} + c \tag{6.31}$$

6.2.3. Bended Upward Position of Dart Loops

When the assembly bends upward the deployment angle changes. Once again joints reside on small, medium and large circles (Figure 6.6). Unit lines of scissor units intersect at the centre of these circles which moves along the $+y$ axis. Thus the deployment angle β increases as the assembly bends upward. In order to calculate the segment angle α'' and the change of the deployment angle β'', the bottom angle (θ_1'') of the kite loop for this position needs to be calculated.

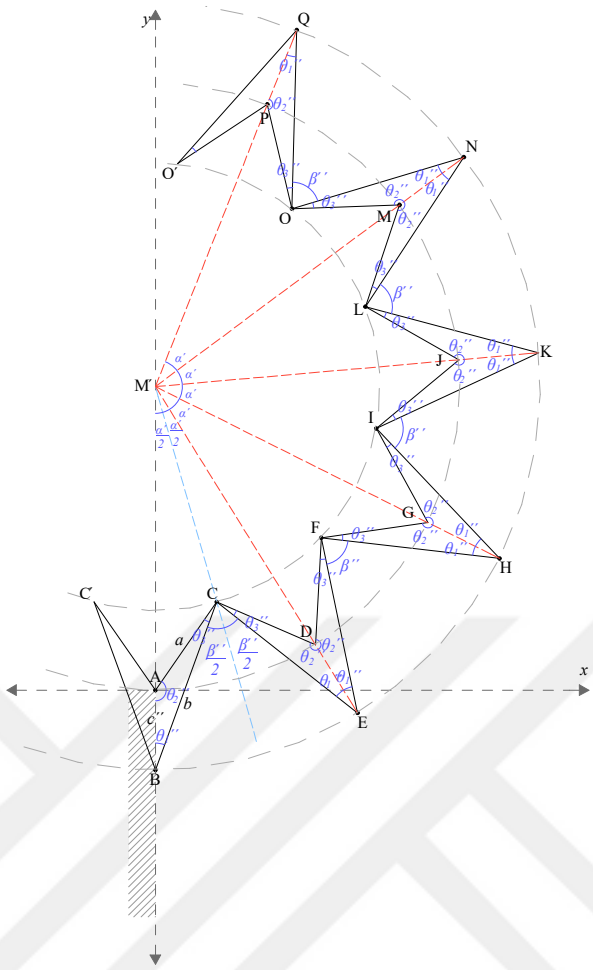

Figure 6.6. Kinematic diagram of the bended upward configuration of the linkage

Deployment angle β'' can be calculated as:

$$\beta'' = \psi - \theta_3'' \tag{6.32}$$

Sum of the two of the interior angles of the triangle is equal an exterior angle. Accordingly, for the triangle Δ BM'C the segment angle of an angulated unit is calculated as:

$$\frac{\alpha'}{2} + \theta_1'' = \frac{\beta''}{2} \tag{6.33}$$

$$\alpha' = \beta'' - 2\theta_1'' \tag{6.34}$$

From Eq. 5.27 it is seen that in the bended upward configuration of the assembly, the segment angle is equal to the difference between the bottom angle of a dart and the

deployment angle between darts. Compared to the downward configuration the new segment angle is has opposite sign.

The small radius of the bended upward configuration of the linkage can be calculated by means of the triangle ΔAM'C. According to the sine law r_{1u} is found as:

$$\frac{a}{\sin \alpha'/2} = \frac{r_{1u}}{\sin\left[-\left(\alpha'/2 - \theta_2''\right)\right]} \tag{6.35}$$

The medium radius can be found by the cosine law:

$$r_{2u} = [r_{1u}^2 + a^2 + 2r_1 a \cos(\theta_2'')]^{1/2} \tag{6.36}$$

The large radius can be found as the sum of the small radius and the long diagonal of the loop:

$$r_{3u} = r_{1u} + c'' \tag{6.37}$$

6.3. Position Analysis

Kinematic analysis is the study of motion characteristics in a known mechanism. One of the main principal goals of the kinematic analysis is to determine the location and orientation of rigid bodies. Location of a rigid body (link) or a particle (point) in a rigid body with respect to a given reference frame is called as the *Position* of that point or body (Söylemez 2000).

In order to understand the kinematic analysis of the proposed system first, we need to calculate the mobility of the linkage. According to the Grübler's equation for planar linkages:

$$M = 3(L - 1) - 2j_1 - j_2 \tag{6.38}$$

Where M is the degree of freedom, L is the number of links, j_1 is the number of joints which have one DoF, and j_2 is the number of 2 DoF joints. In Figure 6.7 there is a kinematic diagram of the linkage. The mobility calculation for this linkage is:

$$M = 3(12 - 1) - 2.16 - 0 = 1 \tag{6.39}$$

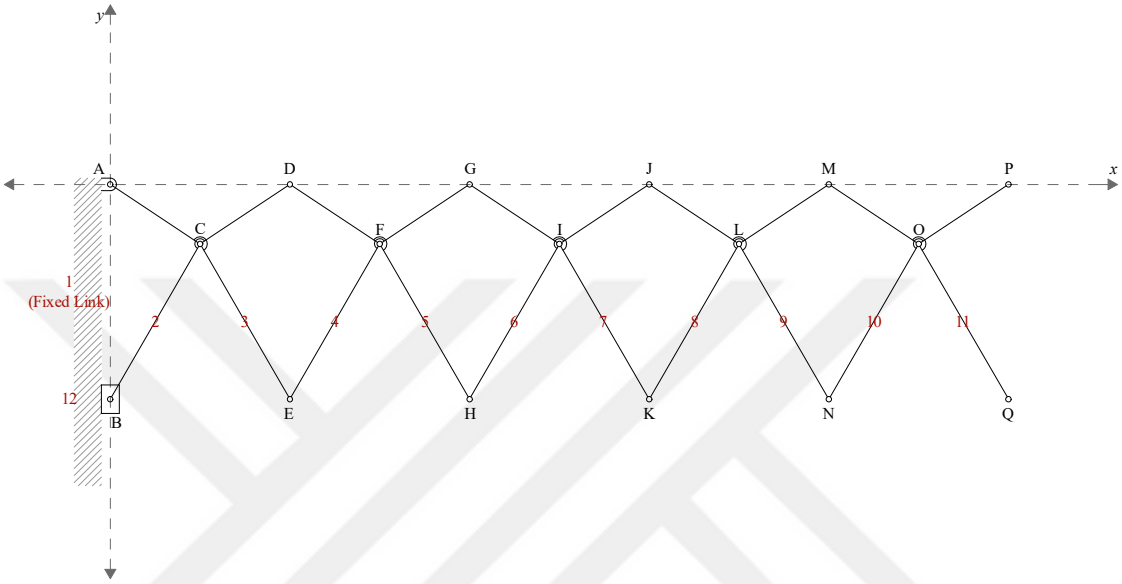

Figure 6.7. Kinematic diagram of the linkage

It is observed that according to the Grübler's mobility formula the degree of freedom of the linkage is 1. Only one parameter is needed to define the positions of all links of the assembly shown in Figure 6.8. This parameter can be chosen as the angle θ_1. All link lengths (a, b) and the angle of the input link (θ_1) are assumed to be known. Thus it is possible to determine c, θ_2 and θ_3 according to the known parameters.

The proposed linkage consists of the following constant parameters:

$$|AC| = |CD| = |DF| = |FG| = |GI| = |IJ| = |JL| = |LM| = |MO| = |OP| = a$$

$$|BC| = |CE| = |EF| = |FH| = |HI| = |IK| = |KL| = |LN| = |NO| = |OQ| = b$$

Variable parameters of the linkage are θ_1, θ_2, θ_3 and $|AB| = |DE| = |GH| = |JK| = |MN| = |PQ| = c$.

Figure 6.8 shows all the variables used in kinematic analysis of the mechanism. According to given lengths of (a, b) and θ_1 variable, all angles (θ_2 and θ_3), c, all coordinates of A, B, …, Q points and angles α_1, α_2, α_3…α_{15} can be found.

In kinematic analysis of the system, firstly point A is assumed as origin (0, 0). While point B could change its position along y axis by the help of a prismatic joint.

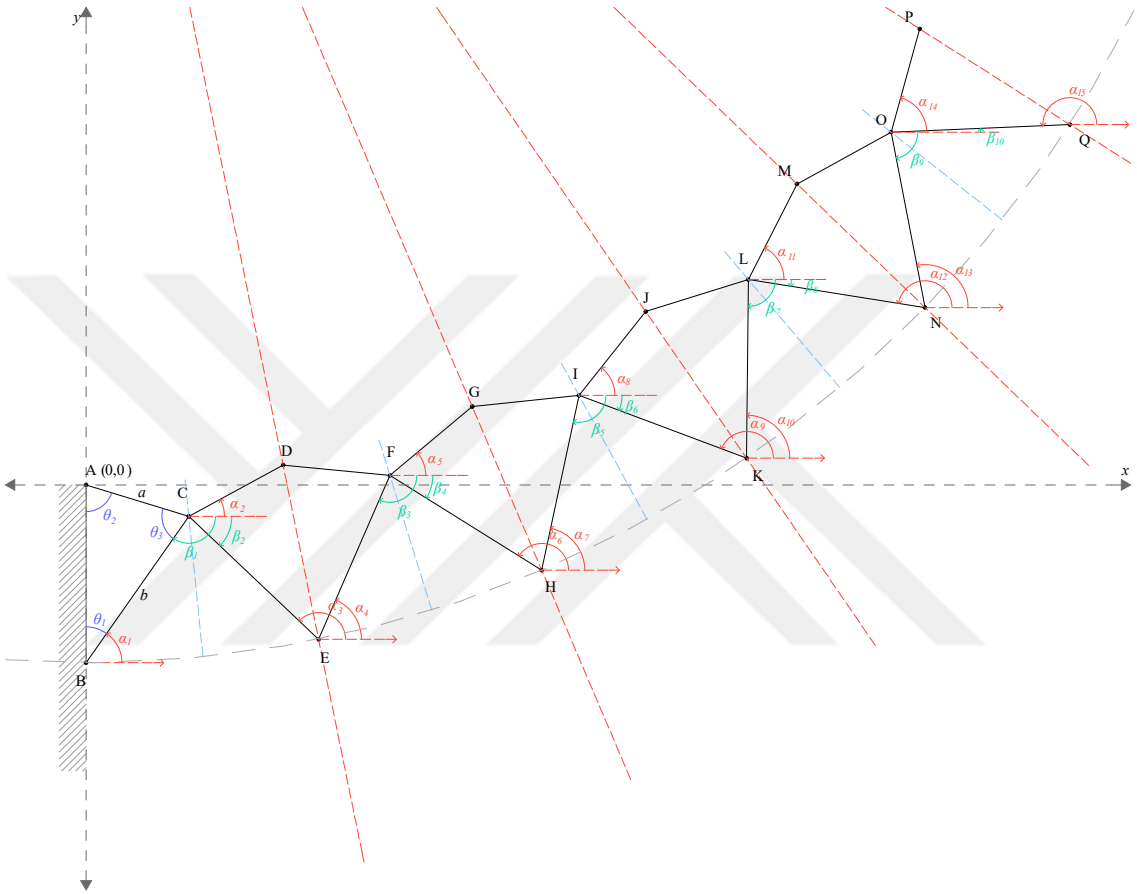

Figure 6.8. The position of the linkage when c=50 and θ_1~35º

A parametric model of this mechanism is constructed in Microsoft Excel®. See (Söylemez, 2008) for use of Excel® in mechanism applications. As an example, the Excel model was constructed for a =30, b =50 and θ_1 = 35º at the initial configuration. After finding the angles θ_2 and θ_3, the variable length c is calculated. Then, the coordinates of the points are calculated. The angles that are needed to find the coordinates of the points are calculated.

The coordinates of the point A is assumed as (0,0). And the coordinates of the point B depends on the variable length c (0, c).

Step 1: In order to calculate the coordinates of the other points first we need to calculate the angle α_1:

$$\alpha_1 = 90° - \theta_1 \tag{6.40}$$

Next, the coordinates of point C are found:

$$C_x = B_x + (b.cos\alpha_1) \tag{6.41}$$

$$C_y = B_y + (b.sin\alpha_1) \tag{6.42}$$

Step 2: In order to calculate the coordinates of point D first, the auxiliary angle β_1 needs to be calculated:

$$\beta_1 = \alpha_2 - 180° \tag{6.43}$$

With the help of the β_1, the angle for point D can be found:

$$\alpha_2 = \beta_1 - \psi \tag{6.44}$$

By finding the angle α_2 the coordinates of point D can be calculated as:

$$D_x = C_x + (a.\ cos\ \alpha_2) \tag{6.45}$$

$$D_y = C_y + (a.\ sin\ \alpha_2) \tag{6.46}$$

Step 3: This step contains two phases. First one is to find the coordinates of point E and the second one is to find the coordinates of point F. In order to find the coordinates of point E first the auxiliary angle should be found:

$$\beta_2 = \alpha_2 - 180° \tag{6.47}$$

$$\alpha_3 = 180° + \beta_2 \tag{6.48}$$

$$E_x = C_x + (b.\cos\alpha_3) \tag{6.49}$$

$$E_y = C_y + (b.\sin\alpha_3) \tag{6.50}$$

$$F_x = E_x + (b.\cos\alpha_4) \tag{6.51}$$

$$F_y = E_y + (b.\sin\alpha_4) \tag{6.52}$$

For the rest of the coordinates of points Step 2 and Step 3 are repeatedly applied. For the coordinates of the points G, J, M and P Step 2 is used. And for the other points H and I, K and L, N and O, and Q Step 3 is used. The Excel sheet is illustrated in Figure 6.9.

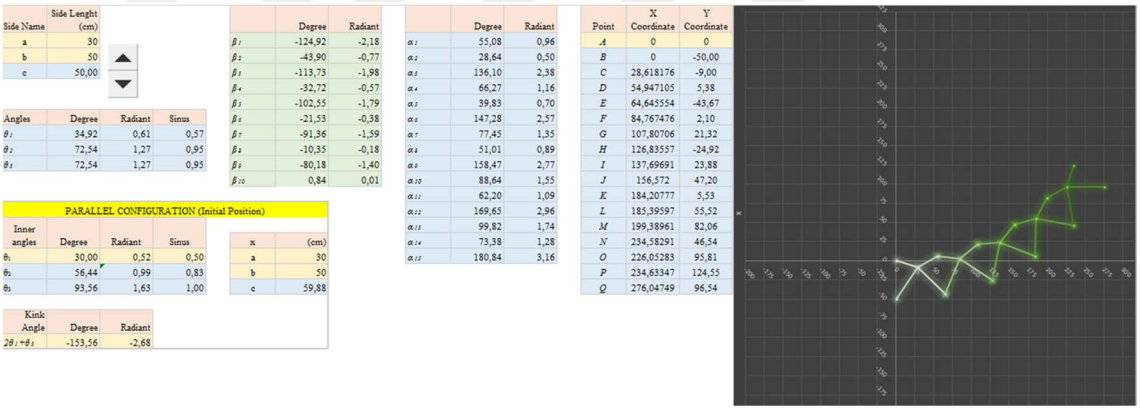

Side Name	Side Lenght (cm)
a	30
b	50
c	50,00

Angles	Degree	Radiant	Sinus
θ_1	34,92	0,61	0,57
θ_2	72,54	1,27	0,95
θ_3	72,54	1,27	0,95

	Degree	Radiant
β_1	-124,92	-2,18
β_2	-43,90	-0,77
β_3	-113,73	-1,98
β_4	-32,72	-0,57
β_5	-102,55	-1,79
β_6	-21,53	-0,38
β_7	-91,36	-1,59
β_8	-10,35	-0,18
β_9	-80,18	-1,40
β_{10}	0,84	0,01

	Degree	Radiant
α_1	55,08	0,96
α_2	28,64	0,50
α_3	136,10	2,38
α_4	66,27	1,16
α_5	39,83	0,70
α_6	147,28	2,57
α_7	77,45	1,35
α_8	51,01	0,89
α_9	158,47	2,77
α_{10}	88,64	1,55
α_{11}	62,20	1,09
α_{12}	169,65	2,96
α_{13}	99,82	1,74
α_{14}	73,38	1,28
α_{15}	180,84	3,16

Point	X Coordinate	Y Coordinate
A	0	0
B	0	-50,00
C	28,618176	-9,00
D	54,947105	5,38
E	64,645554	-43,67
F	84,767476	2,10
G	107,80706	21,32
H	126,83557	-24,92
I	137,69691	23,88
J	156,572	47,20
K	184,20777	5,53
L	185,39597	55,52
M	199,38961	82,06
N	234,58291	46,54
O	226,05283	95,81
P	234,63347	124,55
Q	276,04749	96,54

PARALLEL CONFIGURATION (Initial Position)

Inner angles	Degree	Radiant	Sinus
θ_1	30,00	0,52	0,50
θ_2	56,44	0,99	0,83
θ_3	93,56	1,63	1,00

	(cm)
a	30
b	50
c	59,88

Kink Angle	Degree	Radiant
$2\theta_1+\theta_3$	-153,56	-2,68

Figure 6.9. Analytical position analysis of the angulated scissor linkage in the position of c=50 and θ_1~35º

It is observed that the loops of the assembly transform between kite and dart forms during the motion. While the assembly bends downward, the loops remain as kites and the angle θ_1 decrease continuously. But when the structure bends upward from downward configuration angle θ_1 continues to increase until the loops of the structure turn into triangles. At this position angle θ_2 becomes a right angle (90º). That is, two short sides of a kite loop (a) become collinear. After that, when the structure continues to bend upward angle θ_1 decreases again until the structure reaches maximum bending. Therefore, the linkage can have two different configurations for an angle value of θ_1 such as illustrated in Figures. 6.10 and 6.11.

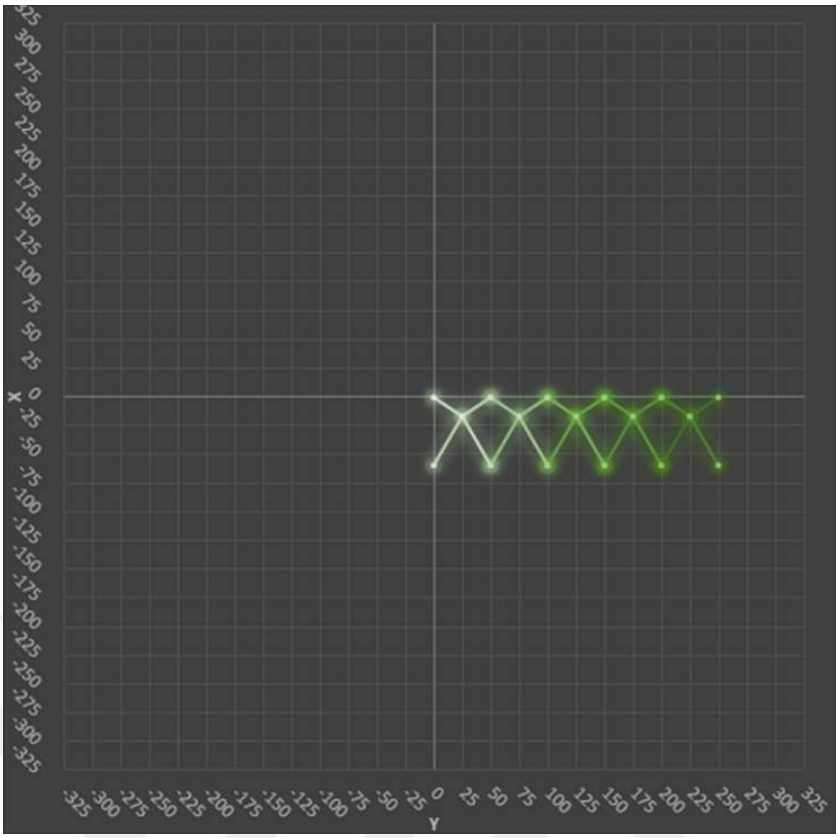

Figure 6.10. Initial position of the linkage c=59,88 cm, θ1 = 30º, θ2 = 56,44º, θ3 = 93,56º

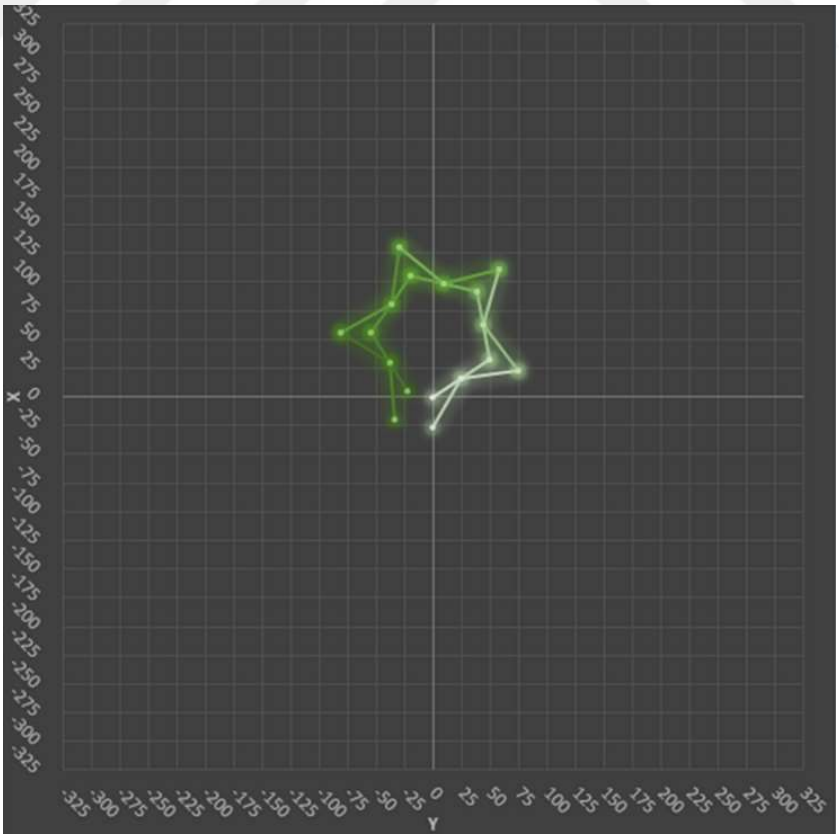

Figure 6.11. Bended upward position of the linkage c=26,72 cm, θ1 = 30º, θ2 = 123,56º, θ3 = 26,44º

6.4. Conclusion

In this chapter the geometrical conditions of the proposed linkages have been investigated. The three defined positions (flat, bended downward and bended upward configurations) have been examined for both of the linkages constructed with kite and dart loops. It is seen that in order to find segment angle and radius of both kite and dart loops the same mathematical formulations are used. In both systems, when the mechanism is in bended and/or downward position they define a centre which moves along the y-axis. When the system is in bended position the centre is on –y axis, while in bended upward position the centre is on +y axis.

It is observed that the linkages have the same geometrical conditions during their motions between convex and concave configurations. Then, by using Microsoft Excel® position analysis of one of the linkages consisting of kite loops has been evaluated. It is observed that during the motion of the linkage, it has two positions for a given bottom angle value. While the linkage is bending upward the bottom angle increases. It reaches maximum value when all the loops of the linkage transform into triangles. At this position the loops of the linkage start to transform from the kite loops into the dart loops. When the linkage keeps bending upward, the bottom angle again decreases.

CHAPTER 7

CONCLUSION

This chapter offers the aforementioned contributions of the dissertation in the development of transformable planar structural linkages.

This thesis is restricted to planar scissor linkages only. In this thesis, common deployable scissor linkages were thoroughly investigated. The geometric and kinematic conditions of the scissor units were examined in detail. In addition to this, the loop types of scissor units and their assembly conditions for every type of scissor units were also revealed. New type of deployable scissor linkages that can transform between convex and concave configurations were developed.

The new type planar angulated scissor assemblies have different configurations that are flat, bended upward and bended downward configurations. It results in remarkable transformation capability compared to the existing ones in the literature. It can even form different configurations with only one input parameter.

In the first type of novel linkages, angulated elements are constructed via kite loops. Moreover, the present study reveals that dart loops could also be used which results in new angulated scissor units.

In the context of the aforementioned framework, a novel type of scissor unit that is derived from kite or dart loops, has been introduced. A novel planar angulated scissor linkage has been developed by the utilization of this unit. Moreover, kinematic analysis of the novel angulated scissor linkage has been presented.

REFERENCES

Akgün, Y., Haase, W., & Sobek, W. (2007). Proposal for a new scissor-hinge structure to create transformable and adaptive roofs. Proceedings of *"IASS 2007 International Association of Spatial Structures*.". Venice.

Akgün, Y. (2010). A Novel Transformation Model for Deployable Scissor-Hinge Structures. PhD dissertation. Izmir Institute of Technology.

Akgün, Y., Gantes, C. J., Kalochairetis, K., & Kiper, G. (2010). A novel concept of convertible roofs with high transformability consisting of planar scissor-hinge structure. *Engineering Structures*, 32, 2873-2883.

Akgün, Y., Gantes, C. J., Sobek, W., Korkmaz, K., & Kalochairetis, K. (2011). A novel adaptive spatial scissor-hinge structural mechanism for convertible roofs. *Engineering Structures*, 33, 1365-1376.

Akgün, Y., Maden, F., & Korkmaz, K. (2013). Design of adaptive structures by kinematic synthesis of mechanisms. In: Paulo J.S (Ed.), "*Structures and Architecture: Concepts, Applications and Challenges."* Ed. Cruz, London: Taylor & Francis, pp 976-982.

Atake, K. (2000). New variations of the scissors technique. In: *"MARAS III: International Conference on Mobile and Rapidly Assembled Structures"*. Madrid, Spain, pp 143-154.

Belda, E. A. P. (2013). The Structures of Emilo Pérez Piñero: Evolution and Types. In Proceeding of the *"First Conference Transformables"* 2013, Seville, Starbooks, pp 31-39.

Buhl, T., Jensen, F. V., & Pellegrino, S. (1984). Shape Optimization of Cover Plates for Retractable Roof Structures. *Computers and Structures Journal*, 82, 1227- 1236.

Calatrava, S. (1981). Zur Faltbarkeit von Fachwerken. PhD dissertation, ETH Zurich.

Chen, Y. (2003). Design of Structural Mechanisms. PhD dissertation, University of Oxford, Oxford, UK.

De Temmerman, N. (2007). Design and Analysis of Deployable Bar Structures for Mobile Architectural Applications. PhD dissertation. Vrije Universiteit Brussel.

Escrig, F. (1984). Expandable space frame structures. Edited by H. Nooshin. In: Proceedings of the *"3rd International Conference on Space Structures."* Guildford, UK: Elsevier Applied Science Publishers, pp 845-850.

Escrig, F. (1985). Expandable space structures. *International Journal of Space Structures*, 1, 79-91.

Escrig, F. (1996). General survey of deployability in architecture. In: Proceedings of the *"Second International Conference on Mobile and Rapidly Assembled Structures II (MARAS 96)",* Seville.

Escrig, F., & Valcárcel, J. P. (1993). Geometry of expandable space structures. *International Journal of Space Structures*, 8, 71-84.

Escrig, F., & Valcárcel, J. P. (1986a). Analysis of expandable space bar structures. In: K. Heki (Ed.) Proceedings of *"IASS Symposium on Shells, Membranes, and Space Frames."* Osaka: Elsevier Science Publishers, pp 269-276.

Escrig, F., & Valcarcel, J. P. (1986b). Great size umbrellas with expendable bar structures. In: Proceedings of the *"1st International Conference on Lightweight Structures in Architecture",* Sydney, University of New South Gales, pp 676-681.

Escrig, F., & Valcárcel, J. P. (1987). Curved expandable space grids. In: Proceedings of the *"International Conference on the Design and Construction of Non-Conventional Structures."* London, pp 157-166.

Fundación Emilio Pérez Piñero. (n.d.). Retrieved January 26, 2017, from http://www.perezpinero.org/

Gantes, C. (1991). A Design Methodology for Deployable Structures. PhD thesis, Massachusetts Institute of Technology.

Gantes, C. J. (2001). Deployable Structures: Analysis and Design. Boston: WIT Press.

Gantes, C.J., Logcher, R. D., Connor, J. J., & Rosenfeld, Y. (1993). Deployability conditions for curved and flat, polygonal and trapezoidal deployable structures. *International Journal of Space Structures*, 8, pp 97-106.

Hanaor, A. & Levy. R. (2001). Evaluation of deployable structures for space enclosures. *International Journal of Space Structures*, 16, 211-229.

Hoberman, C. (1990). Reversibly Expandable Doubly-curved Truss Structure. US Patent No. 4,942,700.

Hoberman, C. (1991). Radial Expansion/Retraction Truss Structures. U.S. Patent No. 5,024,031.

Hoberman, C. (1993). Unfolding architecture. *Architectural Design*, 63, 56-59.

Hoberman, C. (2004). Retractable structures comprised of interlinked panels. U.S. Patent No. 6,739,098.

Hoberman, C. (2013). Mechanical Invention Through Computation - Mechanism Basics, MIT Class 6.S080 Lecture notes.

Hoberman, C. (2016). Hoberman Transformable Design. Retrieved November 08, 2016 http://www.hoberman.com/

Jensen, F. V. (2005). Concepts for retractable roof structures. PhD dissertation, University of Cambridge.

Jensen, F., & Pellegrino, S. (2002). Expandable structures formed by hinged plates. In: G.A.R. Parke and P. Disney (Eds.), Proceedings of *"5th International Conference on Space Structures."* London: Thomas Telford Publishing, pp 263-272.

Jensen, F., & Pellegrino, S. (2005). Expandable 'blob' structures. *Journal of the International Association for Shell and Spatial Structures*, 46, 151-158.

Kiper, G., Söylemez, E. (2010) Irregular polygonal and polyhedral linkages comprising scissor and angulated elements. In: Proc. "*1st IFToMM Asian Conference on Mechanism and Machine Science"* (CD), Taipei (Taiwan), October 21-25, pp 455-459.

Kiper, G. (2011). Design Methods for Planar and Spatial Deployable Structures. PhD dissertation, Middle East Technical University

Kiper, G. (2015) Personal communication.

Kokawa, T. (1995). A trial of expandable arch. In: Proceedings of the *"IASS International Symposium"* 1995 Milano, 2, pp 501-510.

Kokawa, T. (1996). Scissors arch with zigzag-cable through pulley-joints. In: Proceedings of *"Conceptual Design of Structure*." pp 868-875.

Kokawa, T. (1997). Cable scissor arch-marionettic structure. In: *"Structural Morphology Towards the New Millennium, IASS International Colloquium"*, pp 107-114.

Kokawa, T. (2000). Structural idea of retractable loop-dome. *Journal of the International Association for Shells and Spatial Structures*: IASS 41. 111-115.

Korkmaz, K. (2004). An Analytical Study of the Design Potentials in Kinetic Architecture. PhD dissertation. Izmir Institute of Technology.

Langbecker, T. (1999). Kinematic analysis of deployable scissor structures. *International Journal of Space Structures*, 14, 1-15.

Langbecker, T., Albermani, F. (2001). Kinematic and non-linear analysis of foldable barrel vaults. *Engineering structures*, 23, 158-171.

Leonard, I. E., Lewis, J. E., Liu, A. C. F., & Tokarsky, G. W. (2014). Classical Geometry: Euclidean, Transformational, Inversive, and Projective. Somerset: John Wiley & Sons, Incorporated, 2014.

Liao, Q. & Li, D., (2005). Mechanisms for scaling planar graphs. *Chinese Journal of Mechanical Engineering*, 41, 140-143.

Liapi, K. (2001). Transformable structures: design features and preliminary investigation. *Journal of Architectural Engineering*, 7, 13-17.

Maden, F. (2014). Hareketli strüktürler. *Yapı*, 386, 132-136.

Maden, F. (2015). Novel Design Methodologies for Transformable Doubly-Ruled Surface Structures. PhD dissertation. Izmir Institute of Technology.

Maden, F. and Korkmaz, K. (2010). Makas mekanizmaların kinetik mimarideki uygulamaları. *Yapı*, 341,102-107.

Maden, F., Korkmaz, K., & Akgün, Y. (2011). A review of planar scissor structural mechanisms: geometric principles and design methods. *Architectural Science Review*, 54(3), 246-257.

Mira, L. A. (2010). Design and Analysis of a Universal Scissor Component for Mobile Architectural Applications. MSc Thesis, Vrije Universiteit Brussel.

Mira, L. A., Thrall, A. P., & De Temmerman, N. (2014). Deployable scissor arch for transitional shelters. *Automation in Construction*, 43, 123-131.

Pellegrino, S. (2001). Deployable Structures. New York: Springer.

Pellegrino, S. Caltech-Professor Sergio Pellegrino Space Structures Laboratory. Retrieved November 09, 2016, from http://www.pellegrino.caltech.edu/

Petrova, P. (2008). The Range and Limits of Deployable Space Frames based on Scissor-like Elements to Create a Large Structure Totally Arbitrary Curvature. Diplomarbeit, Technischen Universitat Wien.

Piñero, Emilo Pérez. (1961a). A reticular movable theatre. *The Architects' Journal,* 134(30): 299.

Piñero, E., P. (1961b). Project for a mobile theatre. *Architectural Design*, 31(12): 570.

Piñero, E., P. (1962). Expandable space framing. *Progressive Architecture*, 43(6): 154-155.

Piñero, E., P. (1965). Three dimensional reticular structure. U.S. Patent No. 3,185,164.

Rippmann, M. (2007). Curtain Wall: Building Design Semesterarbeit. Stuttgart: Universität Stuttgart-ILEK.

Kelvin., R., Mira, L. A. and De Temmerman, N. 2013. From surface to scissor structure, In: Proceedings of the *"First Conference Transformables"* 2013. Seville: Starbooks, pp. 275-280.

Söylemez, E. (2000). Mekanizma Tekniği. Prestij Ajans Matbaacılık.

Söylemez, E. (2009). Using computer spreadsheets in teaching mechanisms. In: Proceedings of *"EUCOMES 08"*, Springer, pp. 45-53.

Usiskin, Z., Griffin, J., Witonsky, D., & Willmore, E. (2008). The Classification of Quadrilaterals: A Study of Definition. Charlotte, NC: Information Age Publishing.

Van Mele, T., De Temmerman, N., De Laet, L., & Mollaert, M. (2010). Scissor-hinged retractable membrane structures. *International Journal of Structural Engineering*, 1(3-4), 374-396.

Yar, M., Korkmaz, K., Kiper, G., Maden, F., Akgün, Y. & Aktas, E. (2016). A novel planar scissor structure transforming between concave and convex configurations. *International Journal of Computational Methods and Experimental Measurements*. DOI: 10.2495/CMEM-V0-N0-1-9

Wikimedia by Felix Escrig, (Own work), retrieved November 28, 2016 from http://creativecommons.org/licenses/by-sa/3.0, via Wikimedia Commons.

You, Z., & Pellegrino, S. (1997). Foldable bar structures. *International Journal of Solids and Structures*, 34, 1825-1847.

Zuk, W. (1994). The next 100 years of architecture. The Futurist, 28, 16-19.

Zuk, W., & Clark, R. H. (1970). Kinetic Architecture. Van Nostrand Reinhold, New York, USA.